# Investigation of Topology, Instantons, and the Nahm Transform in Lattice QCD using Highly Improved Operators

Sundance Osland Bilson-Thompson

*B.Sc (Hons.) Mathematical Physics*

*Department of Physics and Mathematical Physics*

*The University of Adelaide*

April 24, 2002

*To Larisa,*

*the other half of my soul.*

# Contents

# Abstract

The development in recent years of improvement schemes for the action and topological charge in the context of lattice gauge theory has proven to be an extremely fruitful area of research. These schemes have enabled numerical simulations of Quantum Chromodynamics to accurately approximate continuum behaviour for substantially less computational cost than would be required with unimproved operators. Following the work of LePage [1] [2], and de Forcrand, Perez, and Stamatescu [3] we deduce the form for action and topological charge operators which eliminate $\mathcal{O}(a^2)$ and $\mathcal{O}(a^4)$ discretization errors. The improved action is incorporated into an algorithm to cool a range of gauge field configurations, in order to access the classical behaviour of the fields. We find that we can generate self-dual configurations containing different numbers of instantons, which remain stable after thousands of cooling sweeps. A novel method of improving both operators is introduced which enables us to reconstruct the action as a double-checking mechanism against the more traditionally improved action. Analysis of single-instanton configurations with highly improved operators is used to investigate evidence of the instability of such configurations implied by the Nahm transform [4] on the lattice to extremely high numerical accuracy.

# Declaration of Originality

This work contains no material which has been accepted for the award of any other degree or diploma in any university or other tertiary institution and, to the best of my knowledge and belief, contains no material previously published or written by another person, except where due reference has been made in the text.

I give consent to this copy of my thesis, when deposited in the University Library, being available for loan and photocopying.

5th May 2002

Sundance Osland Bilson-Thompson — Date

# Acknowledgements

I wish to thank my parents Lianne and Gary for always allowing and encouraging me to pursue whatever academic or career path I desired. I would especially like to thank my father for encouraging my confidence with mathematics by showing me, when I was in primary school, how easy it is to multiply and divide by tens. Who would have thought that moving a decimal point would lead to a PhD thesis? Thanks Dad.

I also wish to thank my supervisors, Assoc. Prof. Tony Williams especially for accepting me as a newly-minted honours student, and arranging financial support throughout my candidacy, and Dr. Derek Leinweber for always taking the time to discuss the validity of our ideas, swatting bugs in my Fortran code, and generally being a friendly approachable guy.

I would furthermore like to thank my honours supervisor, Dr. Jim McCarthy, for his enthusiasm, support, guidance and friendship, and Marc Ortleib, for being the best high-school science teacher I ever had, and for introducing me to The Goons, the music of Tom Lehrer, the board game *Diplomacy*, and generously loaning me novels from his personal science fiction library.

No mention of my high-school career would be complete without thanking Matthew Davey, Brad Morton and Andrew Carman for their friendship and insanity. What a team we made! When we were good we were really, really weird, and when we were bad we were the best! And I can still whip all your asses at downball!

Credit also to Myles "Moles" Abbott and Kevin "Zaph" Burfitt. Now that my PhD project is complete I can get to work on developing the next generation of Folding Watch! Thanks guys for your friendship and humour.

Frédéric Bonnet and James Zanotti deserve credit for generating gauge field configurations and writing the original cooling code which I modified, and for calculating lattice spacings respectively. Furthermore Derek Leinweber deserves additional credit for his work on the development of the cooling code, and many of the researchers at the Centre for the Subatomic Structure of Matter have contributed ideas, code, or comments which have ultimately contributed to the software developed by myself and others. In particular I wish to thank Dr. Alex Kalloniatis for helping me understand the continuum dynamics of instantons, and their relevance to hadronic physics. All the friends I made at The University of Adelaide, but especially (in no particular order) Garth Kidd, Crispin Harris, Sam Yates, Richard Harris, Gareth Hodges, Anna Willowhite, Brandon Pincombe, Brendan Watts, Wendy Leadbeater, and Hugh Higgins deserve a mention for sharing interesting or ludicrous conversations, juggling with me, teaching me to play *Go*, giving me back-rubs, and just generally making my undergraduate years more fun than they otherwise would have been. Likewise Patrick Bowman and Stewart Wright deserve thanks for adding a necessary dose of surreality to my indenture at the Centre for the Subatomic Structure of Matter.

Lastly I would like to thank my partner, Larisa Lindsay, for being a proofreader and sounding-board, and for providing necessary emotional support and affection, especially when it was most needed during the task of writing up.

This work was carried out at the Special Research Centre for the Subatomic Structure of Matter and the Department of Physics and Mathematical Physics at the University of Adelaide, using grants of supercomputer time on the CM-5 at the South Australian Centre for Parallel Computing and on the Orion supercomputer at the National Computing Facility for Lattice Gauge Theory.

# Part I

# Introduction

# Chapter 1

# Introduction

*"By space, the universe encompasses me and swallows me up like an atom. By thought I comprehend the world."*

Blaise Pascal

*Pensées*

By far the most successful physical theory humans have ever formulated is Quantum Electrodynamics - QED, which underlies the behaviour of the electromagnetic force. QED describes the dynamics of electrically charged particles in terms of the exchange of gauge bosons (photons), massless uncharged particles with integer spin. QED can be described by the Lagrangian density [5]

$$\begin{aligned} \mathcal{L}_{\text{QED}} &= \mathcal{L}_{\text{Dirac}} + \mathcal{L}_{\text{Maxwell}} + \mathcal{L}_{\text{Int}} \\ &= \bar{\psi}(x)(i\gamma^{\mu}\partial_{\mu} - M)\psi(x) - \frac{1}{4}F_{\mu\nu}F^{\mu\nu} - e\bar{\psi}(x)\gamma^{\mu}\psi(x)A_{\mu} \end{aligned} \tag{1.1}$$

where the first term describes fermions, the second term describes the dynamics of boson fields, and the third term describes the interaction of fermions with bosons. The $\bar{\psi}$ and $\psi(x)$ are therefore fermion creation and annihilation operators while

the $A_\mu$ are photon annihilation and creation operators, and $e = -|e|$ is the charge on the electron. From now on we shall refer to the second term in Equation (1.1) as giving rise to the Yang-Mills action, but here we have denoted it $\mathcal{L}_{\text{Maxwell}}$ to make explicit that Maxwell's Equations (with no sources) follow from the action

$$S = -\frac{1}{4}\int d^4x F_{\mu\nu}F^{\mu\nu} \tag{1.2}$$

as the Euler-Lagrange equations of motion.

Equation (1.1) may be simplified by replacing the partial derivative in the Dirac term by the *gauge covariant derivative*

$$D_\mu \equiv \partial_\mu + ieA_\mu. \tag{1.3}$$

The interaction between fermions and bosons is now encapsulated by the covariant derivative and we may write the QED Lagrangian density as

$$\mathcal{L}_{\text{QED}} = \bar{\psi}(x)(i\gamma^\mu D_\mu - M)\psi(x) - \frac{1}{4}F_{\mu\nu}F^{\mu\nu}. \tag{1.4}$$

This Lagrangian density is invariant under local phase rotations (as we shall see in Section 2.2).

Experimental tests of the predictions of QED have confirmed its accuracy to very high orders. The most impressive example is $a_e$, the anomalous magnetic moment of the electron, the calculated value of which agrees to eleven decimal places with the experimentally deduced value $(10^6 a_e = 11.596521869 \pm 0.0000041)$ .

The successes of QED in turn inspired the formulation of an analogous theory, Quantum Chromodynamics - QCD, intended to describe the strong nuclear force (QED has of course been quite successfully unified with the *weak* nuclear force by Glashow, Salam, and Weinberg who received the 1971 Nobel Prize in Physics for their work). However the fundamental differences between the electromagnetic and strong nuclear forces have made the solution of QCD a far more vexing task than the solution of QED. Whereas there is only one kind of electric charge, and

particles may carry this charge or its opposite (denoted as positive and negative charge respectively) there are three kinds of strong charge (often denoted by the primary colours red, green, and blue) and particles may be charged red, anti-red, green, anti-green, blue, or anti-blue. Furthermore the gauge bosons that carry the strong nuclear force (gluons) themselves carry colour charge. The dynamics of gluons is consequently far more complex than that of photons, as gluons may interact directly with each other, which has profound consequences for any attempts to solve QCD. These differences are reflected in the mathematical representations of the gauge fields. In QED the gauge fields at any point in space are described by complex scalars with unit modulus. These scalars are elements of the Abelian group $U(1)$. By contrast the three colour charges of QCD mean that the fields are represented as $3 \times 3$ hermitian matrices, elements of the non-Abelian group $SU(3)$.

Whereas the electromagnetic force diminishes with the square of distance, and a single charged particle may exist in isolation from its counterparts, QCD displays the property of asymptotic freedom. At short distances as probed by asymptotically large momentum transfer, quarks behave as free particles.

It is well established that quarks are always confined within colour-neutral groupings to form heavier particles (either red plus green plus blue in the case of baryons, anti-red plus anti-green plus anti-blue in the case of anti-baryons, or a colour and the corresponding anti-colour in the case of mesons), but never observed as single isolated particles the way electrons are. As the separation between quarks within a hadron is increased the force between them saturates to a constant value, a very different effect to what is seen with the inverse-square law from electromagnetism. It was the attempt to understand the confinement of quarks which led Wilson (1974) to formulate QCD as a lattice gauge theory [6]. Lattice gauge theory derives its name from the fact that we replace the continuum of space-time by a hyper-cubic lattice of discrete points. Such theories are of

interest because they represent a straightforward non-perturbative approach to studying QCD. One of their more appealing properties is that the lattice serves as an automatic momentum cutoff, regulating the divergent quantities corresponding with self-interaction terms that trouble gauge field theory in the continuum. This property arises because the shortest wavelength which can be modelled on a lattice of spacing $a$ is $\lambda = 2a$. It follows automatically that the maximum momentum permitted on the lattice is $k_{\max} = 2\pi/\lambda = \pi/a$. However this behaviour hints at a darker side to the lattice approximation, as errors of the order of the lattice spacing or the lattice spacing squared are introduced into the calculation of gauge-invariant quantities, leading to discrepancies between quantities calculated on the lattice and their continuum counterparts. In this investigation we shall be concerned with the effect of these discretization errors on the topology of gauge fields, within the framework of the quenched approximation. It is clear that such errors may be reduced by approaching the continuum limit $a \to 0$ and continuum quantities in lattice field theory are ultimately arrived at by *extrapolating* to this limit. However calculations on an arbitrarily fine lattice are not practicable as the computational cost of lattice calculations rises rapidly as we approach the continuum limit. An estimate of this cost has been provided by LePage as

$$\text{cost} \propto \left(\frac{L}{a}\right)^4 \left(\frac{1}{a^2}\right)^{\alpha} \left(\frac{1}{m_\pi^2 a}\right)^{\beta} \tag{1.5}$$

with $L$ the length of the lattice in each dimension, and $\alpha$, $\beta$ in the range 0-1 [7]. In this study we will be looking only at gluon actions, and so we neglect the $m_\pi$ term, but it is still clear that computing power will limit the usefulness of reducing the lattice spacing and so it will be desirable to eliminate discretization errors algebraically.

In 1975 Belyavin, Polyakov, Schwartz, and Tyupkin [8] discovered finite-action self-dual solutions, with non-trivial topology, to the equations of classical Yang-Mills theory. In other words, they had found classically stable solutions which

did not simply correspond to the empty, flat vacuum. These solutions are what we call instantons. They are a consequence of the non-Abelian, self interacting nature of the QCD fields and may be represented as gauge fields of the form

$$A_\mu(x) = \frac{i}{g}\left(\frac{x^2}{x^2+\rho^2}\right)(\partial_\mu G)G^{-1} \tag{1.6}$$

for an $SU(2)$ gauge transformation

$$G(x) = \frac{x_4 \pm i\vec{x}.\vec{\tau}}{(x^2)^{1/2}} \tag{1.7}$$

with $x^2 = x_4^2 + \vec{x}^2$ and $\rho$ is a scale parameter referred to as instanton size. The name instantons is suggestive of their particle-like nature. They have distinct spatial locations, are spherically symmetrical with finite size, and carry a topological "charge" which is conserved in interactions between instantons.

Aside from their intrinsic interest as features of the QCD vacuum, instantons are believed to play an important role in determining the nature of hadronic physics, by affecting the propagation and interaction of quarks (instantons are, after all, non-trivial configurations of the gluon fields, and it is the gluons which mediate the strong interaction between quarks). Instantons have an associated topological charge of $+1$, while anti-instantons have a topological charge of $-1$. In the presence of light fermions the instanton configurations give rise to fermionic zero modes, as demonstrated by the Atiyah-Singer index theorem [9], which states that for the Dirac operator $D = \gamma_\mu(D_\mu + iA_\mu)$ the topological charge of the background gauge field is equal to the index of $D$, that is the difference of the number of negative and positive chirality zero-modes. Instantons and anti-instantons act as "potential wells" which allow quarks to hop from one well to the next, covering large distances [10]. By thus promoting the formation of delocalized zero modes, a collective quark condensate which breaks chiral symmetry may be produced. Furthermore the restrictions placed upon the propagation of quarks via instantons are believed to have a defining role in the types and properties of hadrons

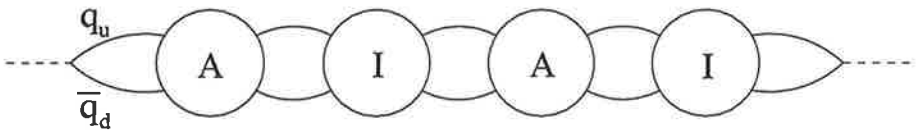


Figure 1.1: The instantons, I, and anti-instantons, A, serve to propagate certain bound quark states such as an up quark and a down anti-quark. Figure after Schaëfer and Shuryak [10].

which may be formed by associated quarks. Since there is only one zero mode per flavour, only quarks of different flavours may travel together, leading for instance to the propagation of a pion formed from an up quark and a down anti-quark, as illustrated in Figure 1.1. Furthermore, quarks flip chirality as they pass through an instanton (or anti-instanton), and hence must pass between instantons and anti-instantons, rather than from one instanton to another, or one anti-instanton to another. Clearly then the density and behaviour of instantons in the QCD vacuum should have a strong bearing on the structure and properties of mesons and nucleons. A more detailed description of the role of instantons in QCD can be found in [10], while other potentially interesting roles for instantons may occur in baryon-number-violating reactions that may be observable in the region where semi-classical calculations are reliable [11], and in direct contributions to deep inelastic scattering [12] [13] [14].

Since instantons are non-trivial classical solutions (minima of the action) of the field equations their dynamics may be investigated by recursively modifying the fields to minimise the action at each lattice site. This procedure is known as cooling, and is based upon a simple prescription for the minimisation of the action. Within the quenched approximation one simply maximises the real part of the trace of Wilson loop terms (as will be discussed in Chapter 6). If one were to consider unquenched QCD, cooling would become substantially more difficult, as

the minimization of the determinant of the fermion matrix is a highly non-trivial problem.

Unfortunately the larger the discretization errors present, the less well cooling works. Since errors in the calculation of the action mean that the cooling process is not perfectly matched to the true structure of the fields, there is a tendency to smooth out their topological structure, eventually rendering it trivial and reducing the total action of the field to zero. Discretization errors may be reduced by simply decreasing the lattice spacing (approaching the continuum limit $a \to 0$). However this approach rapidly increases the computational cost (for a fixed lattice volume) of performing the necessary calculations. Over the last decade or so, scale-independent schemes for eliminating discretization errors have been devised, most notably Symanzik improvement [15] which has been applied by many researchers to eliminate $\mathcal{O}(a^2)$ errors arising in the calculation of the action (a further source of errors is the non-classical self-couplings of the gluon fields. These errors are reduced by the process of tadpole improvement [1]). Cooling with these actions is characterised by a substantial improvement in the stability of instantons. Rather than falling to zero the action tends to plateau for an extended period. However studies of locally self-dual configurations require stability for thousands, not merely hundreds, of cooling sweeps. To achieve the kind of precision required over so many iterations of the cooling algorithm requires improvement beyond the $\mathcal{O}(a^2)$ level.

More recently de Forcrand *et al.* [3] deduced the form for action and topological charge operators which eliminate $\mathcal{O}(a^2)$ and $\mathcal{O}(a^4)$ errors. These highly improved operators are based upon the strategic combination of five distinct planar Wilson loop terms, but also incorporate a free variable which can be tuned to control or eliminate the effect of each loop upon the behaviour of the total resultant operator. By tuning this variable it is possible to create 3-loop, 4-loop and 5-loop operators which all eliminate the errors up to $\mathcal{O}(a^4)$. The question then automat-

ically arises as to whether these highly improved operators are equivalent, since they require different amounts of computational effort, and it would be advantageous to obtain the best results for the least computational cost.
By studying the long-term stability of instantons, de Forcrand *et al.* concluded that the 5-loop operator produces the best results. Following on from this group's work, we are concerned with investigating several properties of instantons on the lattice, each of which is related to the question of which operators have the smallest discretization errors. Since we assume that the closest reproduction of the expected continuum behaviour is characteristic of the smallest errors, this question may be addressed in the following ways;

- All continuum instantons are expected to have an associated action of $S_0 = 8\pi^2/g^2$. Therefore the total action of the field divided by $S_0$ will be equal to the number of instantons present. When we calculate $S/S_0$ then for the whole lattice, we should get an integer value (in the dilute instanton gas approximation). Likewise since each instanton (or anti-instanton) should have an associated topological charge of $+1$ (or $-1$) the total topological charge of the field will be equal to the number of instantons minus the number of anti-instantons. In both cases the closer the value calculated on the lattice is to an integer, the smaller the discretization errors must be.

- Recursive local minimization of the action should ideally approach a value consistent with the structure of the gauge fields on the lattice, that is to say that as instantons come to dominate the configuration, the total action measured on the lattice will arise primarily (and eventually, exclusively) from the associated $S_0 = 8\pi^2/g^2$ action of each instanton or anti-instanton present. However, as noted above, unimproved cooling eventually erases all information from any field configuration, reducing its action to zero. Successfully improved cooling is characterised by a plateauing of the action.

However the question of how many cooling sweeps these plateaux persist for remains an open one. It seems reasonable to use the long-term stability of cooled instantons as a criteria for assessing the validity of various cooling schemes.

- Likewise we expect that instantons should be spherically symmetrical and retain a nearly constant radius as they are cooled, although it must be noted that the action $S_0$ is independent of instanton size. If the instantons shrink or smear out this may be attributed to discretization errors.

- As cooling proceeds the instantons and anti-instantons should eventually annihilate, their topological windings neutralizing each other in the process. Ultimately there will be only instantons or anti-instantons remaining, and the field configuration will be self-dual. At this stage the total action and topological charge over the lattice will be characterised by the relation $S/S_0 = |Q|$. The long-term stability of this self-duality is another important sign of a successfully improved cooling scheme.

This thesis is set out as follows; In Chapter 2 we give an overview of the formulation of lattice gauge theory with the motivation and definition of important concepts, initially for the case of an Abelian field theory, then carrying these over to the non-Abelian case. In Chapter 3 we look at improvement of the action. Chapter 4 deals with the topology of gauge fields and with instanton dynamics. The details of calculating the topological charge are given in Chapter 5 and a novel method of improving both the action and topological charge operators is introduced. In Chapter 6 we present our results by firstly demonstrating that self-dual gluon configurations can reliably be produced by cooling Monte-Carlo-generated gauge fields. To the best of our knowledge this is the first time that self-duality achieved in this manner has been explicitly demonstrated to such high numerical accuracy on the lattice (as high as one part in $10^4$). The stability

criteria discussed above are used to determine which cooling scheme suffers from the smallest discretization errors.

Once we have determined which operators most accurately reproduce the expected continuum behaviour we examine a range of single-instanton configurations to determine if any consequences of the Nahm Transform [16] are manifest in our numerical simulations. The Nahm Transform is a duality transformation which maps a configuration of $Q$ instantons on the 4-torus in $SU(N)$ to a configuration of $N$ instantons on the dual 4-torus in $SU(Q)$ (which implies that a completely self-dual single instanton or anti-instanton configuration cannot exist on the 4-torus, since it would be mappable to an $N$-instanton configuration in $U(1)$, and there are known to be no instantons in as simple a field theory as $U(1)$). Our conclusions are presented in Chapter 7.

# Part II

# Formulation

# Chapter 2

# Formulating Lattice Field Theory

*"Plagiarise!*
*Let no-one else's work evade your eyes!*
*Remember why the good Lord made your eyes,*
*so don't shade your eyes,*
*just plagiarise, plagiarise, plagiarise!*
*Only be sure always to call it please, 'Research'."*

Tom Lehrer

*Lobachevski*

## 2.1 Definitions

Let us begin our investigation with a brief overview of the formulation of lattice gauge theory. The seemingly straightforward act of approximating continuous space-time by a hyper-cubic lattice leads to a series of definitions and gives rise to many problems. The alleviation of some of these problems will form the central theme of the first half of this thesis.

We start by considering a finite volume of space-time. Let us subdivide this volume into a series of cubic cells defined by a regular lattice with spacing $a$. The

value of any gauge field in this region of space is represented by a value at the positions corresponding to the lattice vertices or sites.

In general, continuum symmetries like Lorentz invariance and rotational invariance are compromised on the lattice. However if we work in a quantum field theory in the vicinity of a phase transition where all correlation lengths diverge one can expect that the fact that space-time has been made discrete will not matter. QCD is often argued to exhibit a second-order phase transition as $g \to 0$ and perturbative renormalisation group equations tell us that as $g \to 0$, $a \to 0$ and hence we can make contact with continuum results through the use of perturbation theory. In this case we assume that this commonly-accepted view is accurate enough that our results will remain valid as we extrapolate from the lattice to the continuum.

Because of the discrete step size on the lattice, derivatives are replaced by finite differences, like those seen in basic high school calculus. For instance, if we define the forward derivative of some arbitrary function $f(x)$ as

$$\hat{\partial}^f_\mu f(x) = \frac{1}{a}[f(x+\mu) - f(x)], \tag{2.1}$$

and the backward derivative as

$$\hat{\partial}^b_\mu f(x) = \frac{1}{a}[f(x) - f(x-\mu)], \tag{2.2}$$

we can define the total derivative on the lattice as

$$\begin{aligned} \hat{\partial}_\mu f(x) &= \frac{1}{2}[\hat{\partial}^f_\mu + \hat{\partial}^b_\mu] f(x) \\ &= \frac{1}{2a}[f(x+\mu) - f(x-\mu)]. \end{aligned} \tag{2.3}$$

Notice the use of a hat over the derivative symbol to denote that we're on the lattice, not the continuum.

On the lattice, integrals are replaced with discrete sums over the lattice sites,

incorporating a factor of the lattice spacing for each dimension over which the integral is taken. For four-dimensional space-time

$$\int d^4x \longrightarrow a^4 \sum_x . \tag{2.4}$$

## 2.2 Continuum QED

Let us now look at the simple case of finding a gauge-invariant action for QED, an Abelian gauge theory, in the continuum, and then moving to the lattice to find a gauge-invariant action for lattice QED in an analogous way [17].

Firstly consider the fermion action arising from the Dirac equation

$$S_{\mathrm{F}} = \int d^4x \bar{\psi}(x)(i\gamma^\mu \partial_\mu - M)\psi(x) \tag{2.5}$$

which arises from the Lagrangian density discussed in Chapter 1

$$S = \int d^4x \mathcal{L}(\psi, \partial_\mu \psi). \tag{2.6}$$

This action is invariant under global $U(1)$ transformations

$$\psi(x) \longrightarrow G\psi(x) \tag{2.7}$$

$$\bar{\psi}(x) \longrightarrow \bar{\psi}(x)G^{-1} \tag{2.8}$$

where $G = e^{i\Lambda}$ and the condition that $G$ is a $U(1)$ transformation means that $G^\dagger G = I$ and $\Lambda$ is 1-dimensional (a scalar).

Unfortunately $S_{\mathrm{F}}$ is not invariant under local $U(1)$ transformations, $G(x) = e^{i\Lambda(x)}$. This is bad news because local transformations can be regarded as equivalent to passive transformations arising from an $x$-dependent change of basis. But the laws of physics must be independent of the local choice of basis.

The solution to this dilemma is to make $S_{\mathrm{F}}$ invariant under local transformations. We achieve this by making the replacement

$$\partial_\mu \longrightarrow \partial_\mu + igA_\mu(x) = D_\mu \tag{2.9}$$

where $A_\mu(x)$ is referred to as a gauge field. Having introduced a local gauge transformation $G(x)$ we can now say that $\psi, \bar{\psi}$ and $A$ transform as

$$\begin{aligned} \psi(x) &\rightarrow G(x)\psi(x), \\ \bar{\psi}(x) &\rightarrow \bar{\psi}(x)G^{-1}(x), \\ A_\mu(x) &\rightarrow G(x)A_\mu(x)G^{-1}(x) - \frac{i}{g}G(x)\partial_\mu(x)G^{-1}(x) \end{aligned}$$

under this transformation. We can allow $A_\mu(x)$ to propagate by introducing the Yang-Mills action

$$S_{\text{YM}} = -\frac{1}{4}\int d^4x F_{\mu\nu}(x)F^{\mu\nu}(x) \tag{2.10}$$

where

$$F_{\mu\nu}(x) = \partial_\mu A_\nu(x) - \partial_\nu A_\mu(x) \tag{2.11}$$

is the continuum field-strength tensor.

The gauge-independent action is now

$$\begin{aligned} S_{\text{QED}} &= \int d^4x\bar{\psi}(x)(i\gamma^\mu D_\mu - M)\psi(x) - \frac{1}{4}\int d^4x F_{\mu\nu}(x)F^{\mu\nu}(x) \\ &= S_{\text{F}} + S_{\text{YM}} \end{aligned} \tag{2.12}$$

## 2.3 Lattice QED

Lattice QED is formulated in Euclidean space-time. The Hamiltonian is independent of whether we work in Minkowski space-time or Euclidean space-time and so continuum QED may be transferred to the lattice by simply replacing the time parameter $t$,

$$t \longrightarrow -it. \tag{2.13}$$

In Euclidean space we employ the $\gamma$-matrices, $\gamma_\mu$, $(\mu = 1, 2, 3, 4)$, which obey the algebra $\{\gamma_\mu, \gamma_\mu\} = 2\delta_{\mu\nu}$. The action now becomes

$$iS_{\rm QED} \to -S^E_{\rm QED} = i\int d^4x\bar{\psi}(x)(\gamma_\mu D_\mu - M)\psi(x) + \frac{i}{4}\int d^4x F_{\mu\nu}(x)F_{\mu\nu}(x), \tag{2.14}$$

where the $E$ superscript denotes Euclidean space-time. Next we rewrite the action in terms of dimensionless lattice variables

$$\begin{aligned} M^{\rm Phys} &\longrightarrow \frac{1}{a}M \\ A_\mu^{\rm Phys} &\longrightarrow \frac{1}{a}A_\mu \\ \psi_\alpha^{\rm Phys}(x) &\longrightarrow \frac{1}{a^{3/2}}\psi_\alpha(x) \\ \bar{\psi}_\alpha^{\rm Phys}(x) &\longrightarrow \frac{1}{a^{3/2}}\bar{\psi}_\alpha(x) \\ \partial_\mu\psi_\alpha^{\rm Phys}(x) &\longrightarrow \frac{1}{a^{5/2}}\hat{\partial}_\mu\psi_\alpha(x) \end{aligned}$$

where symbols are dimensionless and the $a$ carries the dimension of length. Notice the hat on the right-hand-side to distinguish the lattice derivative (defined in the Introduction) from the continuum derivative.

The lattice Dirac action becomes

$$S_{\rm F} = \sum_x \frac{1}{2}\bar{\psi}(x)\gamma_\mu(\psi(x+\mu) - \psi(x-\mu)) - g\sum_x \gamma_\mu A_\mu\bar{\psi}(x)\psi(x) - \sum_x M\bar{\psi}(x)\psi(x). \tag{2.15}$$

We wish this action to be invariant under local transformations as before, however we find that terms of the form $\bar{\psi}(x)\psi(y)$ transform as

$$\bar{\psi}(x)\psi(y) \longrightarrow \bar{\psi}(x)G^{-1}(x)G(y)\psi(y). \tag{2.16}$$

What we need is a term which we can introduce, which transforms in exactly the opposite way, to cancel out this gauge variance. Fortunately, such a term exists. It is the Schwinger line integral

$$U(x,y) = e^{ig\int_x^y dz_\mu A_\mu(z)} \tag{2.17}$$

which transforms as $U(x,y) \longrightarrow G(x)U(x,y)G^{-1}(y)$. So we find that

$$\bar{\psi}(x)U(x,y)\psi(y),$$
$$\bar{\psi}(y)U^{\dagger}(x,y)\psi(x),$$

are invariant under local gauge transformations, where

$$U^{\dagger}(x,y) \;=\; U(y,x)$$

since

$$\bar{\psi}(x)U(x,y)\psi(y) \;\rightarrow\; \bar{\psi}(x)G^{-1}(x)\left(G(x)U(x,y)G^{-1}(y)\right)G(y)\psi(y)$$

and clearly the analogous result is true for $U^{\dagger}(x,y)$. With regard to notation, as noted in the Introduction the lattice axes shall be denoted by Greek letters $\mu, \nu...$ while Roman letters shall be used for points in space-time corresponding to the lattice sites. The unit vector in the $\mu$ direction is $\hat{\mu}$, and since the lattice spacing is denoted by $a$, $\mu = a\hat{\mu}$ is a vector with length one lattice spacing, pointing in the $\mu$ direction. Therefore $x$ represents a vertex of the lattice, while $x+\mu$ would represent a lattice site adjacent to $x$ in the positive $\mu$ direction. With this in mind from now on we shall write $U_{\mu}(x)$ in place of $U(x,x+\mu)$. Hence $U_{\mu}(x)$ is the *parallel transport* operator that takes us from the site $x$ on the lattice, one step in the positive $\mu$ direction, and its conjugate takes us one step in the negative $\mu$ direction to arrive at the point $x$ (Figure 2.1).

The gauge-invariant lattice action now becomes

$$S_F = \sum_x \left\{ \frac{1}{2}\bar{\psi}(x)\gamma_{\mu}U_{\mu}(x)\psi(x+\mu) - \frac{1}{2}\bar{\psi}(x+\mu)\gamma_{\mu}U_{\mu}^{\dagger}(x)\psi(x) - M\bar{\psi}(x)\psi(x) \right\} \tag{2.18}$$

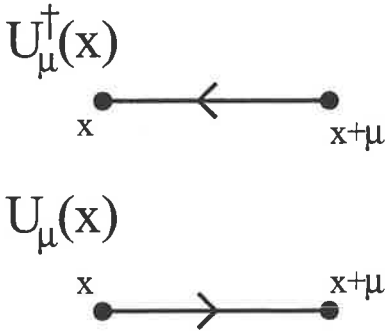


Figure 2.1: The link operator takes us one step forward along a lattice axis from the point $x$, while its conjugate takes us one step backwards to $x$.

(we shall deal with the $F_{\mu\nu}F^{\mu\nu}$ gauge action term below).
Note that with the appropriate substitutions, namely

$$\begin{aligned} U_\mu(x) &= \exp\left\{ig\int_0^a dz A_\mu(x+z\hat{\mu})\right\} \\ &= \exp\left\{ig\int_0^a dz\left(A_\mu(x)+z\partial_\mu A_\mu(x)+\mathcal{O}(z^2)\right)\right\} \\ &= \exp\left\{igaA_\mu(x)+\mathcal{O}(a^2)\right\} \\ &= 1+igaA_\mu(x)+\mathcal{O}(a^2), \end{aligned} \tag{2.19}$$

we readily see that this action goes to the continuum action as $a \to 0$.
In order to complete our construction of the lattice action for QED we wish to find a lattice version of the Yang-Mills action. We want it to be gauge invariant, which means it must be made of closed loops, and we want it to be as local as possible to facilitate computer simulations on the lattice, so it should be made of the smallest loops possible. The obvious candidate then is an elementary plaquette. The operator that takes us around a closed path is called the Wilson loop operator, and is the path-ordered product of the link operators along the path. Remember that path-ordering means we keep the products arranged in the order that we move around the path (in this Abelian case the path-ordering

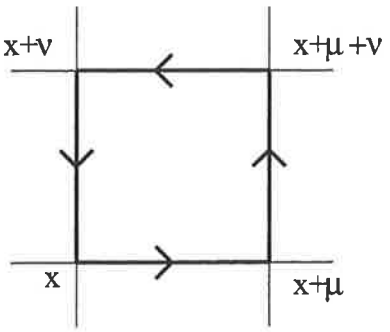


Figure 2.2: The elementary plaquette formed from the product of four link operators.

is irrelevant, but in the non-Abelian case we will look at later it will be very important). The $1 \times 1$ Wilson loop (plaquette) operator at the point $x$ is usually given by

$$W_{\mu\nu}^{(1\times1)}(x) = U_\mu(x)U_\nu(x+\mu)U_\mu^\dagger(x+\nu)U_\nu^\dagger(x), \tag{2.20}$$

as shown in Figure 2.2. Unfortunately constructing the action on the basis of this definition of the plaquette (see Section 2.4) leads to an action beset by quite large discretization errors, when compared to the continuum action. A first step to reducing these errors is the following; rather than expanding the Wilson loop operator around one corner, we shall expand it around the centre point $x_0$, and take the values of $A_\mu$ and $A_\nu$ at the midpoints of the links as illustrated in Figure 2.3.

We know that

$$W_{\mu\nu}^{(1\times1)}(x_0) = U_\mu(x_0 - \frac{\nu}{2})U_\nu(x_0 + \frac{\mu}{2})U_\mu^\dagger(x_0 + \frac{\nu}{2})U_\nu^\dagger(x_0 - \frac{\mu}{2}), \tag{2.21}$$

where

$$U_\mu(x_m) = \exp\left[ig\int_{-\frac{a}{2}}^{\frac{a}{2}} A_\mu(x_m + z\hat{\mu})dz\right] \tag{2.22}$$

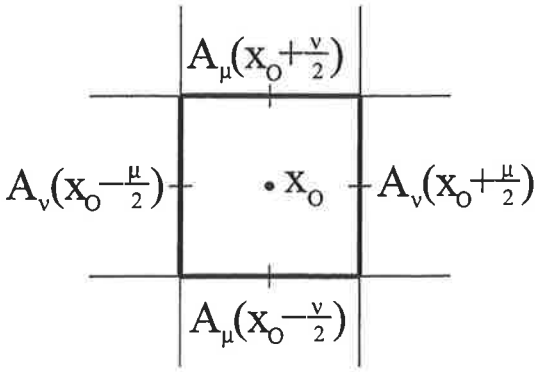


Figure 2.3: How we expand the loop around its centre and evaluate each link at its midpoint. Note that $x_0$ is a half-integer value $x_0 = x + \mu/2 + \nu/2$, and so $A_\mu$ and $A_\nu$ are correctly defined at the midpoints of the links.

and in this case $x_m$ represents the midpoint of each link. Let us now Taylor expand the $A$'s as we did in Equation (2.19). We can explicitly perform this calculation for a link in the $\mu$ direction

$$\begin{aligned} U_\mu(x_m) &= \exp\left\{ig\int_{-\frac{a}{2}}^{\frac{a}{2}} A_\mu(x_m + z\hat{\mu})dz\right\} \\ &= \exp\left\{ig\int_{-\frac{a}{2}}^{\frac{a}{2}} \left(A_\mu(x_m) + z\partial_\mu A_\mu(x_m) + \frac{1}{2}z^2\partial_\mu^2 A_\mu(x_m) + \mathcal{O}(z^3)\right)dz\right\} \\ &= \exp\left\{ig\left(\left[zA_\mu(x_m)\right]_{-\frac{a}{2}}^{\frac{a}{2}} + \left[\frac{1}{6}z^3\partial_\mu^2 A_\mu(x_m)\right]_{-\frac{a}{2}}^{\frac{a}{2}} + \mathcal{O}(z^6)\right)\right\}, \end{aligned} \tag{2.23}$$

where the terms arising from $z\partial_\mu A_\mu(x_m)$ and $\mathcal{O}(z^3)$ terms in the Taylor expansion have been ignored since the symmetric integration limits render their integrals equal to zero.

We therefore conclude that

$$U_\mu(x_m) = \exp\left\{igaA_\mu(x_m) + \mathcal{O}(a^3)\right\}, \tag{2.24}$$

and equivalently

$$U_\nu(x_m) = \exp\left\{igaA_\nu(x_m) + \mathcal{O}(a^3)\right\}. \tag{2.25}$$

It follows that Equation (2.21) can be written in the form

$$\begin{aligned}
W_{\mu\nu}^{(1\times1)}(x_0) &= U_\mu(x_0 - \frac{\nu}{2})U_\nu(x_0 + \frac{\mu}{2})U_\mu^\dagger(x_0 + \frac{\nu}{2})U_\nu^\dagger(x_0 - \frac{\mu}{2}) \\
&= \exp\{igaA_\mu(x_0 - \frac{\nu}{2}) + \mathcal{O}(a^3)\} \\
&\quad \times \exp\{igaA_\mu(x_0 + \frac{\mu}{2}) + \mathcal{O}(a^3)\} \\
&\quad \times \exp\{-igaA_\mu(x_0 + \frac{\nu}{2}) + \mathcal{O}(a^3)\} \\
&\quad \times \exp\{-igaA_\mu(x_0 - \frac{\mu}{2}) + \mathcal{O}(a^3)\} \\
&= \exp\{iga(A_\mu(x_0 - \frac{\nu}{2}) + A_\mu(x_0 + \frac{\mu}{2}) \\
&\quad -A_\mu(x_0 + \frac{\nu}{2}) - A_\mu(x_0 - \frac{\mu}{2}) + \mathcal{O}(a^2))\}.
\end{aligned} \tag{2.26}$$

We can rewrite this product in terms of the loop midpoint $x_0$ by Taylor expanding again,

$$\begin{aligned}
W_{\mu\nu}^{(1\times1)}(x_0) &= \exp\{iga(A_\mu(x_0) - \frac{a}{2}\partial_\nu A_\mu(x_0) \\
&\quad +A_\nu(x_0) + \frac{a}{2}\partial_\mu A_\nu(x_0) \\
&\quad -A_\mu(x_0) - \frac{a}{2}\partial_\nu A_\mu(x_0) \\
&\quad -A_\nu(x_0) + \frac{a}{2}\partial_\mu A_\nu(x_0) \\
&\quad +\mathcal{O}(a^2))\} \\
&= \exp\{iga(a\partial_\mu A_\nu(x_0) - a\partial_\nu A_\mu(x_0) + \mathcal{O}(a^2))\} \\
&= \exp\{iga^2 F_{\mu\nu} + \mathcal{O}(a^3)\}.
\end{aligned} \tag{2.27}$$

We have therefore been able to extract the continuum field strength tensor from the plaquette. We now return to the task of constructing a lattice version of the Yang-Mills action.

## 2.4 The Wilson Action

Wilson (1974) proposed a form for the action for the pure gauge field (Yang-Mills) action on the lattice, based upon the plaquette [6],

$$S_{\text{Wil}}[W_{\mu\nu}^{(1\times1)}] = \beta\sum_x\sum_{\mu<\nu}\left[1-\frac{1}{2N}\left(\text{Tr}\,W_{\mu\nu}^{(1\times1)}+\text{Tr}\,W_{\mu\nu}^{(1\times1)\dagger}\right)\right] \quad (2.28)$$

$$= \beta\sum_x\sum_{\mu<\nu}\left[1-\frac{1}{N}\left(Re\text{Tr}\,W_{\mu\nu}^{(1\times1)}\right)\right] \quad (2.29)$$

for an $SU(N)$ theory, where $Re$ denotes taking the real part of the function, and Tr denotes taking the trace. Note that since the trace of any loop will be complex, taking the real part of the trace is equivalent to taking the average of the trace of the loop and the trace of its conjugate. For if we assume that the elements of $W_{\mu\nu}$ are of the the form $a_{\mu\nu}+ib_{\mu\nu}$ then we see that

$$\begin{aligned}\frac{1}{2}\left(\text{Tr}W_{\mu\nu}+\text{Tr}W_{\mu\nu}^{\dagger}\right) &= \frac{1}{2}(a_{11}+ib_{11}+...+a_{NN}+ib_{NN}\\ &\quad +a_{11}-ib_{11}+...+a_{NN}-ib_{NN})\\ &= (a_{11}+a_{22}+...+a_{NN})\\ &= Re\,(a_{11}+ib_{11}+...+a_{NN}+ib_{NN})\\ &= Re\text{Tr}W_{\mu\nu}.\end{aligned}$$

In this case however, $N=1$ and as a consequence, the trace is trivial. Now we may expand the Wilson loop operator, using the standard Taylor expansion for an exponential function, and find that

$$\begin{aligned}S_{\text{Wil}}[W_{\mu\nu}^{(1\times1)}] &= \beta\textstyle\sum_x\sum_{\mu<\nu} \left[1-\frac{1}{2}\left(1+iga^2\hat{F}_{\mu\nu}-\frac{1}{2}g^2a^4\hat{F}_{\mu\nu}^2\right.\right.\\ &\quad \left.\left.+1-iga^2\hat{F}_{\mu\nu}-\frac{1}{2}g^2a^4\hat{F}_{\mu\nu}^2+\mathcal{O}(a^6)\right)\right]\\ &= \beta\textstyle\sum_x\sum_{\mu<\nu} \left[1-1+\frac{1}{2}g^2a^4\hat{F}_{\mu\nu}^2+\mathcal{O}(a^6)\right]\\ &= \beta\textstyle\sum_x\sum_{\mu,\nu} \frac{1}{4}g^2a^4\hat{F}_{\mu\nu}^2+\mathcal{O}(a^6).\end{aligned}$$

Therefore we have

$$S_{\text{Wil}}[W_{\mu\nu}^{(1\times1)}] \approx \frac{1}{4}\int d^4x F_{\mu\nu}F^{\mu\nu} \text{ (setting } \beta = \frac{1}{g^2}\text{).} \tag{2.30}$$

Notice that when we switch from summing over $\mu$ and $\nu$ given the condition $1 \leq \mu < \nu \leq 4$ to summing over all $\mu, \nu = 1, 2, 3, 4$ we double-up on each $F_{\mu\nu}^2$ in our expression, since $F_{\mu\nu} = -F_{\nu\mu}$. Therefore we have introduced an additional factor of one-half to cancel the effect of this double-counting.

Although we have not dealt with the problem of fermion doubling (see reference [17], Chapter 4), we shall conclude our construction of the lattice action for QED at this point. Our approach has none-the-less motivated the introduction of the link operators and loop operators, and the introduction of the Wilson action. From now on, throughout our discussion of non-Abelian lattice gauge theory we'll concern ourselves exclusively with the pure gauge action.

## 2.5 Non-Abelian Gauge Field Theory on the Lattice

Now we will extend our analysis to non-Abelian field theory, specifically QCD, using the mathematical formalism developed in the Abelian case. The physics in this case is characterised by gauge transformations which are elements of the group $SU(N)$. This means that

$$A_\mu = \sum_{a=1}^{N^2-1} \frac{\lambda^a}{2} A_\mu^a, \tag{2.31}$$

where the $\lambda^a$ are generators of the group $SU(N)$, i.e., these are $N \times N$ hermitian matrices. We similarly find that

$$F_{\mu\nu} = \sum_{a=1}^{N^2-1} \frac{\lambda^a}{2} F_{\mu\nu}^a. \tag{2.32}$$

This ensures that $F_{\mu\nu}$ is an element of the Lie algebra of the group $SU(N)$. We are interested in finding a lattice version of the Euclidean action

$$S = \frac{1}{4}\int d^4x F^a_{\mu\nu}F^a_{\mu\nu}, \tag{2.33}$$

where

$$\mathrm{Tr}(\lambda^a\lambda^b) = 2\delta_{ab} \tag{2.34}$$

and therefore

$$S = \frac{1}{2}\int d^4x \mathrm{Tr}F_{\mu\nu}F_{\mu\nu}. \tag{2.35}$$

Also note that in the non-Abelian case the derivatives in the continuum field strength tensor have been changed from partial derivatives to covariant derivatives,

$$\begin{aligned} F_{\mu\nu}(x) &= D_\mu A_\nu(x) - D_\nu A_\mu(x) && (2.36)\\ &= \partial_\mu A_\nu(x) - \partial_\nu A_\mu(x) + ig[A_\mu(x), A_\nu(x)] && (2.37)\\ &= [D_\mu, D_\nu]. && (2.38) \end{aligned}$$

Because things are now non-Abelian path ordering is important. Since $A_\mu$ and $A_\nu$ are now non-commutative we use the Baker-Cambell-Haussdorf rule to find the form of the loop operator as a single exponential,

$$e^A e^B = \exp\left\{A + B + \frac{1}{2}[A,B] + ...\right\}, \tag{2.39}$$

where the dots (...) denote higher order commutators of the form $[A,[B,C]]$. In the case of the $1 \times 1$ Wilson loop there are four link operators and so the BCH rule implies a more complicated form for the expansion of the loop operator

$$\begin{aligned} e^A e^B e^C e^D &= \exp\{A + B + C + D + \\ &\quad \frac{1}{2}([A,B] + [A,C] + [A,D] \\ &\quad + [B,C] + [B,D] + [C,D]) + ...\}, \end{aligned}$$

where again the dots represent commutators of higher order. Now we are in a position to evaluate the Wilson loop for a non-Abelian theory. Analogously to Equation (2.26) we find that

$$\begin{aligned} W_{\mu\nu}^{(1\times1)}(x_0) &= \exp\Big\{iag\Big(A_\mu(x_0-\frac{\nu}{2})+A_\nu(x_0+\frac{\mu}{2}) \\ &\quad -A_\mu(x_0+\frac{\nu}{2})-A_\nu(x_0-\frac{\mu}{2})+\mathcal{O}(a^2)\Big) \\ &\quad +\frac{(iag)^2}{2}[A_\mu(x_0-\frac{\nu}{2}),A_\nu(x_0+\frac{\mu}{2})] \\ &\quad +\frac{(iag)^2}{2}[A_\mu(x_0-\frac{\nu}{2}),-A_\mu(x_0+\frac{\nu}{2})] \\ &\quad +\frac{(iag)^2}{2}[A_\mu(x_0-\frac{\nu}{2}),-A_\nu(x_0-\frac{\mu}{2})] \\ &\quad +\frac{(iag)^2}{2}[A_\nu(x_0+\frac{\mu}{2}),-A_\mu(x_0+\frac{\nu}{2})] \\ &\quad +\frac{(iag)^2}{2}[A_\mu(x_0+\frac{\mu}{2}),-A_\mu(x_0+\frac{\nu}{2})] \\ &\quad +\frac{(iag)^2}{2}[A_\mu(x_0-\frac{\nu}{2}),A_\nu(x_0-\frac{\mu}{2})] \\ &\quad +\mathcal{O}(g^3a^3,g^2a^4)\Big\}, \end{aligned}$$

where the $g^3a^3$ errors correspond with higher order commutators, the $a^2$ errors correspond with higher order terms in the Taylor expansion of the $A$'s outside the commutators and the $g^2a^4$ errors correspond with higher order terms in the Taylor expansion of the $A$'s inside the commutators. Then as before we Taylor expand around $x_0$ and find that

$$\begin{aligned} W_{\mu\nu}^{(1\times1)}(x_0) &= \exp\Big\{iag\Big(A_\mu(x_0)-\frac{1}{2}a\partial_\nu A_\mu(x_0)+A_\nu(x_0)+\frac{1}{2}a\partial_\mu A_\nu(x_0) \\ &\quad -A_\mu(x_0)-\frac{1}{2}a\partial_\nu A_\mu(x_0)-A_\nu(x_0)+\frac{1}{2}a\partial_\mu A_\nu(x_0)+\mathcal{O}(a^2)\Big) \\ &\quad +\frac{(iag)^2}{2}\Big\{[A_\mu(x_0-\frac{\nu}{2}),A_\nu(x_0+\frac{\mu}{2})]+[A_\mu(x_0-\frac{\nu}{2}),-A_\mu(x_0+\frac{\nu}{2})] \\ &\quad +[A_\mu(x_0-\frac{\nu}{2}),-A_\nu(x_0-\frac{\mu}{2})]+[A_\nu(x_0+\frac{\mu}{2}),-A_\mu(x_0+\frac{\nu}{2})] \\ &\quad +[A_\mu(x_0+\frac{\mu}{2}),-A_\mu(x_0+\frac{\nu}{2})] \\ &\quad [A_\mu(x_0-\frac{\nu}{2}),A_\nu(x_0-\frac{\mu}{2})]+\mathcal{O}(a^2)\Big\}+\mathcal{O}(g^3a^3,g^2a^4)\Big\}. \end{aligned}$$

Collecting terms and expanding the commutators we obtain

$$\begin{aligned} W_{\mu\nu}^{(1\times1)}(x_0) &= \exp\Big\{ ia^2g\left(\partial_\mu A_\nu(x_0) - \partial_\nu A_\mu(x_0) + \mathcal{O}(a)\right. \\ &\quad \left. + \frac{ig}{2}\Big( [A_\mu(x_0), A_\nu(x_0)] - [A_\mu(x_0), A_\mu(x_0)] - [A_\mu(x_0), A_\mu(x_0)] \right. \\ &\quad \left. - [A_\nu(x_0), A_\mu(x_0)] - [A_\nu(x_0), A_\nu(x_0)] + [A_\mu(x_0), A_\nu(x_0)] + \mathcal{O}(a)\Big)\Big\} \\ &= \exp\Big\{ia^2g\Big(\partial_\mu A_\nu(x_0) - \partial_\nu A_\mu(x_0) + ig[A_\mu(x_0), A_\nu(x_0)] + \mathcal{O}(a)\Big)\Big\} \\ &= \exp\left\{ia^2gF_{\mu\nu}(x_0) + \mathcal{O}(ga^3)\right\} \\ &\to \exp\left\{ia^2gF_{\mu\nu}(x_0)\right\} \text{ as } a \to 0 \end{aligned} \tag{2.40}$$

(consistent with the result in the Abelian case) and in this limit $F_{\mu\nu}$ is the non-Abelian continuum field strength tensor.[1]

Clearly, trying to find the higher order terms for a non-Abelian field theory would be prohibitatively difficult. Taking the Taylor expansions of the $A$'s out to higher orders will rapidly increase the number of terms and the number of commutators. Similarly, trying to calculate the form of the Wilson loop for paths with more than four links will rapidly introduce a daunting profusion of terms. We need a better way.

Fortunately, there is one. As was done by LePage [1] we firstly define the closed-loop Product Operator $P_{\mu\nu}^{(m\times n)}(x_0)$ in line with the form of the Wilson action for an $SU(N)$ theory

$$P_{\mu\nu}^{(m\times n)}(x_0) = \frac{1}{N} Re\mathrm{Tr}\mathcal{P}W_{\mu\nu}^{(m\times n)}(x_0), \tag{2.41}$$

(where the $\mathcal{P}$ on the right-hand side denotes path-ordering) so that

$$S_{\mathrm{Wil}} = \beta \sum_x \sum_{\mu<\nu} \left[1 - P_{\mu\nu}^{(1\times1)}\right]. \tag{2.42}$$

[1] As a side point on notation, it is worth mentioning that in some of the literature on this topic the relation $W_{\mu\nu} \equiv \exp\{ia^2gG_{\mu\nu}\}$ where $G_{\mu\nu} = F_{\mu\nu} + \mathcal{O}(a)$ is used.

For the time being we shall only concern ourselves with the plaquette, for the sake of simplicity. The Product Operator is an exponential function, which we can write as a function of an integral around a closed path,

$$P_{\mu\nu}^{(1\times1)} = \frac{1}{N}\mathcal{P}Re\mathrm{Tr}\left\{e^{ig\oint A.dx}\right\}, \tag{2.43}$$

and the expansion of this exponential will be a polynomial in powers of $a$, the lattice spacing (actually, powers of $a^2$, as we can see by inspecting Equation (2.40)). We know that $P_{\mu\nu}^{(1\times1)}$ is invariant under axis interchange ($\mu \leftrightarrow \nu$), since it is proportional to the action, which must be invariant under a change of basis, so the terms at each order in $a$ must also have this property. Since we know that $F_{\mu\nu} = -F_{\nu\mu}$ we may conclude that the lowest order term must contain $F_{\mu\nu}^2$, and all higher order terms must contain even powers of $F_{\mu\nu}$. We also know that the terms at each order must be dimensionless so that the action remains dimensionless. Since $F_{\mu\nu}$ has dimensions of inverse-length-squared, we can conclude that the lowest order term (the $F_{\mu\nu}^2$ term) will be the $a^4$ term (note also that each factor of $F_{\mu\nu}$ carries a factor of $g$ with it). The other factors we expect to find in this expansion are covariant derivatives (because we require local gauge invariance), which have dimensions of inverse-length. Applying the requirements for symmetry and dimensional consistency we deduce that the expansion will be

$$\begin{aligned} P_{\mu\nu}^{m\times n} \;=\; & 1 - g^2\Big(b_1 a^4 \mathrm{Tr}\{F_{\mu\nu}^2(x_0)\} + a^6\mathrm{Tr}\{F_{\mu\nu}(b_2 D_\mu^2 + b_3 D_\nu^2)F_{\mu\nu}\} \\ & + a^6\mathrm{Tr}\{F_{\mu\nu}(b_4 D_\mu D_\nu + b_5 D_\nu D_\mu)F_{\mu\nu}\} + \mathcal{O}(a^8)\Big) \\ & + \mathcal{O}(g^4 a^4) \end{aligned} \tag{2.44}$$

where $b_1, ..., b_5$ are scalar constants, and the $\mathcal{O}(g^4a^4)$ errors are perturbative corrections which can be removed in the act of cooling, as discussed in Section 6.2. Assuming $b_2, b_3, ...$ are non-zero, the non-leading order terms in the expansion will introduce tree-level errors which we shall wish to remove in order to make our definition of the lattice action more accurate. We can find the values of these

constants by the use of a clever trick [1]. Rewriting the line integral $\oint Adx$ in Equation (2.43) as $\oint(A_\mu dx_\mu + A_\nu dx_\nu)$ we see that we can apply the 2-dimensional version of Stoke's theorem (that is, Green's theorem)

$$\oint_c (Jdx + Kdy) = \int\int_R \left(\frac{\partial K}{\partial x} - \frac{\partial J}{\partial y}\right) dxdy. \tag{2.45}$$

Therefore we see that we can readily rewrite our integral around the loop as

$$\oint Adx = \int\int_{-a/2}^{a/2} dx_\mu dx_\nu \left(\partial_\mu A_\nu(x_0 + x) - \partial_\nu A_\mu(x_0 + x)\right). \tag{2.46}$$

Note that we have lost the concept of path-ordering in the transition from a line integral to a double-integral over an area. We will find however, that the differences between Abelian and non-Abelian expansions of the Wilson loop correspond to terms of order $g$. These are removed rapidly by the process of cooling. As a consequence we achieve improvement of both the action and topological charge through the use of an Abelian analysis. A more detailed discussion of this matter will be withheld until the process of cooling is fully described in Section 6.2.
Now we expand the $A$'s around the point $x_0$. If we choose to work in coordinate gauge $A.x = 0$ the derivative terms arising from the Taylor expansion can be seen to be equivalent to covariant derivatives $x_\mu \partial_\mu = x_\mu D_\mu$. Hence we find

$$\begin{aligned}\oint Adx \;=\; & \int\int_{-a/2}^{a/2} dx_\mu dx_\nu \Big(D_\mu A_\nu(x_0) + x_\alpha D_\alpha D_\mu A_\nu(x_0) \\ & + \frac{1}{2} x_\alpha x_\beta D_\alpha D_\beta D_\mu A_\nu(x_0) - D_\nu A_\mu(x_0) - x_\rho D_\rho D_\nu A_\mu(x_0) \\ & - \frac{1}{2} x_\rho x_\sigma D_\rho D_\sigma D_\nu A_\mu(x_0) + \mathcal{O}(x^3)\Big).\end{aligned}$$

Next we sum over the repeated indices, and since our plaquette is a 2-D object we are simply summing over the $\mu$ and $\nu$ directions, thus we find

$$\begin{aligned}\oint A.dx \;=\; & \int\int_{-a/2}^{a/2} dx_\mu dx_\nu \Big( \{D_\mu A_\nu(x_0) - D_\nu A_\mu(x_0)\} \\ & + \{x_\mu D_\mu + x_\nu D_\nu\} \{D_\mu A_\nu(x_0) - D_\nu A_\mu(x_0)\}\end{aligned}$$

$$
\begin{aligned}
&+\{x_\mu x_\nu D_\mu D_\nu\}\{D_\mu A_\nu(x_0) - D_\nu A_\mu(x_0)\} \\
&+\frac{1}{2}\{x_\mu^2 D_\mu^2 + x_\nu^2 D_\nu^2\}\{D_\mu A_\nu(x_0) - D_\nu A_\mu(x_0)\} \\
&+\mathcal{O}(x^3)) \\
= &\int\int_{-a/2}^{a/2} dx_\mu dx_\nu \Big( F_{\mu\nu}(x_0) + \{x_\mu D_\mu + x_\nu D_\nu\} F_{\mu\nu}(x_0) \\
&+\{x_\mu x_\nu D_\mu D_\nu\} F_{\mu\nu}(x_0) + \frac{1}{2}\{x_\mu^2 D_\mu^2 + x_\nu^2 D_\nu^2\} F_{\mu\nu}(x_0) \\
&+\mathcal{O}(x^3)\Big). \qquad (2.47)
\end{aligned}
$$

When we take the integral the terms with odd powers of $x$ vanish, because of the symmetric integration limits. This means that by choosing to expand the plaquette around its centre-point we have set $b_4, b_5 = 0$. Therefore we can neglect these terms in the expansion of the double-integral and hence obtain

$$
\begin{aligned}
\oint A.dx &= \int\int_{-a/2}^{a/2} dx_\mu dx_\nu \left( F_{\mu\nu}(x_0) + \frac{1}{2}\{x_\mu^2 D_\mu^2 + x_\nu^2 D_\nu^2\} F_{\mu\nu}(x_0) + \mathcal{O}(x^3)\right) \\
&= a^2 F_{\mu\nu}(x_0) + \frac{a^4}{24}\left(D_\mu^2 + D_\nu^2\right) F_{\mu\nu}(x_0) + \mathcal{O}(a^6). \qquad (2.48)
\end{aligned}
$$

We now square this result and insert it into the expansion of the plaquette operator

$$
\begin{aligned}
P_{\mu\nu}^{(1\times1)}(x_0) &= \frac{1}{3}\mathcal{P}Re\mathrm{Tr}\left\{e^{ig\oint Adx}\right\} \\
&= \frac{1}{3}\mathcal{P}Re\mathrm{Tr}\left\{\mathbb{1} + ig\oint Adx - \frac{g^2}{2}(\oint Adx)^2 + \mathcal{O}(g^3)\right\} \\
&= \frac{1}{3}\mathcal{P}\mathrm{Tr}\left\{\mathbb{1} - \frac{g^2}{2}(\oint Adx)^2 + \mathcal{O}(g^4)\right\}, \qquad (2.49)
\end{aligned}
$$

where the leading term in the expansion is the $3\times3$ identity matrix, since we are dealing not with the exponential of a scalar quantity, but with matrices. Note that the covariant derivatives in the following and subsequent equations only act

upon the $F_{\mu\nu}$'s inside the square brackets with them. This then gives

$$\begin{aligned}\left(\oint A.dx\right)^2 &= \left(a^2F_{\mu\nu}(x_0)+\frac{a^4}{24}\left[\left(D_\mu^2+D_\nu^2\right)F_{\mu\nu}(x_0)\right]+\mathcal{O}(a^6,A^2)\right)^2 \\ &= a^4F_{\mu\nu}^2(x_0)+\frac{a^6}{24}F_{\mu\nu}(x_0)\left[\left(D_\mu^2+D_\nu^2\right)F_{\mu\nu}(x_0)\right] \\ &\quad +\frac{a^6}{24}\left[\left(D_\mu^2+D_\nu^2\right)F_{\mu\nu}(x_0)\right]F_{\mu\nu}(x_0)+\mathcal{O}(a^8). \qquad (2.50)\end{aligned}$$

Therefore we find

$$\begin{aligned}P_{\mu\nu}^{(1\times1)}(x_0) &= \frac{1}{3}\mathcal{P}\mathrm{Tr}\left\{\mathbb{1}-\frac{g^2}{2}(\oint A.dx)^2+\mathcal{O}(g^4)\right\} \\ &= \frac{1}{3}\mathrm{Tr}\left\{\mathbb{1}-\frac{g^2}{2}a^4F_{\mu\nu}^2(x_0)-\frac{a^6g^2}{48}F_{\mu\nu}(x_0)\left[\left(D_\mu^2+D_\nu^2\right)F_{\mu\nu}(x_0)\right]\right. \\ &\quad \left.-\frac{a^6g^2}{48}\left[\left(D_\mu^2+D_\nu^2\right)F_{\mu\nu}(x_0)\right]F_{\mu\nu}(x_0)+\mathcal{O}(a^8,g^4)\right\} \qquad (2.51) \\ &= 1-\frac{a^4g^2}{6}\mathrm{Tr}F_{\mu\nu}^2(x_0)-\frac{a^6g^2}{72}\mathrm{Tr}F_{\mu\nu}(x_0)\left(D_\mu^2+D_\nu^2\right)F_{\mu\nu}(x_0) \\ &\quad +\mathcal{O}(a^8,g^4), \qquad (2.52)\end{aligned}$$

where we have reordered the factors in the two $\mathcal{O}(a^6)$ terms between Equations (2.51) and (2.52) to make them equal using $\mathrm{Tr}(AB)=\mathrm{Tr}(BA)$. We have therefore determined that $b_1=1/6$ and $b_2,b_3=1/72$.

This is an extremely powerful approach because it avoids explicitly dealing with commutators, and because the steps are identical for any plaquette up to the point where the double integrals are taken. This means that once the expansion in Equation (2.47) has been found, to the desired order, it is possible to evaluate the expression for a larger square, say $P_{\mu\nu}^{(2\times2)}(x_0)$, or for a $2\times1$ rectangle, or any other Wilson loop simply by changing the integration limits!

We then have, for example,

$$\begin{aligned}P_{\mu\nu}^{(1\times2)}(x_0) &= \int_{-a/2}^{a/2}dx_\mu\int_{-a}^{a}dx_\nu\left(D_\mu A_\nu(x_0+x)-D_\nu A_\mu(x_0+x)\right) \\ P_{\mu\nu}^{(3\times1)}(x_0) &= \int_{-3a/2}^{3a/2}dx_\mu\int_{-a/2}^{a/2}dx_\nu\left(D_\mu A_\nu(x_0+x)-D_\nu A_\mu(x_0+x)\right).\end{aligned}$$

In order to find the expansions for various loop sizes more easily, a package was developed for use with the algebraic manipulation software *Mathematica*. This package takes the integration limits and the order to which the expansion should be found as arguments, and returns an answer corresponding to the step shown in Equation (2.48). The code for this package is included in Appendix A.
Note that by inserting the expression for $P_{\mu\nu}^{(1\times1)}(x_0)$ into the term for the Wilson action and setting $\beta = 2N/g^2 = 6/g^2$ we obtain the Yang-Mills action, accurate to $\mathcal{O}(a^2)$,

$$\begin{aligned}
S_{\text{Wil}} &= \beta \sum_x \sum_{\mu<\nu} \left[1 - P_{\mu\nu}^{(1\times1)}(x_0)\right] \\
&= \beta \sum_x \sum_{\mu<\nu} \left[1 - 1 + \frac{a^4 g^2}{6} \text{Tr} F_{\mu\nu}^2(x_0) \right. \\
&\qquad \left. + \frac{a^6 g^2}{72} \text{Tr} F_{\mu\nu}(x_0) \left(D_\mu^2 + D_\nu^2\right) F_{\mu\nu}(x_0) + \mathcal{O}(a^8, g^4)\right] \\
&= \beta \sum_x \sum_{\mu<\nu} \left[\frac{a^4 g^2}{6} \text{Tr} F_{\mu\nu}^2(x_0) + \mathcal{O}(a^6, g^4)\right] \\
&= a^4 \sum_x \sum_{\mu<\nu} \left[\text{Tr} F_{\mu\nu}^2(x_0) + \mathcal{O}(a^2, g^4)\right] \ (\text{setting } \beta = \frac{6}{g^2}) \\
&= a^4 \sum_x \sum_{\mu,\nu} \left[\frac{1}{2} \text{Tr} F_{\mu\nu}^2(x_0) + \mathcal{O}(a^2, g^4)\right].
\end{aligned}$$

Therefore we have

$$S_{\text{Wil}} = \int d^4x \frac{1}{2} \text{Tr} F_{\mu\nu}^2(x_0) + \mathcal{O}(a^2, g^4). \tag{2.53}$$

## 2.6 Summary

In this Chapter we have shown that a gauge theory may be transferred to a space-time lattice. When we do so we find that the links between lattice sites contain the information about the gauge fields. By multiplying these link operators to form gauge-invariant closed loops we obtain a formula for the action which

approximates the continuum Yang-Mills action, but also contains error terms of order $\mathcal{O}(a^2)$ and higher. In the next Chapter we shall turn to the problem of eliminating some of these errors.

# Chapter 3

# Improved Actions

*"Your friend is right Julian, you can't break the laws of physics. But you can bend them!"*

Jack

*Star Trek: Deep Space Nine*

'Chrysalis'

## 3.1 Tree-Level Improvement

Deviations from the continuum action are one of the foremost problems arising with lattice gauge theory, and consequently many approaches to minimising these errors (improvement) have been formulated. A straightforward summary of improved gauge actions is presented in Chapter 12, and of improvements to the Dirac action (which we shall not consider here) in Chapter 13 of [18]. In the following sections we shall consider improvement based primarily upon the approach pioneered by Symanzik [15], and further developed by Lüscher and Weisz [19].

While it is true that we can obtain the Yang-Mills action from the expression for a $1 \times 1$ loop (plaquette), it is also important to note that the $\mathcal{O}(a^4)$ terms for

any other loop differ from those for the plaquette only by a scalar constant, and hence we could equally well use a $1 \times 2$ rectangle or any other loop, and obtain the Yang-Mills action by simply choosing an appropriate value for $\beta$. Apart from being the most local choice of loop there's nothing special about the plaquette. In fact there's no reason why we couldn't obtain the Yang-Mills action using a linear combination of different loop terms. This fact will enable us to classically improve the action, by combining loops to eliminate the lowest order deviations from the continuum action.

So let us consider the terms arising from the $2 \times 1$ and $1 \times 2$ rectangular loops,

$$\begin{aligned} P_{\mu\nu}^{(2\times1)}(x_0) &= 1 - \frac{4a^4g^2}{6}\mathrm{Tr}F_{\mu\nu}^2(x_0) \\ &\quad -\frac{4a^6g^2}{72}\mathrm{Tr}F_{\mu\nu}(x_0)\left(4D_\mu^2 + D_\nu^2\right)F_{\mu\nu}(x_0) + \mathcal{O}(a^8, g^4) \\ P_{\mu\nu}^{(1\times2)}(x_0) &= 1 - \frac{4a^4g^2}{6}\mathrm{Tr}F_{\mu\nu}^2(x_0) \\ &\quad -\frac{4a^6g^2}{72}\mathrm{Tr}F_{\mu\nu}(x_0)\left(D_\mu^2 + 4D_\nu^2\right)F_{\mu\nu}(x_0) + \mathcal{O}(a^8, g^4). \end{aligned} \quad (3.1)$$

The mix of terms is not symmetric as in the plaquette, but we can overcome this by adding the two expansions together. This ensures that the resulting operator is symmetric under axis interchange, as we required in the previous Chapter. Hence we have

$$\begin{aligned} \left((1 - P_{\mu\nu}^{(2\times1)}(x_0)\right) &+ \left((1 - P_{\mu\nu}^{(1\times2)}(x_0)\right) \\ &= \left(2 - P_{\mu\nu}^{(2\times1)}(x_0) - P_{\mu\nu}^{(1\times2)}(x_0)\right) \\ &= \frac{4a^4g^2}{6}\mathrm{Tr}F_{\mu\nu}^2(x_0) + \frac{4a^6g^2}{72}\mathrm{Tr}F_{\mu\nu}(x_0)\left(4D_\mu^2 + D_\nu^2\right)F_{\mu\nu}(x_0) \\ &\quad +\frac{4a^4g^2}{6}\mathrm{Tr}F_{\mu\nu}^2(x_0) + \frac{4a^6g^2}{72}\mathrm{Tr}F_{\mu\nu}(x_0)\left(D_\mu^2 + 4D_\nu^2\right)F_{\mu\nu}(x_0) \\ &\quad +\mathcal{O}(a^8, g^4) \\ &= \frac{8a^4g^2}{6}\mathrm{Tr}F_{\mu\nu}^2(x_0) + \frac{4a^6g^2}{72}\mathrm{Tr}F_{\mu\nu}(x_0)\left(5D_\mu^2 + 5D_\nu^2\right)F_{\mu\nu}(x_0) \\ &\quad +\mathcal{O}(a^8, g^4) \end{aligned}$$

$$= \frac{8a^4g^2}{6}\mathrm{Tr}F^2_{\mu\nu}(x_0) + \frac{20a^6g^2}{72}\mathrm{Tr}F_{\mu\nu}(x_0)\left(D^2_\mu + D^2_\nu\right)F_{\mu\nu}(x_0) + \mathcal{O}(a^8, g^4).$$

Now that we have an expression symmetric in $\mu$ and $\nu$ we can see that we can create an improved action, $S_{\mathrm{I}}$, by forming a linear combination with the expression arising from the plaquette to eliminate the $\mathcal{O}(a^6)$ terms:

$$\begin{aligned}
S_{\mathrm{I}} &= \frac{5}{3}\beta\sum_x\sum_{\mu<\nu}\left[\left(1-P^{(1\times1)}_{\mu\nu}(x_0)\right) - \frac{1}{20}\left\{\left(1-P^{(2\times1)}_{\mu\nu}(x_0)\right) - \left(1-P^{(1\times2)}_{\mu\nu}(x_0)\right)\right\}\right] \\
&= \frac{5}{3}\beta\sum_x\sum_{\mu<\nu}\left[\frac{a^4g^2}{6}\mathrm{Tr}F^2_{\mu\nu}(x_0) + \frac{a^6g^2}{72}\mathrm{Tr}F_{\mu\nu}(x_0)\left(D^2_\mu + D^2_\nu\right)F_{\mu\nu}(x_0)\right. \\
&\qquad - \frac{1}{20}\left(\frac{8a^4g^2}{6}\mathrm{Tr}F^2_{\mu\nu}(x_0) + \frac{20a^6g^2}{72}\mathrm{Tr}F_{\mu\nu}(x_0)\left(D^2_\mu + D^2_\nu\right)F_{\mu\nu}(x_0)\right) \\
&\qquad \left. + \mathcal{O}(a^8, g^4)\right] \\
&= \frac{5}{3}\beta\sum_x\sum_{\mu<\nu}\frac{1}{6}\left[a^4g^2\mathrm{Tr}F^2_{\mu\nu}(x_0) + \frac{a^6g^2}{12}\mathrm{Tr}F_{\mu\nu}(x_0)\left(D^2_\mu + D^2_\nu\right)F_{\mu\nu}(x_0)\right. \\
&\qquad \left. - \frac{2a^4g^2}{5}\mathrm{Tr}F^2_{\mu\nu}(x_0) - \frac{a^6g^2}{12}\mathrm{Tr}F_{\mu\nu}(x_0)\left(D^2_\mu + D^2_\nu\right)F_{\mu\nu}(x_0) + \mathcal{O}(a^8, g^4)\right] \\
&= \frac{5}{3}\beta\sum_x\sum_{\mu<\nu}\frac{1}{6}\left[\frac{5a^4g^2}{5}\mathrm{Tr}F^2_{\mu\nu}(x_0) + \frac{a^6g^2}{12}\mathrm{Tr}F_{\mu\nu}(x_0)\left(D^2_\mu + D^2_\nu\right)F_{\mu\nu}(x_0)\right. \\
&\qquad \left. - \frac{2a^4g^2}{5}\mathrm{Tr}F^2_{\mu\nu}(x_0) - \frac{a^6g^2}{12}\mathrm{Tr}F_{\mu\nu}(x_0)\left(D^2_\mu + D^2_\nu\right)F_{\mu\nu}(x_0) + \mathcal{O}(a^8, g^4)\right] \\
&= \frac{5}{3}\beta\sum_x\sum_{\mu<\nu}\frac{1}{6}\left[\frac{3a^4g^2}{5}\mathrm{Tr}F^2_{\mu\nu}(x_0) + \mathcal{O}(a^8, g^4)\right] \\
&= \frac{5}{3}\beta\sum_x\sum_{\mu<\nu}\left[\frac{3a^4g^2}{30}\mathrm{Tr}F^2_{\mu\nu}(x_0) + \mathcal{O}(a^8, g^4)\right] \\
&= \frac{5}{3}\beta\sum_x\sum_{\mu<\nu}\left[\frac{a^4g^2}{10}\mathrm{Tr}F^2_{\mu\nu}(x_0) + \mathcal{O}(a^8, g^4)\right] \\
&= \sum_x\sum_{\mu<\nu}\left[a^4\mathrm{Tr}F^2_{\mu\nu}(x_0) + \mathcal{O}(a^8, g^2)\right] \text{ (setting } \beta = \frac{6}{g^2}) \\
&= a^4\sum_x\sum_{\mu,\nu}\left[\frac{1}{2}\mathrm{Tr}F^2_{\mu\nu}(x_0) + \mathcal{O}(a^4, g^2)\right].
\end{aligned}$$

Therefore

$$S_{\mathrm{I}} = \frac{1}{2}\int d^4x \mathrm{Tr} F_{\mu\nu}^2(x_0) + \mathcal{O}(a^4, g^2). \tag{3.2}$$

We can see by comparing equations (2.53) and (3.2) that the combination of terms from the square and rectangular plaquettes has given us an action which matches the continuum action to the next order in $a^2$ beyond that of the unimproved Wilson action.

Notice that tree-level improvement has dealt only with those discretization errors which are leading order in $g$. The $\mathcal{O}(g^2)$ errors remain, and we shall examine a process by which these errors are minimised in Section 3.2. Having noted their existence, and the fact that tree-level improvement does not deal with them, we shall henceforth leave the errors of higher order in $g$ as implicit rather than explicit components of our equations. Although such errors are of similar magnitude to $\mathcal{O}(a^4)$, these corrections will be shown to vanish in the process of cooling (see Section 6.2).

Before we proceed any further let us define

$$T_{\mu\nu}^{(m,n)}(x_0) = \frac{3}{g^2}\Big(2 - P_{\mu\nu}^{(m\times n)}(x_0) - P_{\mu\nu}^{(n\times m)}(x_0)\Big), \tag{3.3}$$

so that

$$S_{\mathrm{I}} = \frac{5}{3}\beta \sum_x \sum_{\mu<\nu} \frac{g^2}{6} T_{\mu\nu}^{(1,1)}(x_0). \tag{3.4}$$

The point of this approach is to average the contribution from rectangular loops oriented in different directions. From this definition we can easily see that

$$\begin{aligned} T_{\mu\nu}^{(1,1)}(x_0) &= \frac{3}{g^2}\left\{\frac{a^4g^2}{3}\mathrm{Tr}F_{\mu\nu}^2(x_0) + \frac{a^6g^2}{36}\mathrm{Tr}F_{\mu\nu}(x_0)\left(D_\mu^2 + D_\nu^2\right)F_{\mu\nu}(x_0) + \mathcal{O}(a^8)\right\} \\ &= \left\{a^4\mathrm{Tr}F_{\mu\nu}^2(x_0) + \frac{a^6}{12}\mathrm{Tr}F_{\mu\nu}(x_0)\left(D_\mu^2 + D_\nu^2\right)F_{\mu\nu}(x_0) + \mathcal{O}(a^8)\right\}, \end{aligned}$$

$$
\begin{aligned}
T_{\mu\nu}^{(1,2)}(x_0) &= \frac{3}{g^2}\left\{\frac{4a^4g^2}{6}\mathrm{Tr}F_{\mu\nu}^2(x_0)+\frac{4a^6g^2}{72}\mathrm{Tr}F_{\mu\nu}(x_0)\left(4D_\mu^2+D_\nu^2\right)F_{\mu\nu}(x_0)\right. \\
&\quad \left.+\frac{4a^4}{6}\mathrm{Tr}F_{\mu\nu}^2(x_0)+\frac{4a^6}{72}\mathrm{Tr}F_{\mu\nu}(x_0)\left(D_\mu^2+4D_\nu^2\right)F_{\mu\nu}(x_0)+\mathcal{O}(a^8)\right\} \\
&= \left\{4a^4\mathrm{Tr}F_{\mu\nu}^2(x_0)+\frac{10a^6}{12}\mathrm{Tr}F_{\mu\nu}(x_0)\left(D_\mu^2+D_\nu^2\right)F_{\mu\nu}(x_0)+\mathcal{O}(a^8)\right\}.
\end{aligned}
$$

It is a fairly straightforward exercise to show that $T_{\mu\nu}^{(m,n)}$ may be used to define an improved action as was demonstrated above,

$$
\begin{aligned}
S_{\mathrm{I}} &= \frac{5}{3}\beta\sum_x\sum_{\mu<\nu}\frac{g^2}{6}\left[\left(T_{\mu\nu}^{(1,1)}(x_0)\right)-\frac{1}{10}\left(T_{\mu\nu}^{(1,2)}(x_0)\right)\right] \\
&= \frac{5}{3}\beta\sum_x\sum_{\mu<\nu}\frac{g^2}{6}\left[a^4\mathrm{Tr}F_{\mu\nu}^2(x_0)+\frac{a^6}{12}\mathrm{Tr}F_{\mu\nu}(x_0)\left(D_\mu^2+D_\nu^2\right)F_{\mu\nu}(x_0)\right. \\
&\qquad -\frac{1}{10}\left(4a^4\mathrm{Tr}F_{\mu\nu}^2(x_0)+\frac{10a^6}{12}\mathrm{Tr}F_{\mu\nu}(x_0)\left(D_\mu^2+D_\nu^2\right)F_{\mu\nu}(x_0)\right) \\
&\qquad \left.+\mathcal{O}(a^8)\right] \\
&= \frac{5}{3}\beta\sum_x\sum_{\mu<\nu}\frac{g^2}{6}\left[a^4\mathrm{Tr}F_{\mu\nu}^2(x_0)+\frac{a^6}{12}\mathrm{Tr}F_{\mu\nu}(x_0)\left(D_\mu^2+D_\nu^2\right)F_{\mu\nu}(x_0)\right. \\
&\qquad \left.-\frac{2a^4}{5}\mathrm{Tr}F_{\mu\nu}^2(x_0)-\frac{a^6}{12}\mathrm{Tr}F_{\mu\nu}(x_0)\left(D_\mu^2+D_\nu^2\right)F_{\mu\nu}(x_0)+\mathcal{O}(a^8)\right] \\
&= \frac{5}{3}\beta\sum_x\sum_{\mu<\nu}\frac{g^2}{6}\left[\frac{5a^4}{5}\mathrm{Tr}F_{\mu\nu}^2(x_0)+\frac{a^6}{12}\mathrm{Tr}F_{\mu\nu}(x_0)\left(D_\mu^2+D_\nu^2\right)F_{\mu\nu}(x_0)\right. \\
&\qquad \left.-\frac{2a^4}{5}\mathrm{Tr}F_{\mu\nu}^2(x_0)-\frac{a^6}{12}\mathrm{Tr}F_{\mu\nu}(x_0)\left(D_\mu^2+D_\nu^2\right)F_{\mu\nu}(x_0)+\mathcal{O}(a^8)\right] \\
&= \frac{5}{3}\beta\sum_x\sum_{\mu<\nu}\frac{g^2}{6}\left[\frac{3a^4}{5}\mathrm{Tr}F_{\mu\nu}^2(x_0)+\mathcal{O}(a^8)\right] \\
&= \frac{5}{3}\beta\sum_x\sum_{\mu<\nu}\left[\frac{3a^4g^2}{30}\mathrm{Tr}F_{\mu\nu}^2(x_0)+\mathcal{O}(a^8)\right] \\
&= \frac{5}{3}\beta\sum_x\sum_{\mu<\nu}\left[\frac{a^4g^2}{10}\mathrm{Tr}F_{\mu\nu}^2(x_0)+\mathcal{O}(a^8)\right] \\
&= \sum_x\sum_{\mu<\nu}\left[a^4\mathrm{Tr}F_{\mu\nu}^2(x_0)+\mathcal{O}(a^8)\right] \text{ (setting } \beta=\frac{6}{g^2} \text{ as above).}
\end{aligned}
$$

Hence we see that

$$S_{\mathrm{I}} = a^4 \sum_x \sum_{\mu,\nu} \left[ \frac{1}{2} \mathrm{Tr} F_{\mu\nu}^2(x_0) + \mathcal{O}(a^4) \right]. \tag{3.5}$$

In future we will find it more convenient to work with the $T_{\mu\nu}^{(m,n)}$'s rather than the $P_{\mu\nu}^{(m\times n)}$'s when creating improved actions, since they are symmetrical in terms of $\mu$ and $\nu$, and they automatically eliminate an irrelevant factor of $1/6$, making our algebraic manipulations neater.

## 3.2 Tadpole Improvement

As we've seen above (Section 2.3) the leading term that couples quarks and gluons is of the form $\bar{\psi}(x)U_\mu(x)\gamma_\mu\psi(x+\mu)$. Taking

$$U_\mu(x) \approx 1 + igaA_\mu(x) - \frac{1}{2}g^2a^2A_\mu^2(x) + \mathcal{O}(a^3) \tag{3.6}$$

we see that this contains the $\bar{\psi}(x)gA_\mu(x)\gamma_\mu\psi(x+\mu)$ quark-gluon vertex, but it also contains higher terms that involve couplings of the gluon field to itself. These couplings, arising from terms like $\frac{1}{2}g^2a^2A_\mu^2(x)$ are called 'tadpoles', because of their diagrammatic representation as closed loops [20].

Naively we expect these terms to be suppressed by powers of $a^2$, however since the tadpole loop integral associated with $A_\mu^2(x)$ diverges as $\left(\frac{\pi}{a}\right)^2$ the effect of the powers of the lattice spacing are cancelled, and the only thing suppressing the tadpoles is powers of $g^2$, which are inadequate to the task. The solution to this problem is to rescale the links with $u_0$, the value of the mean link. In essence $u_0$ is a renormalization factor which accounts for the effect of the short-range (ultraviolet) fluctuations arising from the presence of tadpoles [2]. We rescale the link variables

$$U_\mu(x) \to \frac{U_\mu(x)}{u_0}, \tag{3.7}$$

where we have defined the mean link in a gauge-invariant way

$$u_0 = \left\langle P_{\mu\nu}^{(1\times1)}(x)\right\rangle^{\frac{1}{4}}. \tag{3.8}$$

Having defined the mean link, our next step is to introduce it into the action. Doing so to the improved action we found above would result in an action of the form

$$S_{\mathrm{I}} = \frac{5}{3}\beta\sum_x\sum_{\mu<\nu}\frac{g^2}{6}\left[\left(T_{\mu\nu}^{(1,1)}(x_0)\right) - \frac{1}{10u_0^2}\left(T_{\mu\nu}^{(1,2)}(x_0)\right)\right]. \tag{3.9}$$

An example of how well this improvement scheme restores continuum-like behaviour is given by the restoration of rotational invariance in the static quark-anti-quark potential, $V(r)$. For unimproved actions, the computed value of the potential for distances on-axis ($r/a = 1, 2, 3, 4...$) and off-axis ($r/a = \sqrt{2}, \sqrt{3}, \sqrt{5}...$) may be off by as much as 38%, for coarse lattices with $a \approx 0.4$ fm. With improved actions of the kind discussed above these errors are reduced to the order of one-percent [1].

## 3.3 Order $a^4$ Tree-Level Improvement

We have already seen how a simple tree-level improvement scheme can be employed to eliminate the $\mathcal{O}(a^2)$ deviations from the continuum action on the lattice. We now wish to extend this idea to the elimination of the next order of errors. To this end we will begin by looking at the expansion of the loop operator to order $a^8$.

We can tell from Equation (2.47) that for the elementary plaquette

$$\begin{aligned}\oint A.dx \;=\; & a^2F_{\mu\nu}(x_0) + \frac{a^4}{24}\left(D_\mu^2 + D_\nu^2\right)F_{\mu\nu}(x_0) \\ & + \frac{a^6}{1920}\left(D_\mu^4 + D_\nu^4\right)F_{\mu\nu}(x_0) + \frac{a^6}{576}\left(D_\mu^2D_\nu^2\right)F_{\mu\nu}(x_0) \\ & + \mathcal{O}(a^8).\end{aligned} \tag{3.10}$$

For simplicity we will refrain from substituting this result into Equation (2.49), and instead we will simply use it to find the expression corresponding to $T_{\mu\nu}^{(1,1)}$,

$$\begin{aligned} T_{\mu\nu}^{(1,1)} &= \mathrm{Tr}\, a^4 F_{\mu\nu}^2 + \mathrm{Tr}\, \frac{a^6}{24} F_{\mu\nu} \left[ \left( D_\mu^2 + D_\nu^2 \right) F_{\mu\nu} \right] \\ &\quad + \mathrm{Tr}\, \frac{a^6}{24} \left[ \left( D_\mu^2 + D_\nu^2 \right) F_{\mu\nu} \right] F_{\mu\nu} + \mathrm{Tr}\, \frac{a^8}{1920} F_{\mu\nu} \left[ \left( D_\mu^4 + D_\nu^4 \right) F_{\mu\nu} \right] \\ &\quad + \mathrm{Tr}\, \frac{a^8}{1920} \left[ \left( D_\mu^4 + D_\nu^4 \right) F_{\mu\nu} \right] F_{\mu\nu} + \mathrm{Tr}\, \frac{a^8}{576} F_{\mu\nu} \left[ \left( D_\mu^2 D_\nu^2 \right) F_{\mu\nu} \right] \\ &\quad + \mathrm{Tr}\, \frac{a^8}{576} \left[ \left( D_\mu^2 D_\nu^2 \right) F_{\mu\nu} \right] F_{\mu\nu} + \mathrm{Tr}\, \frac{a^8}{576} \left[ \left( D_\mu^2 + D_\mu^2 \right) F_{\mu\nu} \right] \left[ \left( D_\mu^2 + D_\mu^2 \right) F_{\mu\nu} \right] \\ &\quad + \mathcal{O}(g^2, a^8) \qquad (3.11) \\ &= \mathrm{Tr}\, a^4 F_{\mu\nu}^2 + \mathrm{Tr}\, \frac{a^6}{12} F_{\mu\nu} \left[ \left( D_\mu^2 + D_\nu^2 \right) F_{\mu\nu} \right] \\ &\quad + \mathrm{Tr}\, \frac{a^8}{960} F_{\mu\nu} \left[ \left( D_\mu^4 + D_\nu^4 \right) F_{\mu\nu} \right] + \mathrm{Tr}\, \frac{a^8}{288} F_{\mu\nu} \left[ \left( D_\mu^2 D_\nu^2 \right) F_{\mu\nu} \right] \\ &\quad + \mathrm{Tr}\, \frac{a^8}{576} \left( \left[ D_\mu^2 F_{\mu\nu} \right] \left[ D_\mu^2 F_{\mu\nu} \right] + \left[ D_\nu^2 F_{\mu\nu} \right] \left[ D_\nu^2 F_{\mu\nu} \right] \right) \\ &\quad + \mathrm{Tr}\, \frac{a^8}{288} \left[ D_\mu^2 F_{\mu\nu} \right] \left[ D_\nu^2 F_{\mu\nu} \right] \\ &\quad + \mathcal{O}(g^2, a^8). \qquad (3.12) \end{aligned}$$

Since we will be looking at a number of expansions of this type, corresponding to different loops, let us simplify our results by making use of the notation:

$$\begin{aligned} \mathcal{A} &\equiv \mathrm{Tr}\, a^4 F_{\mu\nu}^2 \\ \mathcal{B} &\equiv \mathrm{Tr}\, a^6 F_{\mu\nu} \left[ \left( D_\mu^2 + D_\nu^2 \right) F_{\mu\nu} \right] \\ \mathcal{C} &\equiv \mathrm{Tr}\, a^8 F_{\mu\nu} \left[ \left( D_\mu^4 + D_\nu^4 \right) F_{\mu\nu} \right] \\ \mathcal{D} &\equiv \mathrm{Tr}\, a^8 F_{\mu\nu} \left[ \left( D_\mu^2 D_\nu^2 \right) F_{\mu\nu} \right] \\ \mathcal{E} &\equiv \mathrm{Tr}\, a^8 \left( \left[ D_\mu^2 F_{\mu\nu} \right] \left[ D_\mu^2 F_{\mu\nu} \right] + \left[ D_\nu^2 F_{\mu\nu} \right] \left[ D_\nu^2 F_{\mu\nu} \right] \right) \\ \mathcal{F} &\equiv \mathrm{Tr}\, a^8 \left[ D_\mu^2 F_{\mu\nu} \right] \left[ D_\nu^2 F_{\mu\nu} \right]. \end{aligned}$$

Using these definitions we may say that

$$T_{\mu\nu}^{(1,1)} = \mathcal{A} + \frac{1}{12}\mathcal{B} + \frac{1}{960}\mathcal{C} + \frac{1}{288}\mathcal{D} + \frac{1}{576}\mathcal{E} + \frac{1}{288}\mathcal{F} + \mathcal{O}(a^{10}). \qquad (3.13)$$

In order to find an $\mathcal{O}(a^4)$-improved action we will need to eliminate the terms $\mathcal{B},\mathcal{C},\mathcal{D},\mathcal{E}$, and $\mathcal{F}$ from the expansions of the loop terms. We will consider five other loop terms in addition to $T^{(1\times1)}$, remembering that the rectangular terms of equal dimensions but different orientation must be added together as was the case for the $\mathcal{O}(a^2)$ case in Section 3.1. Therefore we choose the following terms as the basis for our highly-improved gluon action

$$\begin{aligned}
T_{\mu\nu}^{(1,1)} &= \mathcal{A}+\frac{1}{12}\mathcal{B}+\frac{1}{960}\mathcal{C}+\frac{1}{288}\mathcal{D}+\frac{1}{576}\mathcal{E}+\frac{1}{288}\mathcal{F} \\
T_{\mu\nu}^{(2,2)} &= 16\mathcal{A}+\frac{16}{3}\mathcal{B}+\frac{8}{30}\mathcal{C}+\frac{8}{9}\mathcal{D}+\frac{4}{9}\mathcal{E}+\frac{8}{9}\mathcal{F} \\
T_{\mu\nu}^{(1,2)} &= 4\mathcal{A}+\frac{5}{6}\mathcal{B}+\frac{17}{480}\mathcal{C}+\frac{1}{18}\mathcal{D}+\frac{17}{288}\mathcal{E}+\frac{1}{18}\mathcal{F} \\
T_{\mu\nu}^{(1,3)} &= 9\mathcal{A}+\frac{30}{8}\mathcal{B}+\frac{123}{320}\mathcal{C}+\frac{18}{64}\mathcal{D}+\frac{41}{64}\mathcal{E}+\frac{18}{64}\mathcal{F} \\
T_{\mu\nu}^{(3,3)} &= 81\mathcal{A}+\frac{243}{4}\mathcal{B}+\frac{2187}{320}\mathcal{C}+\frac{729}{32}\mathcal{D}+\frac{729}{64}\mathcal{E}+\frac{729}{32}\mathcal{F}.
\end{aligned}$$

Notice that in each case the coefficient of $\mathcal{D}$ and $\mathcal{F}$ is the same, meaning we can regard these two terms as a single term for the purposes of their elimination. We then have only five unknowns, and five equations, meaning that we should freely be able to solve this system of equations to obtain a highly improved action. Further insight can be gained by dividing the term for each loop by the product of the extent of the loop in the $\mu-$direction squared with the extent of the loop in the $\nu-$direction squared, so that for each loop the coefficient of the $\mathcal{A}$ term is made equal to 1. This gives us $T_{\mu\nu}^{(m,n)}/(m^2n^2)$ for each loop (see Table 3.1).

A number of very interesting results emerge from this analysis. Firstly, we see from Table 3.1 that just as the coefficients for $\mathcal{D}$ and $\mathcal{F}$ for any given loop are the same, the numerators of the coefficients of $\mathcal{C}$ and $\mathcal{E}$ are the same, meaning

Table 3.1: Factors from various loops, for the coefficients in the expansion of the action.

| | $\mathcal{A}$ | $\mathcal{B}$ | $\mathcal{C}$ | $\mathcal{D}$ | $\mathcal{E}$ | $\mathcal{F}$ |
|---|---|---|---|---|---|---|
| (1,1) | 1 | $\frac{2}{24}$ | $\frac{2}{1920}$ | $\frac{1}{288}$ | $\frac{2}{1152}$ | $\frac{1}{288}$ |
| (2,2) | 1 | $\frac{8}{24}$ | $\frac{32}{1920}$ | $\frac{16}{288}$ | $\frac{32}{1152}$ | $\frac{16}{288}$ |
| (1,2) | 1 | $\frac{5}{24}$ | $\frac{17}{1920}$ | $\frac{4}{288}$ | $\frac{17}{1152}$ | $\frac{4}{288}$ |
| (1,3) | 1 | $\frac{10}{24}$ | $\frac{82}{1920}$ | $\frac{9}{288}$ | $\frac{82}{1152}$ | $\frac{9}{288}$ |
| (3,3) | 1 | $\frac{18}{24}$ | $\frac{162}{1920}$ | $\frac{81}{288}$ | $\frac{162}{1152}$ | $\frac{81}{288}$ |

that $\mathcal{D}$ and $\mathcal{F}$ can be combined behind a single coefficient

$$\mathcal{D}' = (\mathcal{D} + \mathcal{F}) \tag{3.14}$$

and $\mathcal{C}$ and $\mathcal{E}$ can likewise be combined behind a single coefficient

$$\mathcal{C}' = \left(\mathcal{C} + \frac{1920}{1152}\mathcal{E}\right). \tag{3.15}$$

Secondly we see that when the denominators of the various terms are set to the same value, the numerators of $\mathcal{B}$ for any loop are given by $m^2+n^2$, the numerators for $\mathcal{C}'$ are given by $m^4+n^4$, and the numerators for $\mathcal{D}'$ are given by $m^2n^2$ (the area of the loop squared).

In order to find the form of an improved action we start by assuming that the terms corresponding to each loop are to be multiplied by some constants, $c_1, c_2, c_3, \ldots$ so that the improved action may be written

$$S_{\text{Imp}} = \beta \sum_x \sum_{\mu<\nu} \frac{g^2}{6} \left[c_1 T_{\mu\nu}^{(1,1)} + c_2 T_{\mu\nu}^{(2,2)} + c_3 T_{\mu\nu}^{(1,2)} + \ldots\right]. \tag{3.16}$$

This equation actually represents a series of equations;

$$c_1\mathcal{A}^{(1,1)} + c_2\mathcal{A}^{(2,2)} + c_3\mathcal{A}^{(1,2)} + ... = 1 \quad (3.17)$$

$$c_1\mathcal{B}^{(1,1)} + c_2\mathcal{B}^{(2,2)} + c_3\mathcal{B}^{(1,2)} + ... = 0 \quad (3.18)$$

$$c_1\mathcal{C}'^{(1,1)} + c_2\mathcal{C}'^{(2,2)} + c_3\mathcal{C}'^{(1,2)} + ... = 0 \quad (3.19)$$

$$c_1\mathcal{D}'^{(1,1)} + c_2\mathcal{D}'^{(2,2)} + c_3\mathcal{D}'^{(1,2)} + ... = 0, \quad (3.20)$$

where $\mathcal{A}^{(m,n)}$ represents the coefficient of the $\mathcal{A}$ term from the expansion of $T_{\mu\nu}^{(m,n)}$ and so forth, with the values taken from Table 3.1. de Forcrand *et al.* [3] have already deduced a form for a 5-loop improved action ("5Li") using $T^{(m,n)}/(m^2n^2)$ where $(m,n) = (1,1),(2,2),(1,2),(1,3),(3,3)$. We wish to reproduce their results by deducing the same values for the constants $c_1, c_2, c_3, ...$

To find the values of the improvement constants we use the coefficients in Table 3.1 to construct an equivalent matrix equation with the coefficient matrix $A$ and the constraint vector $B$

$$\begin{bmatrix} 1 & 1 & 1 & 1 & 1 \\ \frac{2}{24} & \frac{8}{24} & \frac{5}{24} & \frac{10}{24} & \frac{18}{24} \\ \frac{2}{1920} & \frac{32}{1920} & \frac{17}{1920} & \frac{82}{1920} & \frac{162}{1920} \\ \frac{1}{288} & \frac{16}{288} & \frac{4}{288} & \frac{9}{288} & \frac{81}{288} \end{bmatrix} = A \quad (3.21)$$

$$\begin{bmatrix} 1 \\ 0 \\ 0 \\ 0 \end{bmatrix} = B. \quad (3.22)$$

We can now write Equations (3.17-3.20) in the form

$$\begin{bmatrix} 1 & 1 & 1 & 1 & 1 \\ \frac{2}{24} & \frac{8}{24} & \frac{5}{24} & \frac{10}{24} & \frac{18}{24} \\ \frac{2}{1920} & \frac{32}{1920} & \frac{17}{1920} & \frac{82}{1920} & \frac{162}{1920} \\ \frac{1}{288} & \frac{16}{288} & \frac{4}{288} & \frac{9}{288} & \frac{81}{288} \end{bmatrix} \begin{bmatrix} c_1 \\ c_2 \\ c_3 \\ c_4 \\ c_5 \end{bmatrix} = \begin{bmatrix} 1 \\ 0 \\ 0 \\ 0 \end{bmatrix} \tag{3.23}$$

and the values of $c_1, c_2, c_3, \ldots$ may be found by using Gauss-Jordan elimination. After performing a series of elementary row operations to reduce $A$ to echelon form, and the same series of row operation on the vector $B$ we find that

$$\begin{bmatrix} 1 & 0 & 0 & 0 & \frac{55}{9} \\ 0 & 1 & 0 & 0 & \frac{64}{9} \\ 0 & 0 & 1 & 0 & -\frac{640}{45} \\ 0 & 0 & 0 & 1 & 2 \end{bmatrix} \begin{bmatrix} c_1 \\ c_2 \\ c_3 \\ c_4 \\ c_5 \end{bmatrix} = \begin{bmatrix} \frac{19}{9} \\ \frac{1}{9} \\ -\frac{64}{45} \\ \frac{1}{5} \end{bmatrix}. \tag{3.24}$$

Therefore we deduce that

$$\begin{aligned} c_1 &= (19 - 55c_5)/9 \\ c_2 &= (1 - 64c_5)/9 \\ c_3 &= (640c_5 - 64)/45 \\ c_4 &= 1/5 - 2c_5 \end{aligned}$$

and $c_5$ is a free variable which we can use to "tune" the action. Of course, we have divided the terms in the actions by the leading order so that the coefficients for $\mathcal{A}$ are all equal to 1. Hence we must compensate by including factors of $1/m^2n^2$ in the final form of the improved action. This can be illustrated by noting, as above, that the terms we used to construct the matrix $A$ were in fact not $T_{\mu\nu}^{(m,n)}$ but $T_{\mu\nu}^{(m,n)}/(m^2n^2)$. Once we have incorporated these factors and the

relevant tadpole improvement terms the final form of the improved action we have deduced is

$$S_{\text{Imp}} = \frac{5}{3}\beta \sum_x \sum_{\mu<\nu} \frac{g^2}{6} \left[ \frac{(19-55c_5)}{9} T^{(1,1)}_{\mu\nu} + \frac{1}{16u_0^4}\frac{(1-64c_5)}{9} T^{(2,2)}_{\mu\nu} + \frac{1}{4u_0^2}\frac{(640c_5-64)}{45} T^{(1,2)}_{\mu\nu} + \frac{1}{9u_0^4}(1/5-2c_5) T^{(1,3)}_{\mu\nu} + \frac{1}{81u_0^8} c_5 T^{(3,3)}_{\mu\nu} \right]. \quad (3.25)$$

It is easy to see that by tuning the variable $c_5$ we can create 3-, 4-, and 5-loop improved actions. If we set $c_5 = 1/10$ we eliminate the contribution from $T^{(1,2)}_{\mu\nu}$ and $T^{(1,3)}_{\mu\nu}$, leaving only three of the five terms and creating a "3-loop" improved action (from now on we shall write $S(3)$ for brevity) and by setting $c_5 = 0$ we eliminate the contribution from $T^{(3,3)}_{\mu\nu}$, leaving four terms and creating a "4-loop" improved action ($S(4)$ for short).

When retaining all five terms corresponding to using a "5-loop" improved action we shall typically choose $c_5 = 1/20$, midway between the $S(3)$ and $S(4)$ values. This value was selected by de Forcrand *et al.* to stabilize the size of instantons on a lattice with twisted boundary conditions in the time direction [3].

To ensure that the reader is clear about what we mean when we speak of each improvement scheme, let us state the following facts explicitly;

- The 1-loop action is the standard Wilson action constructed from the plaquette alone. It contains errors of order $\mathcal{O}(a^2)$.

- The 2-loop action is constructed from the plaquette and the average of the $a \times 2a$ and $2a \times a$ rectangular loops. It contains errors of order $\mathcal{O}(a^4)$, but is free from $\mathcal{O}(a^2)$ errors.

- The 3-loop action is constructed from the plaquette, $2a \times 2a$ and $3a \times 3a$ Wilson loops.

- The 4-loop action is constructed from the plaquette, $2a \times 2a$ and the respective averages of the $a \times 2a$ and $2a \times a$ rectangular loops, and the $a \times 3a$ and $3a \times a$ rectangular loops.

- The 5-loop action is constructed from the plaquette, $2a \times 2a$, $3a \times 3a$, and the respective averages of the $a \times 2a$ and $2a \times a$ rectangular loops, and the $a \times 3a$ and $3a \times a$ rectangular loops.

- The 3-loop, 4-loop, and 5-loop actions are all free from order $\mathcal{O}(a^4)$ errors, but contain (in general) different order $\mathcal{O}(a^6)$ errors. However they still contain $\mathcal{O}(g^2)$ errors at $\mathcal{O}(a^4)$ and higher, as is clear from the error term in Equation (2.49). If not for tadpole improvement the scale of such error terms would be large enough to interfere with the improvement process, rendering the 3-loop, 4-loop, and 5-loop actions approximately as accurate as the 2-loop.

- Since $c_5$ is a tunable parameter, there are actually an infinite number of possible forms for the 5-loop action. We have chosen to concentrate on the action obtained by setting $c_5 = 1/20$. The 3-loop and 4-loop actions are just other special cases of the 5-loop action.

## 3.4 Alternate Improvement Schemes

As mentioned in the introduction to this Chapter, the improvement scheme we have adopted is based upon that developed by Lüscher and Weisz [19]. It is worth taking the time to describe their improvement procedure and detail the differences with the approach we have adopted.

As we have seen, an arbitrary planar loop $L$ can be expanded as

$$L = r_1\mathcal{A} + r_2\mathcal{B} + ... \tag{3.26}$$

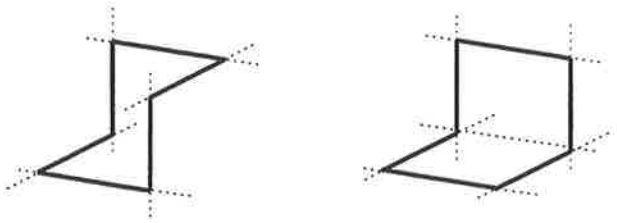

Figure 3.1: Examples of possible non-planar Wilson loops, the parallelogram (left) and bent rectangle (right). Of course, other non-planar loops are possible, involving more than six links.

If we consider the more general case of non-planar loops, other terms arise bearing indices beyond the $\mu, \nu$ that we have so far examined. Additional loops outside the $\mu - \nu$ plane are required to cancel these extra terms. Once again the lattice action can be written as a sum of loop terms weighted with appropriate coefficients. Lüscher and Weisz considered the plaquette plus $1 \times 2$ rectangle and the two other possible choices of six-link Wilson loop depicted in Figure (3.1). Such an improvement scheme eliminates $\mathcal{O}(a^2)$ errors from the lattice action. The $\mathcal{O}(a^2)$-improved action we have described in Section 3.1 is really a special case of this improvement, in which we achieve tree-level improvement while neglecting the non-planar loops. The Lüscher-Weisz action includes very small corrections of order $g^2$, however since the contributions from non-planar loops are so small (the parallelogram term is equal to $-0.00441g^2$ while the bent rectangle term is equal to zero) the action can be improved classically to an excellent approximation, and then tadpole improved to deal with non-classical corrections.

Our calculations are performed on a supercomputer with parallel processing architecture. Since several processors are working on different parts of the lattice at once this approach is extremely rapid, however a "masking" algorithm must be applied, to define which areas of the lattice are to be updated and which are

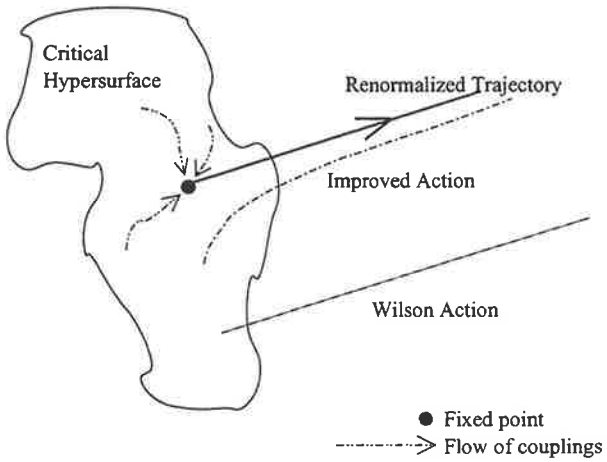


Figure 3.2: . The renormalization group transformations define a flow within coupling space. The renormalized trajectory is an attractor for this flow, and improvement of the action aims to approach the RT arbitrarily closely. Diagram after Gupta [18].

off-limits at any given time, to prevent the Wilson loops used to update different links from overlapping [21]. Restricting our consideration to planar loops greatly improves the efficiency of the masking algorithm. Thirdly, consideration of non-planar loops introduces $g^2$ terms which may be seen as suitable for cancelling the $\mathcal{O}(g^2)$ corrections to the action. However the process of cooling a configuration, to be discussed in Chapter 6, removes such errors anyway. Therefore $\mathcal{O}(g^2)$ corrections are only of concern during the first few sweeps of cooling, and since the research detailed in this thesis is concerned with the behaviour of configurations after several hundred to thousand cooling sweeps, the inclusion of terms to compensate for such corrections would seem unnecessary.

Before concluding, some mention should be made of other approaches to gauge action improvement, especially the "perfect actions" based upon renormalization group transformations (RGT). An RGT may be considered in the space of all

couplings $\{K_\alpha\}$, and specifically we are interested in the hypersurfaces formed by critical points $\{K_\alpha^c\}$ with correlation length $\xi/a = \infty$. At certain fixed points on such hypersurfaces the theory reproduces itself at all length scales, as the renormalized couplings are equal to the original couplings. The sequence of theories defined by repeated use of a RGT induces a flow of couplings, and of particular interest a flow trajectory along the critical hypersurface towards a fixed point, see Figure (3.2). The renormalized trajectory (RT) is the trajectory from a fixed point, to which all critical points sufficiently close to the fixed point eventually tend. What makes this interesting is that an action along the exact RT will be completely free of discretization errors, as there are no scaling violations along the RT. Attempts to improve the action based upon this theoretical framework must contend with the fact that correlation lengths in simulations tend to be much smaller than the extent of the (finite) lattice, $\xi \ll L$. Since the RT attracts flows within the vicinity of the fixed point from which it starts, the action can be improved by estimating the location of the fixed point and adjusting the action to start nearer to it. An example of an approach to improvement based on this idea is the Iwasaki action [22]. Hasenfratz and Neidermayer's classically perfect action [23] is based upon the attempt to take a saddle-point integration of the RGT about the coupling $g = 0$.

The work of Morningstar and Peardon [24] is also worth mentioning. In order to obtain more statistically significant results in the attempt to calculate masses of glueball states, an anisotropic lattice with $a_t \ll a_s$ was adopted. This step is not really an improvement, since it merely corresponds to approaching the continuum limit, albeit in only one dimension. However they then adopted the Lüscher-Weisz action (with tadpole improvement) with the plaquette represented in both the fundamental and adjoint coupling space, in order to avoid a phase transition between weak coupling and strong coupling phases. This approach has been shown to improve the scaling of masses calculated for the glueball spectrum.

## 3.5 Summary

In this Chapter we have seen how the expansions of Wilson loops may be combined to improve the action by removing the classical error terms arising from the lattice discretization of space-time. This process can be extended to any number of loops (in principle), allowing us to remove the errors to any order in $a$. In practice however we have chosen to eliminate the errors up to and including order $\mathcal{O}(a^4)$. We have also seen how tadpole improvement may be employed to improve the action by renormalizing the value of each loop, eliminating the non-classical error terms arising from self-couplings of the gluon fields. In the next Chapter we shall look at the topology of gauge fields and turn our attention to improving the calculation of the topological charge analogously with the improvement of the action.

# Chapter 4

# Topology and Instantons

*"To use the rigorous method of 'handwaving' for solving problems more complex than the addition of positive real integers."*

Item 3

*The Physicists' Bill of Rights*

Anonymous

When we perform simulations on the lattice we attempt to de-emphasise the finite volume of our lattices by imposing periodic boundary conditions to eliminate the existence of an "edge" (although this is not a necessary feature of lattice simulations, and other boundary conditions may be employed). For these reasons it should be specified that what we are studying is an approximation to true QCD, an $SU(3)$ theory on a 4-toroidal mesh of discrete points which approaches full QCD as we take the limit $a \to 0$ (continuum limit), followed by the limit $V \to \infty$ (infinite volume limit). It is expected that topological structures in the $SU(3)$ gauge fields will play a significant role in the physics we simulate on the lattice, and so we would like to examine the field topology that emerges in

the continuum when we examine the semi-classical (low action) solutions to the field equations. We shall find structures that are analogous to particles, and are referred to as instantons and anti-instantons [25]. The presence of instantons and anti-instantons in the QCD vacuum is believed to have an effect on the nature of hadronic physics [10] [14], specifically by acting as "potential wells" which quarks may hop between, thus affecting the possible combination of these quarks to form composite hadronic particles. Both types of pseudo-particles have an associated action of $S_0 = 8\pi^2/g^2$. Instantons in the continuum carry a topological "charge" of $+S_0$, while anti-instantons carry a corresponding charge of $-S_0$. In coming Chapters we shall see that since instantons have discrete action and topological charge, one test of the validity of our simulations is associated with counting the number of instantons and anti-instantons on the lattice.

## 4.1 Homotopy Classes

To understand properly what instantons are and what we mean by topological charge, we will first discuss some introductory topology. Consider the unit circle $e^{i\theta}$ and consider two functions;

$$\begin{aligned} f_0(\theta) &= \exp\{i(n\theta + \theta_0)\} \\ f_1(\theta) &= \exp\{i(n\theta + \theta_1)\}. \end{aligned}$$

Consider also the function

$$F(\theta, t) = \exp\{i[n\theta + (1-t)\theta_0 + t\theta_1]\}.$$

Obviously $F(\theta, 0) = f_0(\theta)$ and $F(\theta, 1) = f_1(\theta)$. We see that $F(\theta, t)$ is a continuous function, and both $f_0(\theta)$ and $f_1(\theta)$ map the unit circle to itself ($S^1 \to S^1$). Since $f_0(\theta)$ and $f_1(\theta)$ may be continuously deformed into each other we say that they are *homotopic* to each other, and $F(\theta, t)$ is called a *homotopy* of these functions.

We will further notice that $f_0(\theta)$ and $f_1(\theta)$ map from a single rotation around the unit circle (the domain is $\theta \in \{0, 2\pi\}$) to $n$ rotations around the unit circle (the range is $f(\theta) \in \{0, 2n\pi\}$). This gives us a sense that the functions $f_0(\theta)$ and $f_1(\theta)$ 'wind around' the unit circle $n$ times, and we call $n$ the 'winding number' or Pontryagin index of these functions. We can therefore divide the space of such mappings into subspaces, called *homotopy classes* or *equivalence classes*, composed of all the functions with the same winding number which can be deformed into each other. Each homotopy class is then characterised by its winding number. This is represented in Figure 4.1. It is also easy and important to observe that we can generate transformations which map between different homotopy classes. A simple example of this is to take powers of the mapping with the lowest non-trivial winding number ($n = 1$)

$$f(\theta) \;=\; e^{i\theta}$$

and produce mappings with higher winding numbers

$$f(\theta)^n \;=\; e^{i\theta n}.$$

One example of a mapping which will become important later is the general function

$$f(x) = \exp\left\{\frac{i\pi x n}{(x^2+\rho^2)^{1/2}}\right\}. \tag{4.1}$$

It is easy to show that the winding number, given by the equation

$$n = \frac{1}{2\pi}\int_{-\infty}^{+\infty} dx\Big(-if^{-1}(x)\partial_x f(x)\Big) \tag{4.2}$$

reproduces the value $n$.

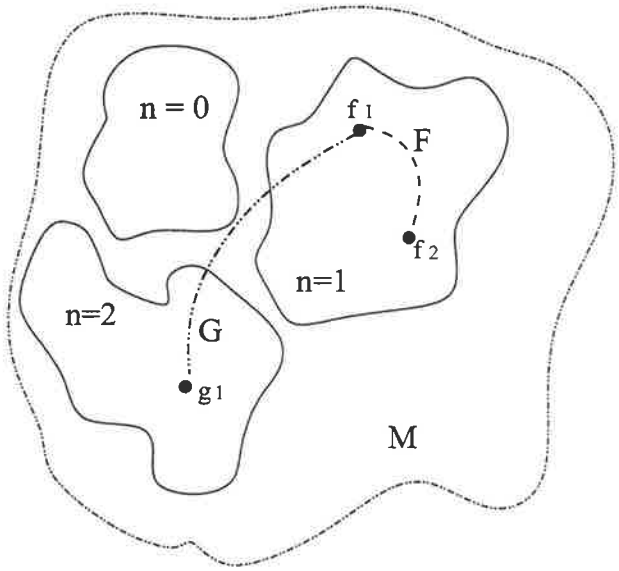


Figure 4.1: The space **M** of mappings from one topological space to another may be subdivided into distinct equivalence classes, each characterised by its own winding number **n**. Homotopies like **F** deform mappings into other mappings within one equivalence class. We can also define mappings like **G** between different equivalence classes.

## 4.2 Vacuum States

Let us begin this Section by noting that points in $n-$dimensional Euclidean space as $|x| \to \infty$ define the same topology as the points on the surface of a sphere $S^{n-1}$ (Figure (4.2)). Therefore, $\mathbb{R}^4$ as $|x| \to \infty$ is topologically equivalent to $S^3$. Now consider the gauge group $SU(2)$.[1] $SU(2)$ is defined by three parameters, since all elements of the group can be written in the form $U = \exp\{i\epsilon.\tau\} =$

[1]Since any group $SU(N)$ can be constructed from subgroups which are elements of $SU(2)$, the results of the following Sections will readily generalise to arbitrary values of $N$, so long as $N \geq 2$.

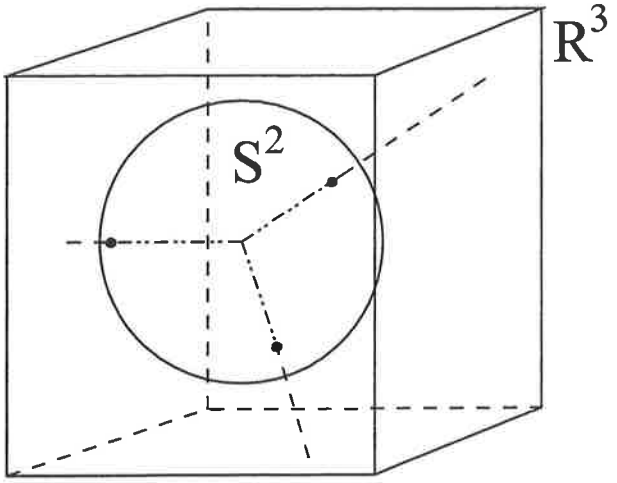


Figure 4.2: Points at infinity in Euclidean $n-$space can be uniquely defined by $n-1$ angles $\theta_1, \theta_2, ..\theta_{n-1}$ and therefore may be treated as if they were points on a sphere $S^{n-1}$.

$a_0\mathbb{1} + i\vec{a}.\vec{\tau}$. We can see that

$$a_0^2 + \vec{a}^2 = 1 \tag{4.3}$$

from the property $UU^\dagger = U^\dagger U = \mathbb{1}$. Clearly Equation (4.3) is the equation of a sphere, so we are justified in treating $SU(2)$ as topologically equivalent to $S^3$. The value of the gauge fields at any point in space is given by a function which assigns an element of the gauge group manifold (in this case $SU(2)$) to each point in space-time. In other words the vacuum state is a mapping from $\mathbb{R}^4 \rightarrow SU(2)$, which as we have just seen is equivalent to a mapping $S^3 \rightarrow S^3$. It seems reasonable to anticipate that such mappings exhibit a winding number, as did the simple $S^1 \rightarrow S^1$ mappings we examined above. In the $SU(2)$ case, we find [26] that the generalisation of Equation (4.2) yields

$$n = \frac{-1}{2\pi} \int_{-\infty}^{+\infty} d^3x \, (\epsilon_{ijk} A_i A_j A_k) \tag{4.4}$$

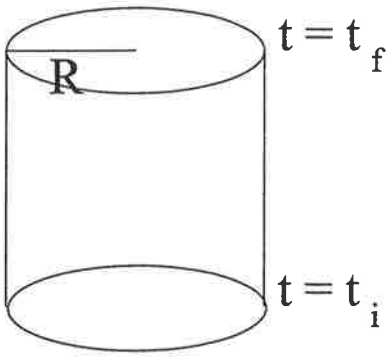


Figure 4.3: Space-time within a hyper-cylinder capped by two 3-spheres, with extent $t_f - t_i$ in the time direction.

where

$$A_i(x) = f^{-1}(x)\partial_i f(x). \tag{4.5}$$

Let us now consider some region of space-time contained within a hyper-cylinder, with extent $t \in [t_i, t_f]$ in the temporal direction. We require that $F_{\mu\nu}(x) \to 0$ at spatial infinity, so that the action will be finite, but as we have already seen $|x| \to \infty$ in $n+1$ dimensions defines the same geometry as the sphere $S^n$ and so we shall say that $F_{\mu\nu}(x) = 0$ outside some very large radius $|x| = R$ as depicted in Figure 4.3. From this point on we shall work in the temporal gauge $A_4(x) = 0$ for simplicity, although our results shall be gauge-invariant and therefore this choice does not matter.

Under a gauge transformation $G$ we have that

$$A_\mu \to A'_\mu = G^{-1}A_\mu G + G^{-1}\partial_\mu G. \tag{4.6}$$

In order for the action to be finite we require that $F_{\mu\nu} \to 0$ as $|x|$ goes to infinity. At first glance this may appear to imply that the fields go to zero at infinity, but

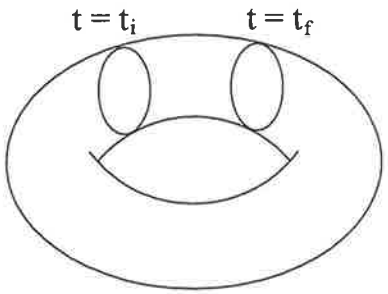


Figure 4.4: A hyper-cylinder section of a space-time torus capped by two spheres ($S^2$), with extent $t_f - t_i$ in the time direction.

in fact it only requires the weaker condition

$$A_\mu(x) \to A'_\mu(x) = G^{-1}\partial_\mu G \tag{4.7}$$

as $|x|$ goes to infinity, which in turn implies that

$$A_4(x) \to A'_4(x) = 0 = \partial_4 G \tag{4.8}$$

because of our gauge-fixing condition. The requirement that $F_{\mu\nu}(x) = 0$ as $|x| \to \infty$ means that the field is pure gauge and time-independent

$$A_i(x) \to A'_i(\vec{x}) = G^{-1}\partial_i G \quad \text{where} \quad i = 1, 2, 3. \tag{4.9}$$

Let us choose a form for the gauge field at the top and bottom surfaces of our hyper-cylinder to be pure gauge and have $A_\mu(\vec{x})$ be independent of direction $\vec{x}$ as $|\vec{x}| \to \infty$. This latter condition ensures that the gauge field on these surfaces has finite energy. In $3+1$ space-time this implies that at $t = t_i$ and $t = t_f$ the gauge field is given by a pure gauge mapping of $S^3 \to SU(2)$. Since at $t = t_i$ and $t = t_f$ the gauge field is pure gauge and since we have $A_\mu(\vec{x})$ independent of direction as $\vec{x} \to \infty$ on these surfaces, we can compactify these surfaces to $S^3$ and hence define a winding number on each surface,[2] $n_i$ and $n_f$, for the $t_i$ and

[2]This is of course analogous to mapping $\mathbb{R}^2 \cup \{\infty\}$ to a sphere $S^2$ with the "north pole" identified with all points at infinity.

$t_f$ surfaces respectively. These integers $n_i$ and $n_f$ characterize different classical vacua of QCD and we can study the tunnelling between them. The difference of the winding numbers $n_f - n_i$ will be identified with the "topological charge" between the equal time surfaces $t_i$ and $t_f$. If $n_f - n_i = 1$ the tunnelling probability [27] is given by the exponential

$$\exp\{-S_{\text{inst}}\}, \tag{4.10}$$

where $S_{\text{inst}}$ is the action associated with a single instanton. In the next Section we will determine this value and relate it to the topological charge.

As we are working in the temporal gauge, Equation (4.6) implies that $G$ takes the form [28]

$$\partial_4 G(x) = -A_4(x)G(x), \tag{4.11}$$

which in turn implies that

$$G(x) = \exp\left\{\frac{\pm\vec{\tau}.\vec{x}}{g(x^2+\rho^2)^{1/2}}\left(\tan^{-1}\frac{x_4}{(x^2+\rho^2)^{1/2}} + \theta_0\right)\right\}. \tag{4.12}$$

Since we are free to choose a value for the integration constant $\theta_0$ we define it to be

$$\theta_0 = \left(n + \frac{1}{2}\right)\pi, \tag{4.13}$$

then if we take the spatial components of $A_\mu(x)$ to be zero at $x_4 = \pm\infty$ it follows that as the field configuration evolves from time $x_4 = -\infty$ to $x_4 = +\infty$

$$G(x)|_{x_4=-\infty} = \exp\left\{i\pi\frac{\pm\vec{\tau}.\vec{x}}{g(x^2+\rho^2)^{1/2}}n\right\} \tag{4.14}$$

and

$$G(x)|_{x_4=+\infty} = \exp\left\{i\pi\frac{\pm\vec{\tau}.\vec{x}}{g(x^2+\rho^2)^{1/2}}(n+1)\right\}. \tag{4.15}$$

We therefore see that the instanton field defines a gauge transformation that continuously deforms a vacuum state with winding number $n$ into a vacuum state

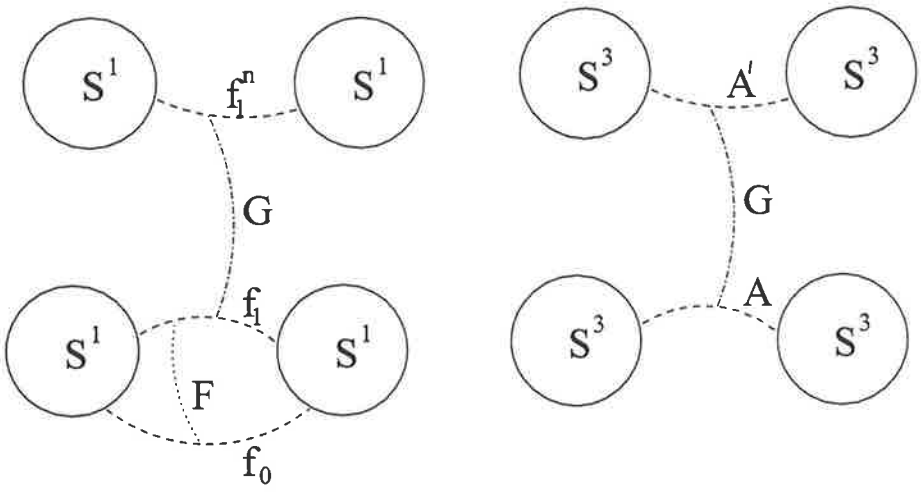


Figure 4.5: Comparison of mappings between homotopy classes and gauge transformations between vacuum states. The function $F$ is a homotopy that connects the mappings $f_0$ and $f_1$ within the same class. The function $G$ represents mapping $f_1$ to $f_1^n$. Analogously a gauge transformation $G$ takes us from one vacuum state $A$ to another state $A'$ with a different winding number.

with winding number $n+1$. The gauge transformation defined by an instanton is therefore a mapping between homotopy classes that differ by one unit of winding number. Figure 4.5 represents this situation, and compares it with the situation discussed for $S^1 \to S^1$ mappings dealt with in Section 4.1 We therefore conclude that if the vacuum state at $t = t_i$ has a different winding number to that at $t = t_f$, then somewhere within our hyper-cylinder there will exist an instanton which tunnels between the two vacuum states. If we now embed our hyper-cylinder within a 4-torus as in Figure 4.4 we see that if we wrap the initial and final times around completely so that the vacuum states are equal, the winding within the hyper-cylinder must be contained within the transformation $G$.

## 4.3 Instanton Solutions to Field Theory

Let us now turn our attention to the type of structures we expect to see in the continuum occurring as classical (low-action) solutions to the field equations. Is a trivial condition, in which the action is zero everywhere, the only stable minimum action solution? At first this may be what we expect, but in 1975 Belavin *et al.* [8] showed that it is possible for non-zero local minima of the action to exist. These solutions are non-dissipative configurations whose (finite) energy remains localised rather than being radiated to infinity (although we shall see that they have an arbitrary scale and hence may approach infinite size). We shall now follow their reasoning to deduce the form of the solutions to Euclidean Yang-Mills theory in $SU(2)$ which we identify as instantons. This theory is characterised by the action

$$S_E = \frac{1}{2g^2}\int d^4x \mathrm{Tr}(F_{\mu\nu}F^{\mu\nu}) \tag{4.16}$$

with the gauge fields

$$A_\mu = \sum_{a=1}^{3} \frac{\tau^a}{2} A_\mu^a, \tag{4.17}$$

the field strength tensor

$$F_{\mu\nu} = \sum_{a=1}^{3} \frac{\tau^a}{2} F_{\mu\nu}^a \tag{4.18}$$

(remember that we're working in $SU(2)$ not $SU(3)$, so there are three generators, not eight, and the $\tau^a$ are the three Pauli matrices), and the Lagrangian density

$$\mathcal{L} = \frac{1}{2g^2}\mathrm{Tr}F_{\mu\nu}F^{\mu\nu} \tag{4.19}$$

with $A_\mu \to iA_\mu/g, F_{\mu\nu} \to iF_{\mu\nu}/g$ for convenience, as per [28]. It follows therefore that

$$F_{\mu\nu} = \partial_\mu A_\nu - \partial_\nu A_\mu + [A_\mu, A_\nu] \tag{4.20}$$

is the field strength tensor, and the dual field strength tensor is defined by

$$\widetilde{F}_{\mu\nu} = \frac{1}{2}\epsilon_{\mu\nu\lambda\rho}F_{\lambda\rho}. \tag{4.21}$$

We may write the winding number of a configuration in terms of the (unobservable) gauge-dependent current [28] [29]

$$K_\mu = -\epsilon_{\mu\nu\lambda\rho}\mathrm{Tr}(A_\mu\partial_\lambda A_\rho + \frac{2}{3}A_\nu A_\lambda A_\rho). \tag{4.22}$$

It can be easily shown that

$$\partial_\mu K_\mu = -\frac{1}{2}\mathrm{Tr}F_{\mu\nu}\widetilde{F}_{\mu\nu}. \tag{4.23}$$

Therefore we may convert between a volume integral and a surface integral over $S^3$ at infinity

$$\int d^4x \mathrm{Tr}F_{\mu\nu}\widetilde{F}_{\mu\nu} = \frac{1}{2}\int_S d\sigma_\mu K_\mu. \tag{4.24}$$

Rewriting $K_\mu$ in terms of the $A_\mu$ and comparing with Equation (4.4) we find that

$$n = \frac{1}{16\pi^2}\int d^4x \mathrm{Tr}F_{\mu\nu}\widetilde{F}_{\mu\nu}. \tag{4.25}$$

Let us now look at the action of a field configuration. It is trivial to see that

$$\mathrm{Tr}\int (F_{\mu\nu} \pm \widetilde{F}_{\mu\nu})^2 d^4x \geq 0 \tag{4.26}$$

and we can show that

$$(F_{\mu\nu} \pm \widetilde{F}_{\mu\nu})^2 = 2(F_{\mu\nu}F_{\mu\nu} \pm F_{\mu\nu}\widetilde{F}_{\mu\nu}), \tag{4.27}$$

because $F_{\mu\nu}F_{\mu\nu} = \widetilde{F}_{\mu\nu}\widetilde{F}_{\mu\nu}$ and $F_{\mu\nu}\widetilde{F}_{\mu\nu} = \widetilde{F}_{\mu\nu}F_{\mu\nu}$ from the Equation (4.21) and the properties of the Levi-Cevita symbol. Therefore we have

$$\begin{aligned}
\frac{1}{2}\int \mathrm{Tr}(F_{\mu\nu} \pm \widetilde{F}_{\mu\nu})^2 d^4x &\geq 0 \\
\Rightarrow \frac{1}{2}\int \mathrm{Tr}(F_{\mu\nu}F_{\mu\nu} \pm F_{\mu\nu}\widetilde{F}_{\mu\nu}) d^4x &\geq 0 \\
\Rightarrow \frac{1}{2}\int d^4x \mathrm{Tr}F_{\mu\nu}F_{\mu\nu} &\geq |\frac{1}{2}\int d^4x \mathrm{Tr}F_{\mu\nu}\widetilde{F}_{\mu\nu}| \\
\Rightarrow S_E &\geq |\frac{1}{2}\int d^4x \mathrm{Tr}F_{\mu\nu}\widetilde{F}_{\mu\nu}| = 8\pi^2 n \\
\Rightarrow S_E &\geq \frac{8\pi^2 n}{g^2} \equiv S_0 n, \qquad (4.28)
\end{aligned}$$

where we have used Equation (4.25). Clearly the Euclidean action is bounded below by the quantity $S_0 n$ and is minimised when $F_{\mu\nu} = \pm\widetilde{F}_{\mu\nu}$ i.e., when the configuration is locally self-dual or anti-self dual. It is obvious that the trivial solution $A_\mu = 0$ with winding number $n = 0$ satisfies this self-duality condition. What is interesting is that other non-trivial solutions are also allowed.

Without going into explicit detail [8] let us just state that $SU(2)$ transformations of the form

$$G(x) = \frac{x_4 \pm i\vec{x}.\vec{\tau}}{(x^2)^{1/2}}, \qquad (4.29)$$

where $x^2 = x_4^2 + \vec{x}^2$ give rise to a gauge field

$$A_4(x) = \frac{\pm\vec{\tau}.\vec{x}}{g(x^2+\rho^2)}, \qquad \vec{A}(x) = \frac{((\vec{\tau}\times\vec{x}) \mp \vec{\tau}x_4)}{g(x^2+\rho^2)} \qquad (4.30)$$

for $x \gg \rho$ where $\rho$ is an arbitrary parameter usually referred to as instanton size [28]. Note that we are working in Euclidean space-time and so the time component of 4-vectors carries the fourth index, not the zeroth.

Given the name 'instantons' and the fact that they have a charge-like property which is conserved in interactions (analogously with the processes of pair-creation and annihilation observed with fermions) it is tempting to think of them as particles. However the standard interpretation of instantons treats them as tunnelling

amplitudes between vacuum states with different winding numbers (as we have seen in Equations (4.14) and (4.15)).

The topological charge may be related to a quantity called the Chern-Simons term which is related to the current $K_\mu$ in an obvious manner [30]

$$CS[A_i] = -\int d^3x \epsilon_{ijk} \mathrm{Tr}(A_i \partial_j A_k + \frac{2}{3} A_i A_j A_k). \tag{4.31}$$

At classical minima this quantity is related to the winding number

$$\begin{aligned} CS[U^{-1}\partial_i U] &= \frac{1}{3}\int d^3x \epsilon_{ijk} \mathrm{Tr}(U^{-1}\partial_i U U^{-1}\partial_j U U^{-1}\partial_k U) \\ &= 8\pi^2 n_U, \end{aligned}$$

where $n_U$ is the winding number of $U$. We can show that the winding number is additive since

$$CS[U^{-1}A_i U + U^{-1}\partial_i U] = CS[A_i] + \frac{1}{3}\int d^3x \epsilon_{ijk} \mathrm{Tr}(U^{-1}\partial_i U U^{-1}\partial_j U U^{-1}\partial_k U). \tag{4.32}$$

We therefore deduce that the topological charge in the case of a tunnelling event from a state $\vec{A} = 0$ to a state $\vec{A} = U^{-1}\partial_i U$ as illustrated in Section 4.2 is given by

$$Q \propto CS[U^{-1}\partial_i U] - CS[0]. \tag{4.33}$$

The topological charge associated with an instanton is therefore the *difference* of the winding numbers of the vacuum states between which it tunnels,

$$Q = n_f - n_i. \tag{4.34}$$

As noted in Chapter 1 instantons are believed to play an important role in hadronic physics by acting as "potential wells" within the gluon fields, modifying the manner in which quarks may associate with each other, dependent upon their flavours and chiralities. The density of instantons within the QCD vacuum may therefore be expected to play a major role in determining the type of hadrons that are permitted to form, and their physical properties.

## 4.4 Summary

In this Chapter we have made a cursory examination of the non-trivial local minima of the Yang-Mills action in the continuum. These solutions to classical Yang-Mills theory are referred to as instantons. We have seen that they are self-dual field configurations which correspond to tunnelling events between vacuum states with different winding numbers. We have furthermore seen that instantons (and in the anti-self dual case, anti-instantons) have an associated action of $S_0 = 8\pi^2/g^2$ (independent of their size) and a quantity called topological charge which is related to their role as tunnelling amplitudes. It follows from these observations that in a configuration consisting purely of instantons and anti-instantons the total action and topological charge will fulfil the conditions $S/S_0 = n_I + n_A$ and $Q = n_I - n_A$ where $n_I$, $n_A$ are the number of instantons and anti-instantons respectively.

In the coming Chapters we shall use the action and topological charge as important "observables" in our lattice simulations. In the next Chapter we shall turn to the task of eliminating discretization errors from the lattice topological charge operator, in analogy to the improvement of the action carried out in Chapter 3.

# Chapter 5

# Topology on the Lattice

*"Science is a way of trying not to fool yourself."*

Richard Feynmann

In order to study topology on the lattice, we can take the straightforward step of shifting the continuum formula for the $SU(3)$ topological charge, which is an integral over all space-time of the charge density [31]

$$q(x) = \frac{1}{32\pi^2}\epsilon_{\mu\nu\rho\sigma}\mathrm{Tr}\Big(F_{\mu\nu}(x)F_{\rho\sigma}(x)\Big) \tag{5.1}$$

to the lattice, and replace the integral in the continuum with a sum over all lattice sites.

$$Q = \sum_x q(x). \tag{5.2}$$

As one would expect, discretization errors affect the lattice topological charge operator, and it is desirable to improve this operator analogously with the improvement procedure carried out on the action. There are two obvious ways of achieving this.

The first is to calculate a series of operators $Q_1, ..., Q_5$ which are then combined

to create an improved operator. This method is exactly analogous to the action improvement procedure detailed in Chapter 3.

The second method involves combining loop terms to create an improved version of $F_{\mu\nu}$, and then using this improved field strength tensor directly in Equation (5.4) to perform an improved calculation of the topological charge. Furthermore, since the action is ultimately based upon $F_{\mu\nu}$ it is also possible to directly "reconstruct" the action from the improved field strength tensor as an alternative to the procedure used in Chapter 3.

## 5.1 Topology on the Lattice

The $SU(3)$ topological charge in the continuum takes the form

$$Q = \frac{1}{32\pi^2} \int d^4x \epsilon_{\mu\nu\rho\sigma} F_{\mu\nu} F_{\rho\sigma}. \tag{5.3}$$

Correspondingly the $SU(3)$ topological charge density on the lattice is given by

$$q(x) = \frac{1}{m^2 n^2} \frac{1}{32\pi^2} \epsilon_{\mu\nu\rho\sigma} F_{\mu\nu}^{(m\times n)}(x) F_{\rho\sigma}^{(m\times n)}(x) \tag{5.4}$$

and we sum over all lattice sites (equivalently to taking the integral in the continuum form) to obtain the total topological charge.

To determine the topological charge we choose to calculate $F^{(m\times n)}$ not from a single $m \times n$ loop but from the clover term (Figure (5.1)) used in the Sheikholeslami-Wohlert improved quark action [32] [33]. In the standard clover term we would set $m = n = 1$, so that we are making a calculation based on the plaquette.

Just as it is desirable to improve the action to obtain more continuum-like results, so it is desirable to produce an improved topological charge operator. de Forcrand *et al.* calculate the topological charge operator using a variation of the standard clover operator which is improved similarly to the action. That is, they employ

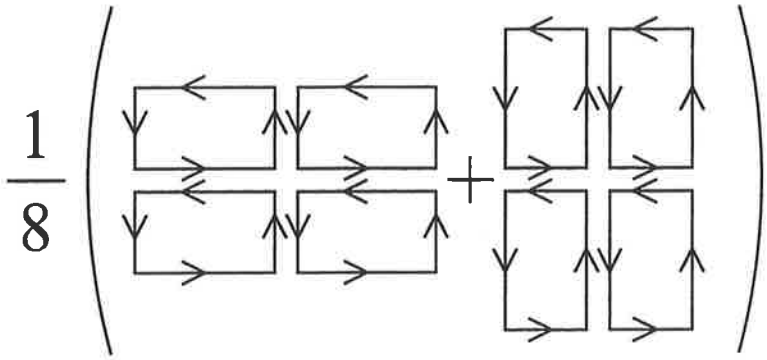

Figure 5.1: The four $m \times n$ loops and four $n \times m$ loops used to construct the clover term from which we determine the topological charge. Notice that this reduces to one-eighth of eight plaquettes in the case $m = n = 1$.

a set of loops of various sizes to calculate a set of topological charge operators $Q_1, ..., Q_5$ based upon clover terms corresponding to different choices of $m$ and $n$. These operators are then combined, each being weighted by a constant, so as to produce an improved topological charge operator. Their $N$-loop improved topological charge operator is therefore defined as

$$\sum_{i=1}^{N} c_i Q_i, \tag{5.5}$$

where the $c_i$ are improvement constants (de Forcrand *et al.* use the same values as in the improved action [3]), and the $Q_i$ are topological charge operators corresponding to a particular choice of $m \times n$ loop. In our construction of the improved action and topological charge operators we have chosen to incorporate appropriate tadpole improvement factors, $u_0$, the values of which are updated during the cooling process, however de Forcrand *et al.* use a fixed mean-link value of one.

There is another way of improving the topological charge which we have chosen to employ, and which is the topic of the next Section.

## 5.2 Improving the Field-Strength Tensor

Consider the form taken by the equation for the expansion of the $(1 \times 1)$ loop operator

$$W_{\mu\nu}^{(1\times1)} = e^{ig\oint Adx} = \left\{1 + ig\oint Adx - \frac{g^2}{2}(\oint Adx)^2 + ...\right\}. \tag{5.6}$$

The third term on the right-hand side is simply the second term squared, so in principle we can construct both the action (which requires the first and third terms) and the topological charge (which requires only the second term) from the second term on the right. In order to extract this term we cannot simply take the imaginary part of $W_{\mu\nu}^{(1\times1)}$ since $A$ has real and imaginary parts. Instead we make the following construction

$$\begin{aligned} W_{\mu\nu}^{(1\times1)} &= 1 + ig\oint Adx - \frac{g^2}{2}(\oint Adx)^2 + \mathcal{O}(g^3) \\ W_{\mu\nu}^{(1\times1)\dagger} &= 1 - ig\oint Adx - \frac{g^2}{2}(\oint Adx)^2 + \mathcal{O}(g^3). \end{aligned}$$

Hence we have

$$\Rightarrow \frac{-i}{2}\left(W_{\mu\nu}^{(1\times1)} - W^{(1\times1)\dagger} - \frac{1}{3}\mathrm{Tr}(W_{\mu\nu}^{(1\times1)} - W_{\mu\nu}^{(1\times1)\dagger})\right) = g\oint Adx + \mathcal{O}(g^3) \tag{5.7}$$

where we have subtracted one-third of the trace to enforce the tracelessness of the Gell-Mann matrices.

This definition introduces an extremely important difference between the improved action and the improved topological charge operator in our calculation. Rectangular loops in perpendicular directions must be added and averaged. But to calculate the action, the terms corresponding to Equation (2.48) are squared first, while for the topological charge the rectangular terms are averaged and then the result is squared. This makes the values of the $\mathcal{O}(a^8)$ terms in the topological

charge operator different from those in the action, and therefore we would expect the improvement coefficients $k_1, ..., k_5$ to be different to the values of the action improvement constants $c_1, ..., c_5$. In the next Section we shall look in more detail at determining the values of these constants[1].

In order to construct an improved field-strength tensor we will need to expand the integral term in the Wilson loop operator, to determine the coefficients of the terms at various orders in $a$. We can do this in the manner described in Section 2.5 using Green's theorem to convert the surface integral to a double integral. But first, since we intend to calculate the topological charge from a clover term we must calculate a series of clover terms, then combine these to create our improved $F_{\mu\nu}$, and construct the topological charge operator from this tensor.

Let us begin by following similar steps to those used in the improvement of the action. We define

$$\begin{aligned}
\mathcal{A} &\equiv a^2 F_{\mu\nu} \\
\mathcal{B} &\equiv a^4 \left(D_\mu^2 + D_\nu^2\right) F_{\mu\nu} \\
\mathcal{C} &\equiv a^6 \left(D_\mu^4 + D_\nu^4\right) F_{\mu\nu} \\
\mathcal{D} &\equiv a^6 \left(D_\mu^2 D_\nu^2\right) F_{\mu\nu}.
\end{aligned}$$

Let us now denote by $C^{(m,n)}$ the combination of terms extracted from the expansion of a Wilson loop as per Equation (5.7) corresponding with the loops used to construct a clover term (Figure 5.1). Hence from Equation (2.46) with

[1] de Forcrand *et al.* use $c_1, ..., c_5$ for the improvement of both the action and topological charge, as their improved operators are constructed from a combination of unimproved operators built from individual loops. By contrast we construct an improved field-strength from combinations of loops, and define our improved operators from this quantity.

appropriate choices of integration limits, we see that

$$\begin{aligned} C^{(m,n)} = \tfrac{1}{8} \Bigg\{ & \int_0^{ma} dx_\mu \int_0^{na} dx_\nu \left(\partial_\mu A_\nu - \partial_\nu A_\mu\right) \\ & + \int_{-ma}^{0} dx_\mu \int_0^{na} dx_\nu \left(\partial_\mu A_\nu - \partial_\nu A_\mu\right) \\ & + \int_{-ma}^{0} dx_\mu \int_{-na}^{0} dx_\nu \left(\partial_\mu A_\nu - \partial_\nu A_\mu\right) \\ & + \int_0^{ma} dx_\mu \int_{-na}^{0} dx_\nu \left(\partial_\mu A_\nu - \partial_\nu A_\mu\right) \\ & + \int_0^{na} dx_\mu \int_0^{ma} dx_\nu \left(\partial_\mu A_\nu - \partial_\nu A_\mu\right) \\ & + \int_{-na}^{0} dx_\mu \int_0^{ma} dx_\nu \left(\partial_\mu A_\nu - \partial_\nu A_\mu\right) \\ & + \int_{-na}^{0} dx_\mu \int_{-ma}^{0} dx_\nu \left(\partial_\mu A_\nu - \partial_\nu A_\mu\right) \\ & + \int_0^{na} dx_\mu \int_{-ma}^{0} dx_\nu \left(\partial_\mu A_\nu - \partial_\nu A_\mu\right) \Bigg\} . \end{aligned} \tag{5.8}$$

In order to determine the forms of these elements of the clover term we may use the *Mathematica* package detailed in Appendix A. We find that

$$C^{(1,1)} = \mathcal{A} + \frac{1}{6}\mathcal{B} + \frac{1}{120}\mathcal{C} + \frac{1}{36}\mathcal{D}$$

$$C^{(2,2)} = 4\mathcal{A} + \frac{8}{3}\mathcal{B} + \frac{8}{15}\mathcal{C} + \frac{16}{9}\mathcal{D}$$

$$C^{(1,2)} = 2\mathcal{A} + \frac{5}{6}\mathcal{B} + \frac{17}{120}\mathcal{C} + \frac{2}{9}\mathcal{D}$$

$$C^{(1,3)} = 3\mathcal{A} + \frac{5}{2}\mathcal{B} + \frac{41}{40}\mathcal{C} + \frac{3}{4}\mathcal{D}$$

$$C^{(3,3)} = 9\mathcal{A} + \frac{27}{2}\mathcal{B} + \frac{243}{40}\mathcal{C} + \frac{81}{4}\mathcal{D}$$

and of course we also include appropriate tadpole improvement factors. Notice that since the order $\mathcal{O}(a^6)$ terms in each $F_{\mu\nu}$ will be "promoted" to $\mathcal{O}(a^8)$ (and

Table 5.1: Coefficients from various loops, for the expansion of $F_{\mu\nu}$.

| | $\mathcal{A}$ | $\mathcal{B}$ | $\mathcal{C}$ | $\mathcal{D}$ |
|---|---|---|---|---|
| (1,1) | 1 | $\frac{1}{6}$ | $\frac{1}{120}$ | $\frac{1}{36}$ |
| (2,2) | 4 | $\frac{8}{3}$ | $\frac{8}{15}$ | $\frac{16}{9}$ |
| (1,2) | 2 | $\frac{5}{6}$ | $\frac{17}{120}$ | $\frac{2}{9}$ |
| (1,3) | 3 | $\frac{5}{2}$ | $\frac{41}{40}$ | $\frac{3}{4}$ |
| (3,3) | 9 | $\frac{27}{2}$ | $\frac{243}{40}$ | $\frac{81}{4}$ |

higher) by taking the product $F_{\mu\nu}F_{\rho\sigma}$, while the $\mathcal{O}(a^8)$ terms will be promoted to $\mathcal{O}(a^{10})$ (and higher). Consequently since we wish to eliminate $\mathcal{O}(a^8)$ errors from the product, we need only expand out to (and eliminate) order $\mathcal{O}(a^6)$ corrections in $F_{\mu\nu}$. We therefore have five equations and four unknowns, so we may freely solve the equations arising from the values listed in Table 5.1.

Next, as in Section 3.3 we construct a matrix from the values of these coefficients and perform Gauss-Jordan elimination to determine the values of the improvement constants. We find that they are

$$\begin{aligned} k_1 &= 19/9 - 55k_5 \\ k_2 &= 1/36 - 16k_5 \\ k_3 &= 64k_5 - 32/45 \\ k_4 &= 1/15 - 6k_5 \end{aligned}$$

and once again the coefficient of the $3 \times 3$ loop (in this case $k_5$) is a tunable free parameter. We can see that if we set $k_5 = 1/90$ we will make $k_2 = k_4 = 0$, eliminating the contribution from the $C^{(1,2)}$ and $C^{(1,3)}$ loops - creating a "3-loop" improved field strength tensor. We may create a "4-loop" improved field strength tensor in three different ways, by setting $k_5 = 0, 19/495$, or $1/576$. For simplicity we have concentrated on a 4-loop improved tensor with $k_5 = 0$ throughout this

investigation, as we have seen no evidence that either of the other two choices produce a better operator, in preliminary investigations. From now on when we refer to the 4-loop improved field strength tensor, topological charge, or reconstructed action we shall mean that $k_5 = 0$ rather than either of the other two possible values.

In this thesis we shall use the value $k_5 = 1/20$ when we calculate a 5-loop improved field strength tensor, analogous to the improved action.

## 5.3 The Reconstructed Action

As mentioned in the introduction to this Chapter, the topological charge operator is not the only useful operator which can be constructed from the improved $F_{\mu\nu}$. We may also square our improved $F_{\mu\nu}$ and construct an improved action from it, to compare with the improved action we have already calculated. This simple procedure merely involves taking the improved tensor we have already described above, with the same improvement coefficients, and inserting it directly into the equation for the Yang-Mills action on the lattice,

$$S = \beta \sum_x \sum_{\mu,\nu} \frac{1}{2} g^2 a^4 F_{\mu\nu}^2. \tag{5.9}$$

This "reconstructed" action may serve to let us double-check that the improvement scheme for $F_{\mu\nu}$ is in agreement with the standard improvement scheme for the action. Since the improvement constants are different to those previously calculated for the action the comparison of the "reconstructed" action with the corresponding improved action[2] should serve to provide two separate lines of analysis.

[2]From now on we shall refer to the reconstructed action and the cooling action, for reasons which will become clear in Chapter 6.

## 5.4 Summary

In this Chapter we have seen how the continuum form of the topological charge operator may be transferred to the lattice. After considering one method of removing discretization errors from the topological charge operator, we have detailed a method based on the direct improvement of the lattice field strength tensor. This improved tensor may be inserted into the definitions of the topological charge and the Yang-Mills action.

The reconstructed action which we obtain from this procedure is a useful tool for checking the validity of our improvement schemes, since we would hope that the cooling action and reconstructed action (when both constructed from the same number of loops) will calculate consistent values for the action of any given configuration. Furthermore, since they are constructed in different ways we shall expect that they will differ in the size of their discretization errors at $\mathcal{O}(a^6)$ (in other words, at orders higher than the order of improvement). Therefore the magnitude of the discrepancies between the cooling action and the reconstructed action indicate the relative magnitude of the $\mathcal{O}(a^6)$ errors in each.

The improved topological charge operator is an important tool for determining the number of instantons present in a configuration. These operators shall be put to direct use in the next Chapter.

# Part III

# Results

# Chapter 6

# Results

*"Do not condemn me forever to the treadmill of mathematical calculations. Leave me some room for philosophical speculation - my sole delight."*

Johannes Kepler

We have now reached the point where we understand some of the interesting properties of gauge fields in the continuum and can transfer these to the lattice. When we do so, the values of the fields at any point in space-time are assumed by values assigned to the lattice links. We can use our lattice approximations to compute numerical quantities related to the topological properties of gauge fields, eliminating discretization errors to high order. The approach we shall use to generate fields with non-trivial topology to study is *thermalisation*, which creates Monte-Carlo-generated gauge field configurations, followed by *cooling*, which removes the short-range quantum fluctuations.

The cooling algorithm relies upon a recursive calculation of the local action, followed by a consequent updating of the link values to minimise the local action at each lattice site. We use the improved actions calculated in Sections 3.2 and 3.3

for this purpose and refer to these as the *cooling actions*. The value of the cooling action at each sweep determines how the links are updated in order to minimise the action. The reconstructed actions (Section 5.3) are used as an independent means of assessing the action of the field configuration at each sweep, but play no role in updating the link values. Each iteration, in which the cooling algorithm is applied to each link once and once only, is called a sweep. Each sweep may be thought of as a step that takes us through configuration space towards a minimum value of the action. As the minima of the action at each point in space-time correspond with either a trivial field or an (anti-)instanton, many sweeps (i.e., many iterations of the cooling algorithm) should cause the entire configuration to approach a self-dual configuration.

In the continuum, as we approach self-duality, we would expect a volume of the QCD vacuum to contain some number of instantons and anti-instantons. Since each (anti-)instanton has, in theory, a topological charge of $(-1) + 1$ it is only unpaired (anti-)instantons which will contribute to the topological charge measured in this volume. If we allow the topological structures within the fields to move, instanton-anti-instanton (I-A) pairs will annihilate (since such pairs are not minima of the action) but these annihilation processes will not alter the total topological charge.

On the lattice we expect a similar behaviour. When we apply the cooling algorithm to a field configuration we expect the short-range high-frequency components of the field to be removed rapidly, and as cooling proceeds instanton-anti-instanton (I-A) pairs will move together. We would hope that, as in the continuum, the total topological charge will be given by $Q = n_I - n_A$ where $n_I$ is the number of instantons and $n_A$ is the number of anti-instantons. Unfortunately discretization errors, when too large, can be expected to ruin this result, leading to non-integer topological charge. We would hope that improved topological charge operators will diminish these discretization errors, and therefore

we may judge which improvement scheme works best based upon how close the topological charge it produces comes to an integer value. Since the I-A pairs do not contribute to the total topological charge on the whole lattice we would expect the total charge to settle down after very few cooling sweeps (after the short-range components of the field have been suppressed) and remain roughly constant thereafter. However since all (anti-)instantons will contribute to the action, we should expect that the action will continue to shrink until all I-A pairs annihilate. At this stage we should be converging towards a completely self-dual configuration, consisting solely of instantons or anti-instantons or a trivial background.

In this Chapter we will demonstrate that cooling with an algorithm based on the naive Wilson (plaquette) action eventually erases all information from the lattice, not only eliminating short-range fluctuations and annihilating I-A pairs but spoiling single (anti-)instantons until they disappear altogether. This is because the discretization errors in the plaquette action are so large. We will demonstrate that improved actions alleviate this problem, causing the action to stabilise at a certain point, beyond which the (anti-)instantons do not shrink significantly, in fact remaining stable for hundreds to thousands of cooling sweeps. We will investigate which action is the best using the difference between the achieved stable values and the closest integer, and the duration for which this stability is maintained as criteria. We will similarly assess which topological charge operator is best using the same criteria.

Throughout the remainder of this thesis we shall use the following notation, which was partially introduced in Section 3.3. The $n$-loop improved cooling action, divided by $S_0$, shall be referred to as $S(n)$. The reconstructed action based on an $n$-loop improved field-strength tensor, and likewise divided by $S_0$, will be denoted by $S_R(n)$. Hence we expect that (neglecting discretization errors), in a configuration consisting wholly of instantons and anti-instantons, $S_R(n) = S(n) = n_I + n_A$.

We shall continue to use the notation $S/S_0$ when discussing instanton behaviour in the continuum, or in the general case, when no particular improvement scheme is being considered. The topological charge operator based on an $n$-loop improved field-strength tensor will be denoted $Q(n)$.

## 6.1 Thermalization

In Lattice Gauge Theory the values of the fields at each point in the region of space-time simulated by our lattice are represented by values assigned to the links. In the case of a $U(1)$ theory (QED), the links would assume (complex) scalar values. In the case of the $SU(3)$ theory which is relevant to the study of the QCD vacuum, an $SU(3)$ matrix will be assigned as a value to each of the lattice links. To simulate the quantum nature of the fields, we wish to introduce an element of randomness to these values. However we do not want to assign these values in a completely random manner, since such randomly generated field configurations would most likely have enormous actions, and hence they would correspond to states far from the classically preferred low-action configurations. Therefore the values assigned to the link field configurations must be weighted with an appropriate Boltzmann factor.

The configurations used in our investigations are generated using the Cabibbo-Marinari pseudo-heatbath algorithm [34]. This is a general procedure for updating the values of $SU(N)$ link variables for any value of $N$. In outline, the algorithm consists of the following steps:

- select a set of $SU(2)$ subgroups of $SU(N)$ (call this set $B$) such that there is no left ideal (this means that, with the exception of the whole group, there is no subset of $SU(N)$ which is invariant under left multiplication by $B$). Let us denote each of these subgroups by $SU(2)_i$ for $i = 1, ..., m$

- update each link variable by multiplying each value by $m$ matrices belonging to the subgroups $SU(2)_i$. The new value of the link variable is then given by the product

$$U' = a_m a_{m-1} ... a_1 U, \tag{6.1}$$

where $U$ is the old link value, and the matrices $a_1, ..., a_m$ are selected randomly with the measure

$$dP(a_k) = d^{(k)}a_k \frac{\exp\left\{-\beta S(a_k U^{(k-1)})\right\}}{\int_{SU(2)_k} da \ \exp\{-\beta S(a U^{(k-1)})\}}, \tag{6.2}$$

where $d^{(k)}a_k$ is the Haar measure on $SU(2)_k$ and $a_k \in SU(2)_k$.

We generate $SU(3)$ configurations by working explicitly with three $SU(2)$ subgroups which are then diagonally embedded in $SU(3)$. At each link update we cycle over these $SU(2)$ subgroups twice. From a cold start (all link values set to the identity) we thermalize for 5000 sweeps using a 2-loop improved action and a fixed mean-link value, and then select configurations every 500 sweeps to create an ensemble of configurations with non-trivial topology, but which are statistically distinct from each other.

## 6.2 Cooling

Once the process of thermalization is complete we have a set of gauge field configurations on the lattice to study, however for typical lattice spacings these configurations are extremely "rough", i.e., they vary significantly over very short scales (typically from one lattice site to the next). In order to study the topological structure of the field we need to find a way of smoothing the short-range (ultraviolet) fluctuations out of the fields. Several schemes for doing this have been developed and utilised, but the particular scheme we are concerned with is called

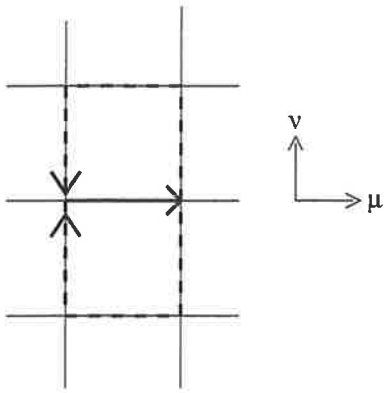


Figure 6.1: The positive and negative staples $\tilde{U}_\mu$ (dotted) adjoining a link $U_\mu$ (bold).

cooling. Cooling is a recursive process which locally drives the action towards a minimum value, but (hopefully) leaves the larger scale structure of the gauge fields unaffected. The algorithm is simple to understand in $SU(2)$ and may be extended to $SU(3)$ by embedding the $SU(2)$ matrices as subgroups within $SU(3)$. Each element of $SU(2)$ may be parametrized as $U = a_0\mathbb{1} + i\vec{a}.\vec{\tau}$ with $a$ real and $a_0^2 + \vec{a}^2 = 1$. We will here consider minimisation of the action calculated from the plaquette for simplicity, so let $\tilde{U}_\mu$ be a staple (the section of the plaquette not including the link to be updated)

$$\tilde{U}_\mu = U_\nu(x+\mu)U_\mu^\dagger(x+\nu)U_\nu^\dagger(x). \tag{6.3}$$

Therefore the plaquette is

$$W_{\mu\nu}^{(1\times 1)} = U_\mu(x)\tilde{U}_\mu. \tag{6.4}$$

Since we calculate the action by summing over all lattice directions at each site there are six staples associated with each link (in the positive and negative directions of the three axes perpendicular to the link - see Figure 6.1). Hence we are

lead to define

$$k\bar{U} = \sum_{\alpha=1}^{6} \tilde{U}_\alpha, \tag{6.5}$$

where $\bar{U}$ is an element of $SU(2)$ and

$$k^2 = \det\left(\sum_{\alpha=1}^{6} \tilde{U}_\alpha\right). \tag{6.6}$$

The local action is proportional to

$$Re\mathrm{Tr}(\mathbb{1} - U_\mu(x)\tilde{U}_\mu), \tag{6.7}$$

which is clearly minimized when we maximize $U_\mu(x)\bar{U}$, i.e., when $Re\mathrm{Tr}(U_\mu(x)\bar{U}) = Re\mathrm{Tr}(\mathbb{1})$. This may be achieved by updating the link values such that

$$U_\mu(x) \longrightarrow \bar{U}^{-1} = \bar{U}^\dagger = \frac{\left(\sum_{\alpha=1}^{6} \tilde{U}_\alpha\right)^\dagger}{k}. \tag{6.8}$$

In practice, a naive cooling scheme based upon the plaquette action will destroy topological structure over the whole lattice if it proceeds for long enough. There are two main ways of dealing with this problem. The first is to use the fact that cooling affects the small-scale properties of the field faster than it affects the large-scale properties and hence try to stop or limit or scale the cooling process at an appropriate stage or in an appropriate manner so that parts of the lattice far from each other remain thermally isolated. The approach we adopt is to cool the lattice using an improved action calculation, on the basis that most of the loss of information in the cooling process comes about because the action we are minimising has discretization errors and hence if we use a more accurate action, the cooling process will become more stable. As detailed previously, our improved action incorporates tadpole improvement which accounts for non-classical self-couplings of the gluon fields. The cooling process rapidly wipes out the short-range fluctuations of the fields, eliminating the small-scale physics responsible for

the perturbative $\mathcal{O}(g)$ and higher corrections to the action mentioned, among other places, in Section 3.1. Similarly the tadpole improvement factor $u_0$ rapidly tends to one. Hence the cooling process makes a classically improved action more accurate over the course of the first few dozen sweeps as these perturbative short-range effects, neglected in the derivation of the improved action, are removed.
Since the cooling iterations gradually bring separated parts of the lattice into contact with each other, as cooling proceeds we should expect to see annihilation of instanton-anti-instanton pairs, as these regions of the field with opposite winding come together and "untwist", like oppositely directed twists in a ribbon spontaneously flattening out.
Throughout the remainder of this Chapter we shall be dealing with configurations that are cooled towards a self-dual configuration containing only instantons or anti-instantons. It is important to note that instantons are completely self-dual objects. For ease of discussion we shall from-time-to-time refer to both nearly-self dual objects and completely self-dual objects as instantons. However, when we need to be precise we shall refer to nearly-self dual objects as pseudo-instantons, because they will become instantons if cooled sufficiently, and completely self-dual objects shall be referred to as true instantons.

## 6.3 Cooling Code used in this Research

The code used to produce the final results contained in this thesis was developed originally as Connection Machine Fortran (CMF) running on a CM-5 supercomputer. This software was then ported across to the Sun super-cluster (Orion) used by the National Computing Facility for Lattice Gauge Theory, and converted to High-Performance Fortran. In its final form, the code consists of a series of shared modules to perform the input and output of data, and standard functions such as the multiplication of link variables. The modules directly related to the calcu-

lation of highly-improved operators total approximately 2500 lines of code. Since this does not include the other shared modules which are required to complete the functionality of the software, we have deemed it unnecessary and inappropriate to include this code in an appendix to this thesis.

## 6.4 Effect of Cooling on Gauge Field Structure

Let us begin by examining the difference between cooling with the standard Wilson action and with the $S(2)$ action - that is, the order $\mathcal{O}(a^2)$-improved action constructed from $T_{\mu\nu}^{(1,1)}$ and $T_{\mu\nu}^{(1,2)}$, which we deduced the form of in Section 3.1. To analyse the effect of cooling algorithms incorporating different action operators we have proceeded as follows: From an original collection of one hundred configurations (numbered as they were saved in the process of thermalization i.e., the $1^{st}$ configuration saved is denoted configuration 01, the $2^{nd}$ configuration saved is denoted configuration 02, and so on), we cooled each for twenty sweeps with 3-loop cooling and a 3-loop improved topological charge operator to find what value their topological charges would plateau at (since, as mentioned above, $Q$ plateaus much sooner than the action). The configurations were then grouped together according to the modulus of their topological charge. Configurations were then chosen at random from groups with different topological charges. This is intended to demonstrate that the observed behaviour of the action and topological charge as we cool are consequences of the chosen cooling scheme, rather than consequences of the total number of (anti-)instantons present. This matter will be looked at in further detail when we discuss the Nahm transform in Section 6.6. Once a configuration was selected on the basis of its topological charge we cooled the original thermalised configuration in our investigations (not the corresponding configuration that had already been cooled for twenty sweeps, unless otherwise explicitly stated). The results which follow were produced on a

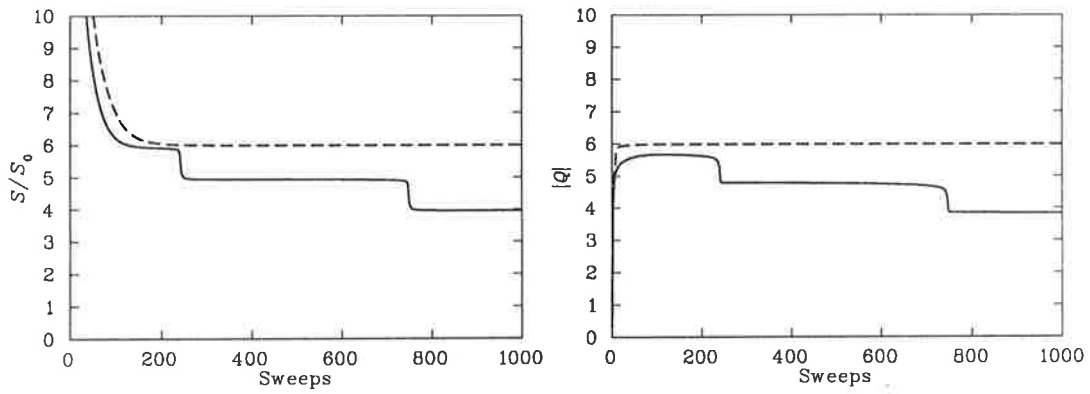


Figure 6.2: Action (left) and topological charge (right) of configuration 89 cooled with 1-loop (solid line) and 2-loop (dashed line) cooling schemes after 1000 sweeps.

$12^3 \times 24$ lattice, at $\beta = 4.60$ with a lattice spacing of $a = 0.125$ fm.

The diagram on the left of Figure 6.2 shows the action against sweep number for a configuration cooled with the Wilson action and $S(2)$. It can be clearly seen that the Wilson action drops to a temporary plateau, but eventually destabilises and drops by approximately one unit around sweep number 250, and again around sweep number 750. It should also be noted that these plateaux occur somewhat below integer values. However the $S(2)$ cooling scheme plateaus at a value much closer to integer (in this case 6.00) and remains at this value without destabilising. On the right of Figure 6.2 we see the comparable plot of the topological charge (calculated with the $Q(1)$ operator in the 1-loop cooling case, and with the $Q(2)$ operator in the 2-loop cooling case) of the same configuration as it is cooled with the Wilson action and $S(2)$. Again we can see that when cooled with the Wilson action the configuration destabilises at various intervals. Since the annihilation of an I-A pair does not change the total topological charge we must conclude that these drops in charge are due to the destruction of single instantons by the high level of discretization errors in the Wilson action. The topological charge curve corresponding to $S(2)$ cooling is significantly more stable. Figures 6.3 and 6.4

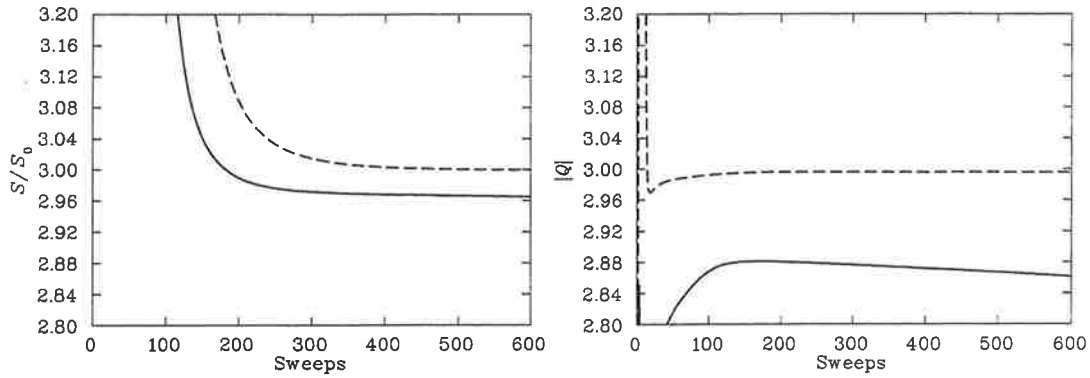


Figure 6.3: Action (left) and topological charge (right) of configuration 14 cooled with 1-loop (solid line) and 2-loop (dashed line) cooling schemes after 600 sweeps. Notice the different vertical scale used for this configuration, compared with configurations 89 and 22 (Figures 6.2 and 6.4).

show equivalent results for two other configurations at the same lattice size and spacing.

In Figures 6.2 and 6.4 (configurations 89 and 22 respectively) we can clearly see that the action and topological charge corresponding to cooling with the Wilson action plateau repeatedly for a period of several hundred sweeps but then drop by an increment of approximately one over a very brief interval. We interpret this as clear evidence that the Wilson cooling scheme not only eliminates short-range fluctuations and annihilates I-A pairs, but because of the large discretization errors present it also destroys single instantons. This is not observed with $\mathcal{O}(a^2)$ or (as we shall see shortly) $\mathcal{O}(a^4)$-improved cooling.

It is obvious from these results (but worth noting explicitly) that the charge and action drop (eventually to zero, if cooling proceeds for long enough) after achieving nearly equal values. In other words, an approximately self-dual condition is reached globally.

Let us now turn to an examination of Figure 6.3 (configuration 14). Unlike the

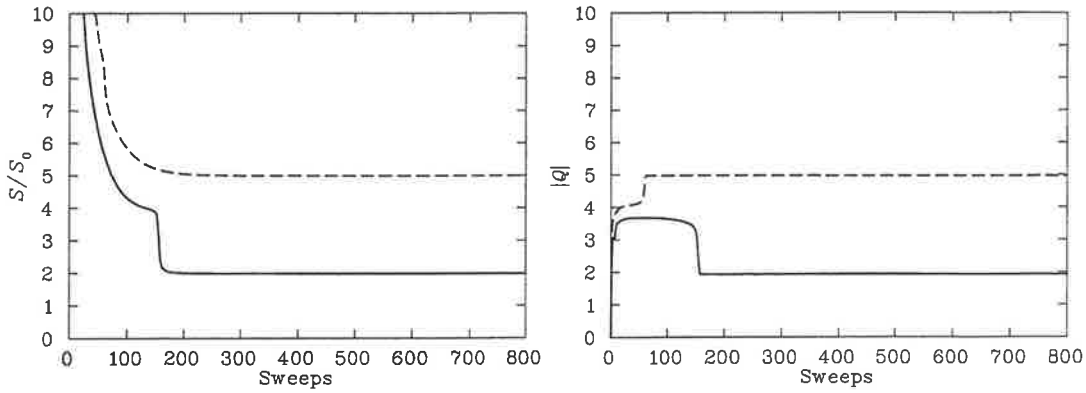


Figure 6.4: Action (left) and topological charge (right) of configuration 22 cooled with 1-loop (solid line) and 2-loop (dashed line) cooling schemes after 800 sweeps.

other two configurations, this one does not destabilise under cooling with the Wilson action, at least not in the first 600 cooling sweeps. What are we to make of this result? It is clear that even though the Wilson action does not destabilise as dramatically as we have seen above, the values of the action and topological charge obtained from Wilson cooling are still significantly further from integer values than those obtained with $S(2)$ cooling, as can be clearly seen at the scale we have chosen to use for Figure 6.3. Furthermore the topological charge calculated in the 1-loop cooling case is observed to drop steadily, having peaked after approximately 100 cooling sweeps. Presumably the configuration could destabilise if it was allowed to cool for long enough. But perhaps the main lesson we should learn from this observation is that each configuration reacts in a different way to cooling in general, and to different cooling schemes in particular, depending on its initial structure. This may become important later when we attempt to determine which of the $\mathcal{O}(a^4)$-improved cooling schemes is best.

Based upon these results we shall henceforth disregard the 1-loop cooling action, as it is obviously beset by pathological discretization errors.

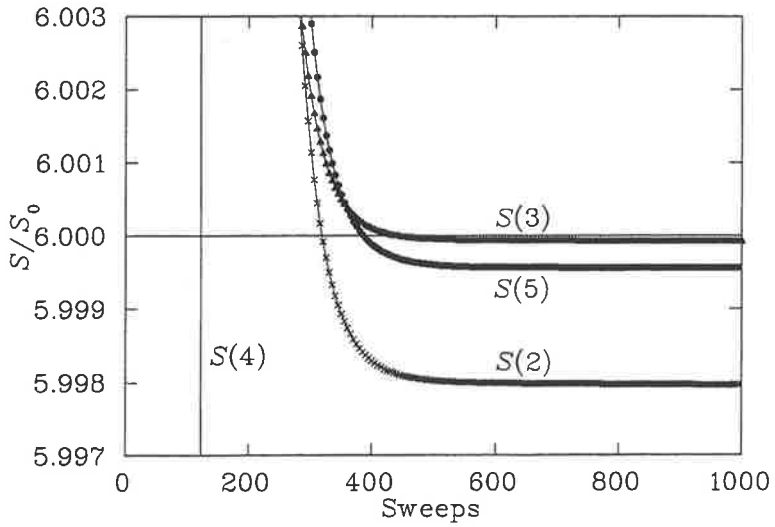


Figure 6.5: Action values over the first 1000 cooling sweeps of configuration 89 cooled with the 2-loop (crosses, $S(2)$), 3-loop (triangles, $S(3)$), 4-loop (vertical line, $S(4)$) and 5-loop (circles, $S(5)$) actions. Note that the 4 loop action drops to a value near 5.00, while the other actions plateau near 6.00. Configuration 89 is clearly sensitive to the detailed form of the improvement scheme in the early stages of cooling.

## 6.5 Non-Trivial Self-Duality from Improved Cooling

As we have observed above, improving the action is an effective means of preventing (anti-)instanton configurations from destabilising. We have seen that if we cool a configuration for long enough all the high-frequency fluctuations in the field will be eliminated, all I-A pairs will annihilate, and we will be left with a configuration which will consist exclusively of either instantons only or anti-instantons only. This configuration will be characterised by the condition that $S/S_0 = |Q|$. Of course, we wish this self-duality to be stable for hundreds of

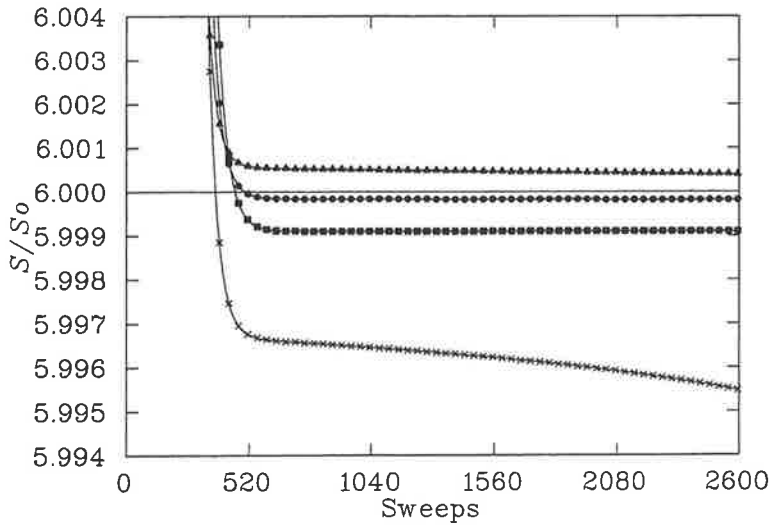


Figure 6.6: Action values over the first 2600 cooling sweeps of configuration 32 cooled with the $S(2)$ action (crosses), $S(3)$ action (triangles), $S(4)$ action (squares) and $S(5)$ action (circles).

cooling sweeps, and therefore we shall wish to cool with an action other than the standard Wilson action. It is also desirable to come as close as possible to true self-duality, not merely to approximate it, in order to study instanton dynamics. Since we know that both the action and topological charge in the continuum will be integers, we shall now attempt to determine which cooling scheme gives the most continuum-like results, that is, which improved action and topological charge operators produce results that are the closest to integers. We reason that these operators have the smallest discretization errors and are therefore best suited to studying the development of $S/S_0$ and $|Q|$ of any configuration as we cool it towards self-duality.

The most obvious way to compare the accuracy of different operators is to plot the values of the action that we obtain over several hundred cooling sweeps, when we cool with each different improvement scheme (and do likewise with the

Table 6.1: Action values from various improvement schemes for configuration 89.

| Sweep | $S(1)$ | $S(2)$ | $S(3)$ | $S(4)$ | $S(5)$ |
|---|---|---|---|---|---|
| 50 | 8.25034 | 10.07139 | 9.72154 | 10.76830 | 10.15204 |
| 100 | 6.21981 | 7.01505 | 6.85311 | 6.71974 | 7.05783 |
| 200 | 5.91257 | 6.04598 | 6.03297 | 5.13985 | 6.05030 |
| 500 | 4.94277 | 5.99802 | 5.99995 | 4.99965 | 5.99960 |
| 1000 | 3.95857 | 5.99796 | 5.99992 | 4.99943 | 5.99956 |

Table 6.2: Action values from various improvement schemes for configuration 32.

| Sweep | $S(1)$ | $S(2)$ | $S(3)$ | $S(4)$ | $S(5)$ |
|---|---|---|---|---|---|
| 50 | 10.58719 | 12.11866 | 12.52191 | 13.42492 | 12.96696 |
| 100 | 7.56851 | 8.72035 | 9.33105 | 9.84850 | 9.59557 |
| 200 | 5.95054 | 6.28744 | 6.19932 | 6.38768 | 6.28359 |
| 500 | 4.90163 | 5.99681 | 6.00061 | 5.99946 | 6.00000 |
| 1000 | 2.96931 | 5.99647 | 6.00051 | 5.99910 | 5.99984 |

topological charge). Figures 6.5 and 6.6 show examples of this on configurations 89 and 32 respectively. It can be quite clearly seen that the 3-loop and 5-loop improvement appear to give the most integer-like results. Table 6.1 shows some values of the action obtained with the various cooling schemes on configuration 89 against sweep number. We can see that the 1-loop, 2-loop, and 4-loop operators all underestimate the action (they produce values which may be close to 6.00, but have none-the-less dropped well below it, and of course the 1-loop cooling is unstable). The 3-loop and 5-loop improved actions drop slightly below 6.00, but remain within 1 part in $10^4$ of an integer value. For comparison Table 6.2 shows a set of equivalently produced data for configuration 32. One of the most notewor-

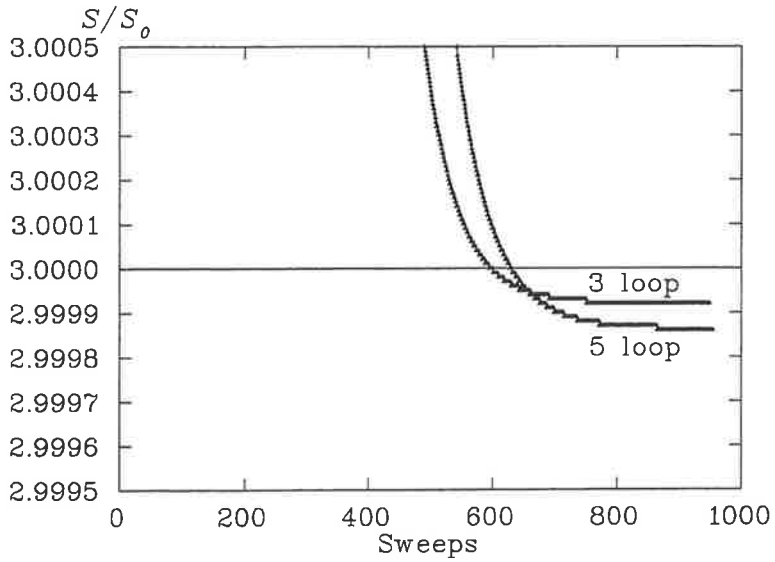


Figure 6.7: Action values over the first 1000 cooling sweeps of configuration 39 cooled with the $S(3)$ action and $S(5)$ action.

thy results of this analysis is the fact that the 4-loop cooling stabilises at a value one unit below the values attained by the 2-loop and the other $\mathcal{O}(a^4)$-improved cooling schemes when applied to configuration 89. While all of our improvement schemes have no $\mathcal{O}(a^4)$ errors by construction, they will in general have different $\mathcal{O}(a^6)$ errors. It is furthermore known that a newly thermalized configuration is very rough on the scale of the lattice spacing. It is therefore likely that the effect of differently improved cooling schemes on thermalized configurations will be determined by the $\mathcal{O}(a^6)$ errors in each cooling action. It is unsurprising then that some cooling schemes should eliminate structures that others leave intact. However, we are attempting to stabilise the large-scale and medium-scale structures in the gauge fields we study. Since the other improved cooling schemes appear to produce mutually consistent results on all configurations, and stabilise closer to integer values, we shall disregard the 4-loop cooling scheme for now. Other

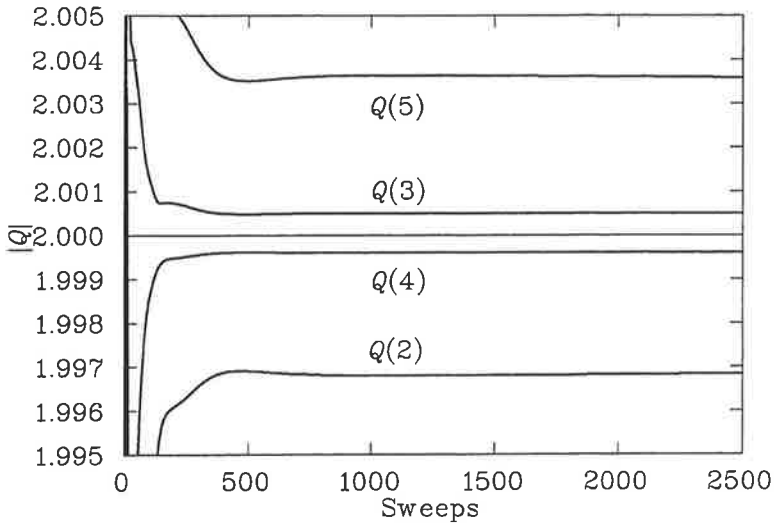


Figure 6.8: Topological charge of configuration 27 cooled with the 3-loop cooling scheme after 2500 sweeps. The 3-loop and 4-loop topological charge improvement schemes appear to be significantly more accurate than either the 2-loop or 5-loop improvement schemes. This demonstrates that $k_5 = 1/20$ was not the optimal choice for this improvement constant.

possible comparisons of results arising from 4-loop cooling and other $\mathcal{O}(a^4)$ improvement schemes (i.e., calculations of topological susceptibility [35], the static quark-anti-quark potential, and chiral symmetry breaking [36]) are left for future investigation. We shall henceforth concentrate on the 3-loop and 5-loop cooling. This leaves us in a somewhat ambiguous position with regard to the relative merits of the 3-loop and 5-loop cooling schemes. We therefore examine one further randomly selected configuration. This configuration (configuration 39) plateaus at an $S/S_0$ value of approximately 3.00 under 3-loop and 5-loop improved cooling. The profiles of $S/S_0$ against sweep number for this configuration are shown in Figure 6.7. In this case the 3-loop comes slightly closer to an integer value although both actions are extremely close to each other as they plateau. This is a 2-1 result in favour of the 3-loop cooling, but the sample size is admittedly

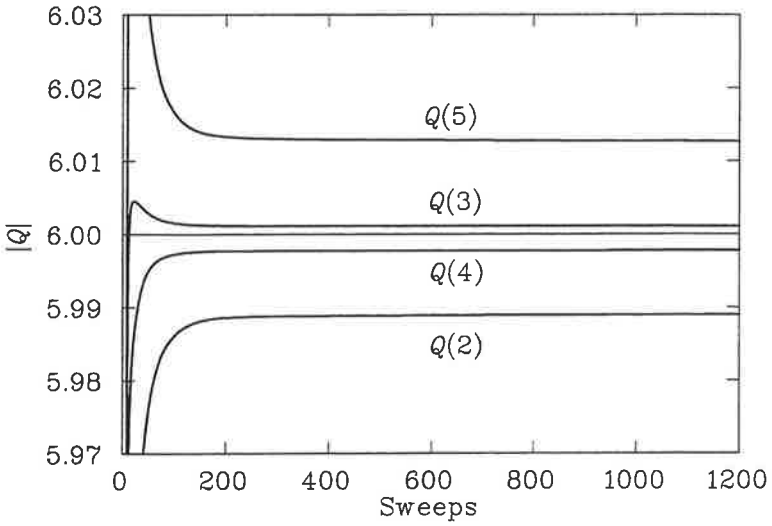


Figure 6.9: Topological charge of configuration 89 cooled with 3-loop cooling schemes after 1200 sweeps. As with configuration 27, the 3-loop and 4-loop topological charge improvement schemes appear to be significantly more accurate than either the 2-loop or 5-loop improvement schemes.

quite small, and the results obtained from 3-loop and 5-loop cooling are both extremely close to the integer values we would expect in the continuum. These results then seem to indicate above all else that there is no single $\mathcal{O}(a^4)$ improvement scheme (i.e., no single choice for the constant $c_5$, since as noted previously 3-loop and 4-loop improvement are merely special cases of 5-loop improvement) which unambiguously gives the best performance in all cases. Each configuration is different, and reacts to differently improved cooling in a unique way. Since the 3-loop and 5-loop cooling both produce excellent results, without any *a priori* knowledge to guide us the decision to use 3-loop or 5-loop improvement for the action should be based upon considerations other than the long-term stability of the results they produce and how continuum-like these results are.

From this point onwards then we choose to study configurations cooled with the $S(3)$ action, since this requires less computational cost than the $S(5)$ action.

Table 6.3: Reconstructed action, $S_R$, and topological charge, $Q$, values from various configurations, each cooled with the $S(3)$ action.

| Config | Sweep | $S(3)$ action | $S_R(2)$ | $S_R(3)$ | $S_R(4)$ | $S_R(5)$ |
|---|---|---|---|---|---|---|
| 89 | 1071 | 5.99992 | 5.98908 | 6.00110 | 5.99777 | 6.01278 |
| 27 | 1400 | 2.00013 | 1.99687 | 2.00055 | 1.99965 | 2.00370 |
| 90 | 1046 | 1.99999 | 1.99849 | 2.00012 | 1.99978 | 2.00133 |
| 56 | 2446 | 1.99996 | 1.99878 | 2.00002 | 1.99979 | 2.00083 |
| Config | Sweep | $S(3)$ action | $Q(2)$ | $Q(3)$ | $Q(4)$ | $Q(5)$ |
| 89 | 1071 | 5.99992 | 5.98899 | 6.00109 | 5.99777 | 6.01267 |
| 27 | 1400 | 2.00013 | 1.99680 | 2.00050 | 1.99961 | 2.00364 |
| 90 | 1046 | 1.99999 | 1.99848 | 2.00011 | 1.99977 | 2.00132 |
| 56 | 2446 | 1.99996 | 1.99878 | 2.00002 | 1.99979 | 2.00083 |

Let us now assess which topological charge operator gives the most accurate results. This is of course equivalent to determining which improvement scheme for $F_{\mu\nu}$ is the best. Figure 6.8 shows the development of the topological charge of configuration 27 over the course of four thousand cooling sweeps with the 3-loop improved cooling action. The 1-loop topological charge is too far from an integer value to be seen on the scale we have chosen for this diagram. Of course, all improvement schemes are doing extremely well here overall, in the sense that they take $Q$ to within 0.2% of an integer within a few hundred sweeps. We are looking at very fine differences in performance indeed, but we can clearly see that the 3-loop and 4-loop operators produce noticeably better results than either the 2-loop or 5-loop operators. Figure 6.9 shows equivalent results for configuration 89, over 1000 sweeps. This time we see that the 3-loop operator gives marginally more integer-like results than those observed with the 4-loop operator. Again the

Table 6.4: Reconstructed action, $S_R$, and cooling action, $S$, values from configurations 89 and 32 cooled with the $S(3)$ and $S(5)$ actions.

| Config | Sweep | $S(3)$ | $S_R(3)$ | $S_R(5)$ | $S(5)$ | $S_R(3)$ | $S_R(5)$ |
|---|---|---|---|---|---|---|---|
| 89 | 200 | 6.03297 | 6.03417 | 6.04644 | 6.05030 | 6.05190 | 6.06444 |
| | 600 | 6.00010 | 6.00130 | 6.01296 | 5.99957 | 6.00116 | 6.01320 |
| | 1000 | 5.99992 | 6.00110 | 6.01284 | 5.99956 | 6.00115 | 6.01314 |
| 32 | 500 | 6.00061 | 6.00300 | 6.02465 | 6.00000 | 6.00319 | 6.02541 |
| | 1000 | 6.00051 | 6.00284 | 6.02385 | 5.99984 | 6.00298 | 6.02486 |
| | 2000 | 6.00044 | 6.00266 | 6.02260 | 5.99983 | 6.00290 | 6.02429 |

1-loop, 2-loop and 5-loop operators are substantially more inaccurate.

Since the improved $F_{\mu\nu}$ plays no role in the link updates as we cool the configurations, we may safely take an ensemble of configurations that have already been cooled to near self-duality and assess their topological charge and reconstructed action from this point only. To assess the performance of the $F_{\mu\nu}$ improvement on other configurations we have presented the values of 2-, 3-, 4-, and 5-loop reconstructed actions and topological charges calculated on four different configurations, all cooled with a 3-loop improved action, in Table 6.3. The columns are the configuration number, the sweep number at which the calculation was performed, the value of the cooling action, the values of $S_R(2)$, $S_R(3)$, $S_R(4)$, and $S_R(5)$, and the values of $Q(2)$, $Q(3)$, $Q(4)$, and $Q(5)$. We can see that in each case the 3-loop and 4-loop improved topological charge and reconstructed actions produce results that are both closest to integer values, and in closest agreement to the value of the cooling action. In the majority of cases the 3-loop operators produce the most integer-like results, and in all cases the 3-loop results most closely match the values of the cooling action (and hence seem to be accurately

assessing the structure of the fields which is produced by the cooling algorithm). A further comparison, between results for 3-loop cooling and 5-loop cooling, is presented in Table 6.4. In this case we wish to determine whether the choice of cooling action affects the dependability of the reconstructed action. We have not chosen to consider the 4-loop cooling action as it has already been deemed unsuitable. We see that the 3-loop reconstructed action gives values closer to the cooling action used in each case (whether the cooling action is 3-loop or 5-loop), and hence appears to be a more accurate probe of the structure of the fields produced by the cooling algorithm, as noted in the previous paragraph, than the 5-loop operator.

For these reasons we conclude that the 3-loop improved field-strength tensor is the most dependable of those assessed. The 3-loop operator is also slightly cheaper (in a computational sense) than the 4- or 5-loop operators. While the numerical evidence therefore suggests that the 3-loop improvement has the smallest $\mathcal{O}(a^6)$ errors of those examined, it would be possible, but time-consuming, to verify this algebraically and this issue is left for future work.

## 6.6 The Nahm Transform on the Lattice

As mentioned in the Introduction, the Nahm transform is a mapping from a configuration on a torus to the corresponding dual configuration on the dual-torus. Suppose $A_\mu$ is a self-dual $SU(N)$ potential with topological charge $Q$ on the torus, where the operator $D_z = \sigma_\mu(\partial_\mu + A_\mu + 2\pi i z_\mu)$ with $z_\mu \in \mathbb{R}$ has $Q$ zero-modes satisfying $D_z(x)\Psi_z^\alpha(x) = 0$, then

$$\hat{A}_\mu^{\alpha\beta}(z) = i \int d^4x \Psi_z^\alpha(x)^\dagger \frac{\partial}{\partial_\mu} \Psi_z^\beta(x) \tag{6.9}$$

defines the Nahm transform of $A_\mu$ [16]. Applying the transform to $\hat{A}_\mu$ gives back $A_\mu$. But what is really interesting about this transform is that $\hat{A}_\mu$ is an $SU(Q)$ potential with topological charge $N$. In other words, the Nahm transform exchanges the roles of colour and topological charge.

It has been known for some time [37] that there are no $|Q| = 1$ instanton solutions on the 4-torus. A corollary of the Nahm transform [4] provides a straightforward way of explaining this situation. This corollary states that it is impossible for a single $|Q| = 1$ instanton to exist on the torus, because this would require the existence of $N$ instantons in $U(1)$ on the dual torus, but this is not allowed since there are no instantons in $U(1)$ field theory (as it is too simple, lacking the self-interactions of a non-Abelian field theory). We should note explicitly that it is *self-dual* $S/S_0 = 1$ solutions which are forbidden on the torus. There is nothing to prevent *either* $|Q|$ *or* $S/S_0$ from being exactly equal to one, but they may not both be equal to one at the same time. Since the lattices upon which we are performing our simulations have untwisted periodic boundary conditions, this consequence of the Nahm transform will be relevant in our simulations when the gauge fields are sufficiently smooth that the topological charge and $S/S_0$ take near-integer values.

Now that we have determined that the 3-loop action and topological charge operators are the most favourable for studying continuum-like physics we are in a position to analyse the behaviour of $|Q| = 1$ configurations to determine if any evidence of the effect of the instability of such configurations implied by the Nahm transform can be detected numerically, for sufficiently smooth gauge fields on the lattice.

If single-instanton configurations (i.e., strictly self-dual) are not allowed on the torus, how would we expect $Q$ and $S/S_0$ to behave as such a configuration is cooled towards self-duality? It seems reasonable that the action and topological charge will approach each other to within a certain range, but never become

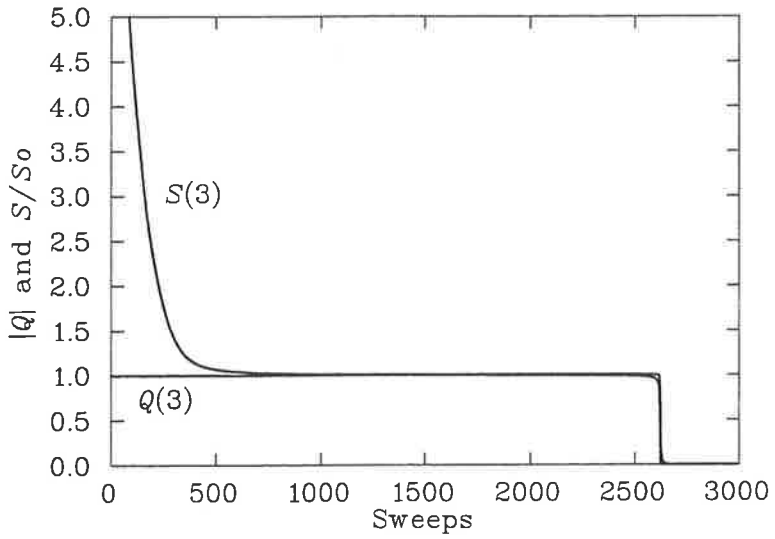


Figure 6.10: Topological charge and action values of configuration 11 (single instanton).

equal. In that case the action may stabilise at some non-integer value. We may also anticipate that the instanton size compared to the torus size will be a relevant parameter. The instanton action is independent of its size $\rho$ in the continuum and hence an arbitrarily small instanton on a finite 4-torus will look like a finite-size instanton on an arbitrarily large 4-torus. This is relevant because as the torus becomes arbitrarily large it will better approximate Euclidean space-time. As the cooling algorithm monotonically decreases the action, we may expect the topological charge to be "forced" downwards as the action decreases, and perhaps the instanton will destabilise, but this is not an *a priori* certainty. It is possible that the action will simply stabilise, as we observed for multiple-instanton configurations, but at a value well above integer.

Fortunately we do not have to guess, and we shall not keep the reader in suspense. Figure 6.10 shows the action and topological charge of configuration 11, which cools towards a single-instanton state. At the scale we have chosen to represent

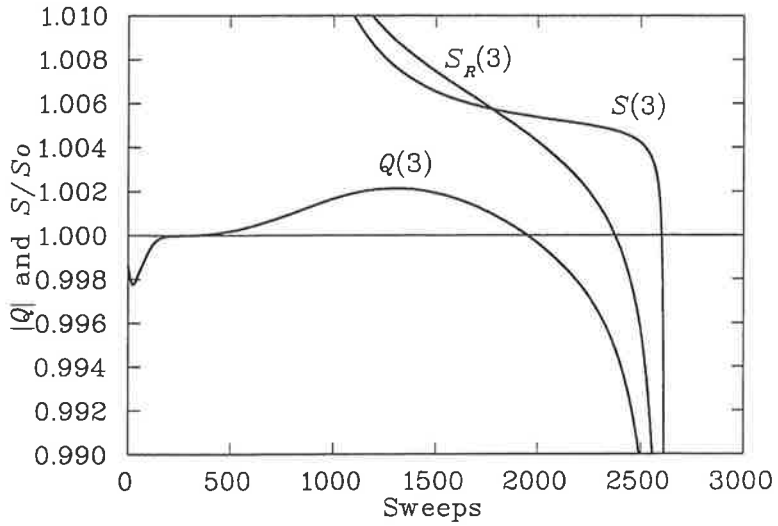


Figure 6.11: Topological charge, action, and reconstructed action values of configuration 11 (single instanton). All operators are 3-loop improved.

in this graph, the configuration looks highly self-dual. However it is obvious that the configuration destabilises and the single instanton present on the lattice disappears. This disappearance can be attributed to the instability implied by the Nahm transform, however to be certain let us examine the behaviour of this configuration at a smaller scale (Figure 6.11). Now we see that the configuration clearly never reaches self duality (at least, not until it destabilises and becomes trivially self-dual). In fact, if we look beyond the dramatic collapse of both the action and topological charge we will notice that for at least 1000 cooling sweeps before the final collapse the topological charge was rising and then slowly falling back down. It appears as though the configuration was somehow prevented from becoming self dual by letting $S/S_0$ fall to the same value as the topological charge. To be certain that this behaviour is not simply an instability in the cooling algorithm which has not manifested itself previously in a noticeable manner, we compare the results from configuration 11 with the results from configuration

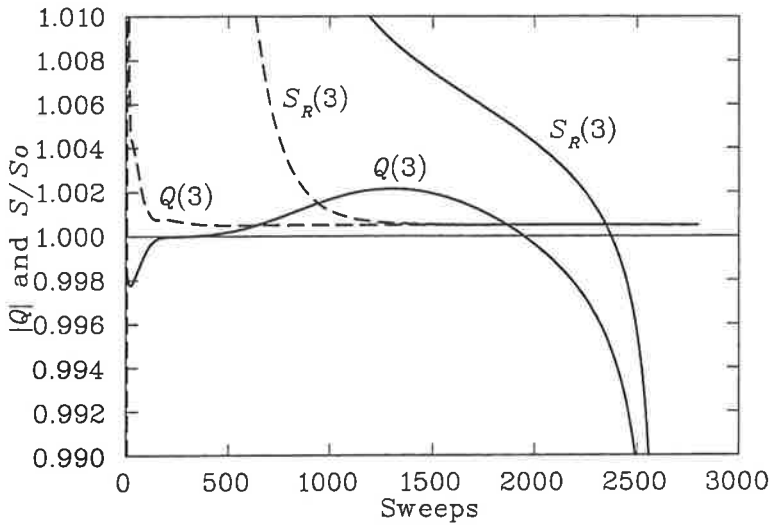


Figure 6.12: Topological charge and reconstructed action values of configuration 11 (single instanton, solid lines) and configuration 27 (two instantons, dashed lines). The values for configuration 27 have been reduced by an increment of 1.00 to overlap them with those of configuration 11. Clearly configuration 11 is not behaving in a stable manner (see text).

27, a two-instanton configuration. In order that we may easily compare their behaviour, we have subtracted one from the value of $S/S_0$ and $|Q|$ for configuration 27 (so that these values approach 1.00 not 2.00) and overlayed the two sets of data in Figure 6.12. Clearly configuration 27 achieves a remarkable level of self-duality, and actually comes within 0.0005 units of an integer value, remaining stable well after the point at which the configuration 11 has undergone its dramatic collapse. It therefore seems reasonable to ascribe this difference in behaviour to the different structures of the gauge fields in each configuration. We have indeed discovered numerical confirmation of the consequences of the Nahm transform.

We shall now attempt to answer the question of how a single-instanton configu-

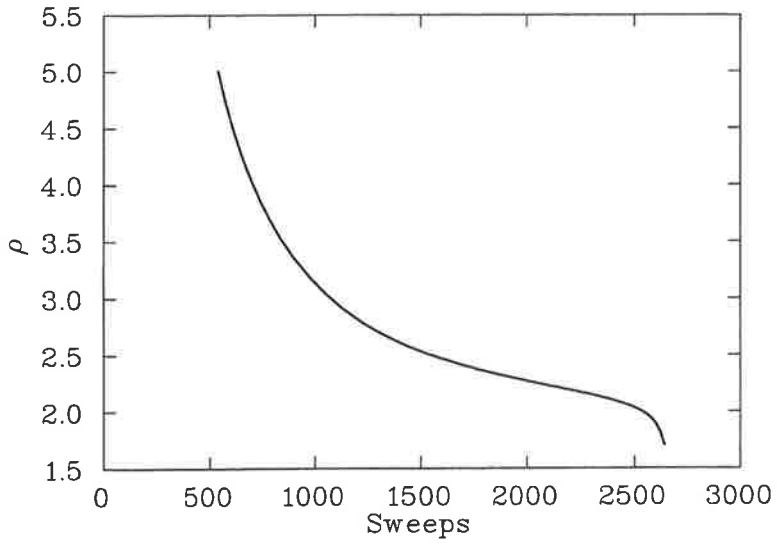


Figure 6.13: Size of the single instanton ($\rho$ measured in lattice units) in configuration 11. Before sweep 500 many peaks are present in the action density, making it difficult to accurately determine the parameters of a specific peak. After sweep 2500 the instanton rapidly disappears and hence its size parameter cannot be measured accurately.

ration on the torus destabilises. One hypothesis, proposed by Van Baal, suggests that on the lattice any single instanton will shrink until it becomes too small to be accurately represented on a discrete space-time and "drops through" the lattice. Alternatively it is possible that the instanton simply "fades away", maintaining a fairly constant size (as measured by the parameter $\rho$) while the action everywhere on the lattice decreases uniformly. In order to answer this question we fit the structure of the gauge fields on the lattice to the theoretical form in Equation (4.30).[1] The relevant fit parameters are the coordinates of the centre of each instanton, the scale parameter $\rho$ and an overall scale factor which normalises the field values to the theoretical values for a continuum instanton.

[1] Other studies using cooling and fitting with instantons have been performed. See reference [38], for instance.

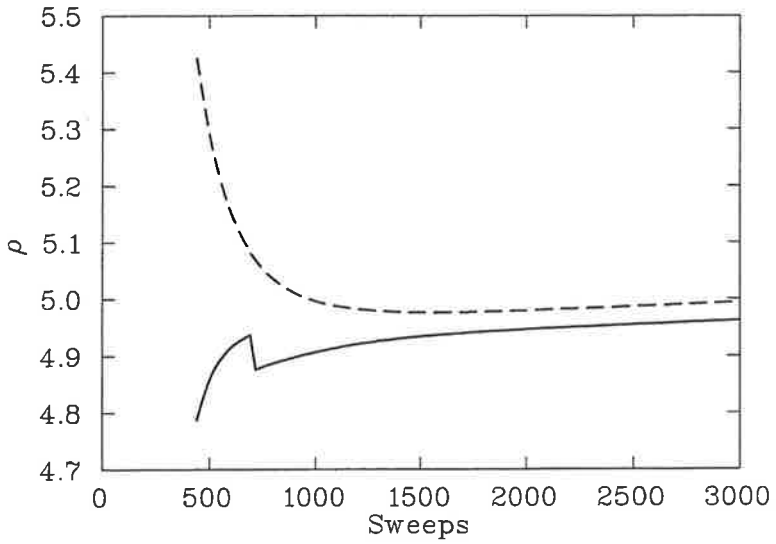


Figure 6.14: Size of the two instantons ($\rho$ measured in lattice units) in configuration 27. The sudden drop in size of one instanton is attributed to a complex interaction between the two instantons as they move apart.

In Figure 6.13 we can see how the instanton radius varies with sweep number. Clearly the instanton is shrinking, by a factor of approximately three as the cooling proceeds over the course of two thousand sweeps. We can also see that the instanton shrinks rapidly at the point where it destabilises. For comparison we also show the sizes of the two instantons in configuration 27 (Figure 6.14) and their separations (Figure 6.15). We can see that after an initial period of fluctuation the instantons settle on very stable, mutually consistent sizes. Furthermore each instanton changes size by a factor of no more than 1.10, much less than the dramatic changes observed over the same range of cooling sweeps for the single instanton in Figure 6.13.

To demonstrate the reproducible nature of these results, we have carried out an equivalent analysis on another configuration with a single pseudo-instanton (configuration 64), and another configuration with two instantons (configuration 90).

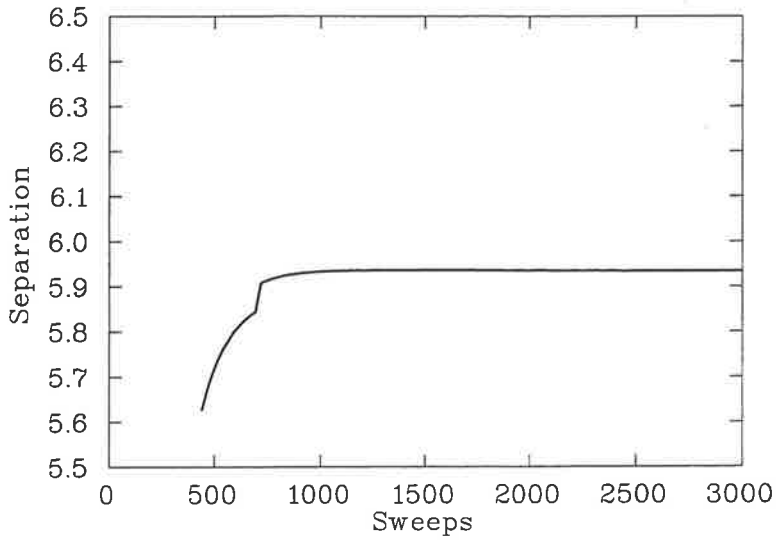


Figure 6.15: Separation of the two instantons (measured in lattice units) in configuration 27. The sudden jump at around sweep number 700 is believed to be due to an interaction between the two instantons as they move apart, since this may affect how well the fitting algorithm judges their size and position.

In Figures 6.16, 6.17, and 6.18 we can see the same type of behaviour of the action, topological charge, and size parameter $\rho$ as was observed with configuration 11. In Figures 6.19 and 6.20 we can see that the two instantons in configuration 90 remain stable for at least 3000 cooling sweeps, converging upon the same size, and ultimately drifting apart very slowly.

A further detail to be noted when we consider Figures 6.11 and 6.17 is the fact that the topological charge remains almost flat at 1.00 from sweep 200 to sweep 500. This is a dramatic confirmation of the consequences of the Nahm transform, because these plateaux coincide with the presence of a group of what we may call 'transitory instantons'. As the configuration is cooled, some regions become trivial, while others become instantons. But some parts of the field cool to become closely associated I-A pairs. Thus they do not affect the overall topo-

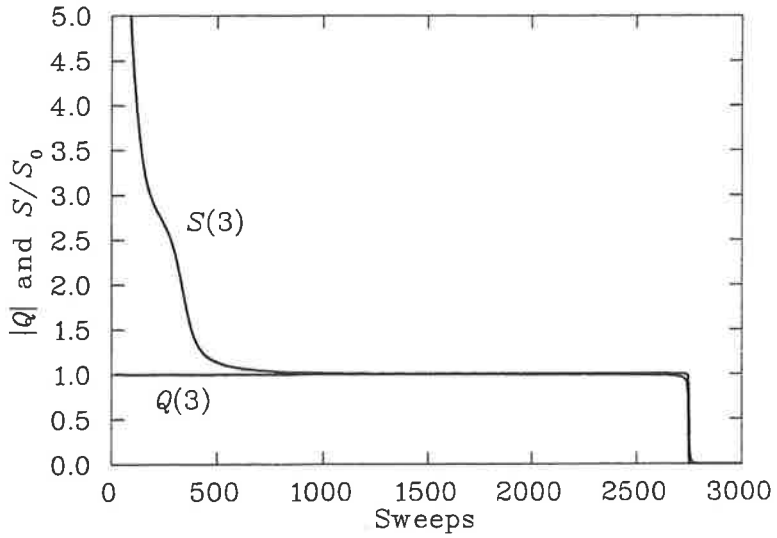


Figure 6.16: Action and topological charge of the single instanton in configuration 64. As with configuration 11 we can see that the configuration destabilises around sweep 2500.

logical charge. Their presence is detected by the code developed to determine instanton size and location, since during the early stages of the cooling process the number of instantons identified by the fitting code often increases and then decreases gradually as the I-A pairs annihilate.[2] While there is more than one instanton on the lattice, the Nahm transform will not make them unstable. It does not appear to be a coincidence that in the period leading up to sweep 400 the instanton fitting code identifies multiple peaks, but only identifies a single peak for each configuration shortly before the point where the topological charge begins to rise, as seen in Figure 6.21. We may therefore confidently assert that the instability we observe with configurations 11 and 64 is due solely to the fact that they contain only a single instanton.

[2]Other instances of such multiple peaks have been observed in [39].

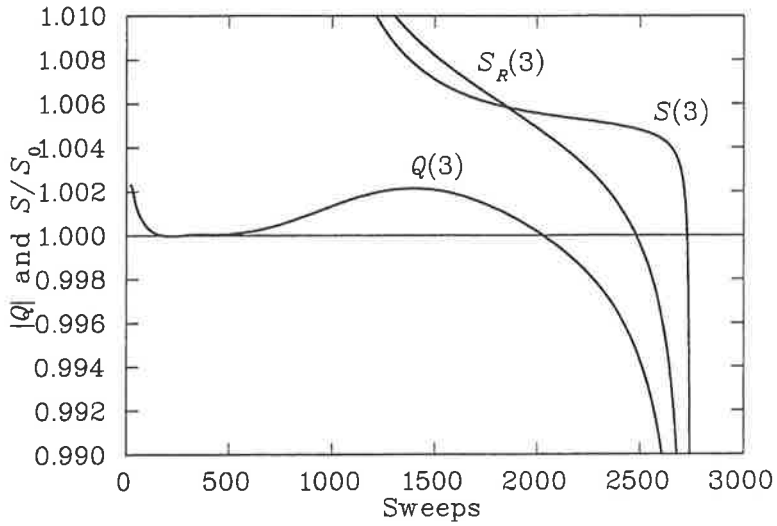


Figure 6.17: Small-scale plot of the action and topological charge of the single instanton in configuration 64. As with configuration 11 we can see that the charge plateaus briefly, rises above 1.00 and then drops again, as the entire configuration destabilises.

## 6.7 Summary

In this Chapter we have numerically examined the various improvement schemes for the cooling action and lattice field-strength tensor described in earlier Chapters. Our results indicate that the best cooling actions are those free from $\mathcal{O}(a^4)$ discretization errors, and of these the 3-loop and 5-loop actions appear to give equally good results in general, although some configurations achieve more continuum-like values of the action and topological charge when cooled with one action or the other. Given this near equivalence, the extra computational cost and time required to use the 5-loop action recommends the 3-loop action as the best choice for studies requiring many hundreds to thousands of cooling sweeps. We have also determined that the 3-loop improvement of the field-strength tensor produces the most continuum-like values of the topological charge and recon-

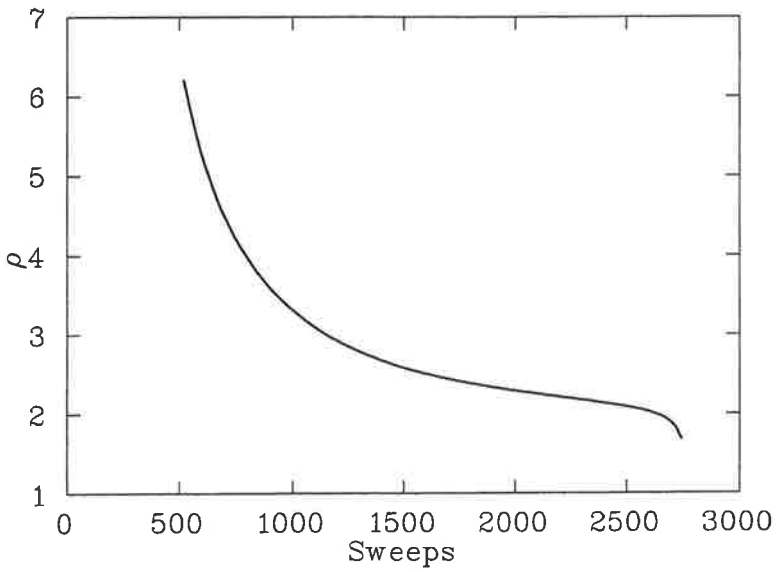


Figure 6.18: Size of the single instanton ($\rho$ measured in lattice units) in configuration 64. The similarity to Figure 6.13 is remarkable.

structed action over a range of configurations, when used with either the 3-loop or 5-loop cooling action. The extremely small differences between the calculated values and those we would expect in the continuum, and the extra computational cost of implementing higher-level improvement make it seem unlikely that tree-level improvement to order $\mathcal{O}(a^6)$ will be either necessary or desirable in the near future.

We have applied $\mathcal{O}(a^4)$-improved cooling and an $\mathcal{O}(a^4)$-improved topological charge operator to the analysis of the relative stability and self-duality of single and multiple-instanton configurations on the (untwisted) 4-torus. We have found that $|Q| = 2$ configurations achieve a very high level of self-duality and remain stable for at least 3000 cooling sweeps. However $|Q| \doteq 1$ configurations do not achieve self-duality and eventually destabilise, becoming topologically trivial. Our results suggest the following model for how such configurations destabilize: when a single pseudo-instanton exists on the 4-torus, it is impossible for this ob-

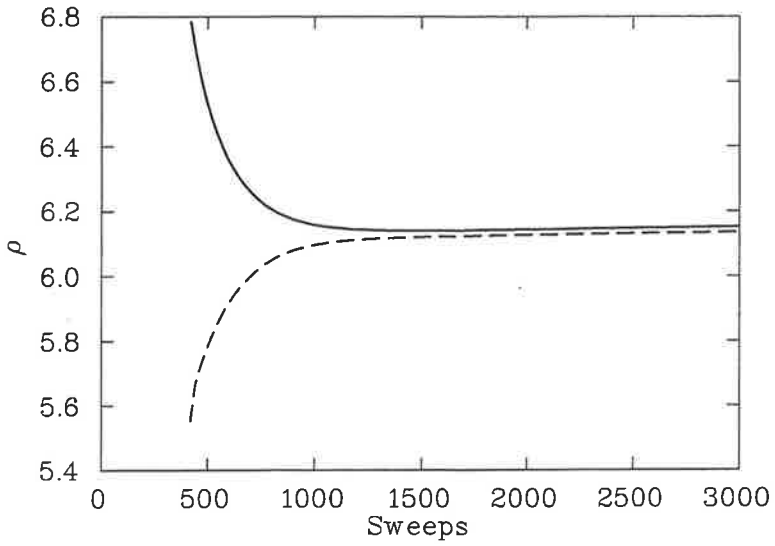


Figure 6.19: Size of the two instantons ($\rho$ measured in lattice units) in configuration 90.

ject to become a true instanton by achieving a self-dual state $|Q| = S/S_0 = 1$. The periodic boundary of the torus allows the pseudo-instanton to wrap around each direction and interact with itself in some destructive or destabilizing manner. Since the only scale parameters in this situation are the size of the instanton and the dimensions of the torus (which may be regarded as one parameter - instanton size as a fraction of torus size), the pseudo-instanton shrinks, so that the torus on which it exists effectively approaches the infinite volume limit, thereby becoming more similar to Euclidean 4-space. The action (and topological charge) of a continuum instanton is independent of its size, however since the space-time in which this lattice pseudo-instanton exists is discrete, once it has shrunk below a certain size, the improvement used to minimize discretization errors becomes overwhelmed and the action and topological charge of the pseudo-instanton are driven away from consistent (i.e., self-dual) values. At this point the pseudo-instanton becomes critically unstable under the influence of the cooling algorithm and it is destroyed. The pseudo-instanton therefore succeeds in becoming self-dual, but it

is a Pyrrhic victory, as it only manages to achieve a trivial self-duality.

One further interesting point remains to be made, regarding the dynamics of two-instanton configurations. If we consider Figure 6.20 we can see that the two instantons in configuration 90 are drifting apart, albeit slowly. Since the instantons overlap (i.e., the instanton separation is less than $\rho_1 + \rho_2$) this seems to indicate that the instantons are in some manner repelling each other. This idea is compatible with the view that a single instanton shrinks in order to minimise the extent to which it interacts with itself, as it wraps around the periodic boundary of the lattice. By contrast, multiple instantons are able to move apart rather than being forced to shrink. An interesting question that then arises is how the instantons would behave if allowed to cool for a sufficiently long time that they no longer overlap. Would they stop separating, or drift until they were opposite each other on the torus (the maximum possible separation)? If they did achieve maximum separation would they then begin to shrink and eventually disappear? These are interesting questions, but since we estimate that it would require approximately one *million* cooling sweeps, at the observed rate of separation, for the instantons to achieve this maximum separation, the answers shall be left for future work.

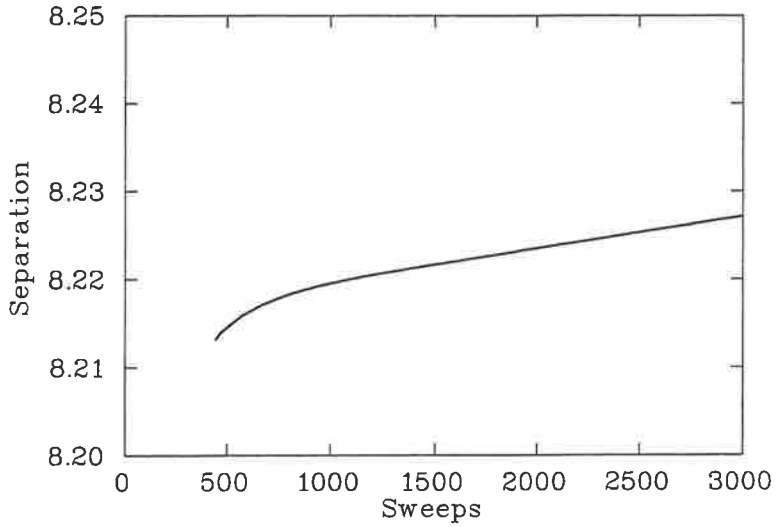


Figure 6.20: Separation of the two instantons (measured in lattice units) in configuration 90. Clearly they are drifting apart, but only very slowly.

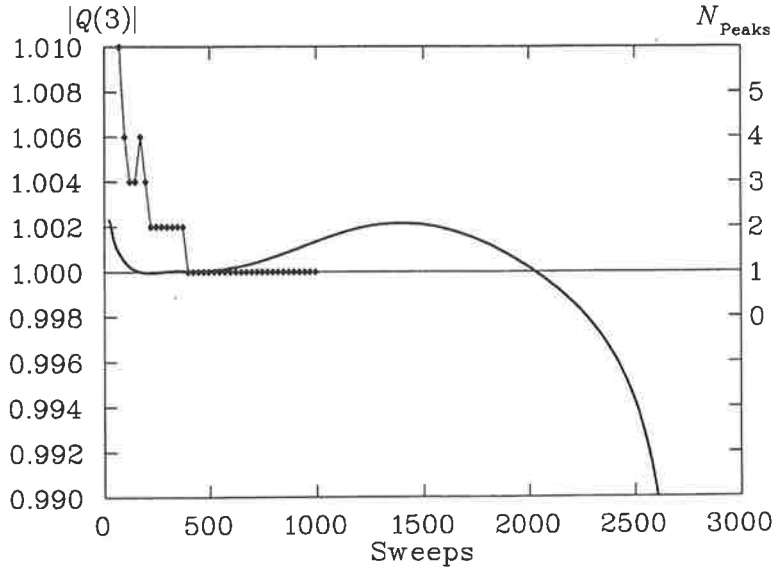


Figure 6.21: Topological charge for the first 3000 sweeps (left scale) and number of instanton-like peaks in the local action density (right scale) for the first 1000 sweeps, of the single-instanton configuration 64. Notice that the topological charge is almost a perfect integer until $N_{Peaks} = 1$.

# Chapter 7

# Conclusions

*"It may be a tad fanciful, and to be honest I'm not sure if the physics holds up. But it could happen. We've been wrong so many times before, why stop now?"*

Nicola Jones

Lattice gauge theory has developed over the last two decades into a highly successful and useful method for studying non-perturbative physics. While much work remains to be done it is clear that the development of algorithms based upon improved operators show great promise for minimizing discretization errors, allowing lattice simulations to reproduce continuum physics very precisely, and in some cases to shed light on continuum behaviour which is not yet fully understood in an analytical sense.

Of particular interest are methods for smoothing out short-range fluctuations in the fields. We have here investigated cooling, an iterative numerical method for finding minima of the local action density of the fields.

We have seen in the preceeding discussion that the use of cooling to examine the

continuum behaviour of gauge fields is a useful tool, but it is essential to improve the action utilised in the cooling algorithm in order to obtain results that agree with those we expect from continuum analyses. Unimproved cooling is beset by pathological discretization errors which eventually eliminate all non-trivial local minima of the action.

The action is improved by algebraically combining gauge-invariant terms calculated on the lattice. The combination of these terms removes classical errors arising from the fact that we have transferred our continuum field theory to a discrete space-time. This method works well, but grows complicated as we move to higher orders of improvement. We have seen that eliminating $\mathcal{O}(a^2)$ discretization errors produces a great improvement in the quality of results, and further work to eliminate $\mathcal{O}(a^4)$ discretization errors produces noticeable, but less pronounced, subsequent improvement. Considering that the values of $S/S_0$ and $Q$ calculated with this level of improvement achieve values within 1% of integers after at most a few hundred cooling sweeps it seems unlikely that there will be enough gained by moving to $\mathcal{O}(a^6)$ improvement to make the associated extra computational effort worthwhile.

In addition to this classical improvement, tadpole improvement may be employed to mitigate the effect of non-classical self-couplings of the gluon fields.

We have utilised the total action and the total topological charge of configurations as we cool them to investigate the behaviour of these configurations. We have seen that (when normalised by $S_0$) the values attained come within fractions of a percent of integer values. These results remain stable for several thousand iterations of the cooling algorithm (except in the special case of $S/S_0 = 1$ configurations). Furthermore, measurements of the size parameters of the instantons produced by this cooling process maintain the extreme stability exhibited by the total action and total topological charge, indicating that the instantons are not being "spread out" or forced to shrink by the effect of the cooling algorithm,

reinforcing the viewpoint that these instantons are stable objects. This excellent agreement with continuum results makes us confident that all results obtained by the same methods are likewise physically valid, and hence we should be able to reproduce other continuum quantities and effects in our simulations. This facilitates the use of highly-improved cooling to investigate the stability of $|Q| = 1$ configurations. We have found that when such configurations approach self-duality, the single pseudo-instanton present shrinks rapidly. We theorise that this occurs as a means of minimizing the extent to which the pseudo-instanton wraps around the periodic boundary of the lattice. As this occurs, the topological charge of the configuration moves away from an integer value. Since the topological charge is bounded above by the action, both quantities are eventually forced downwards as the cooling algorithm monotonically decreases the action. Eventually the pseudo-instanton becomes too small, crossing the dislocation threshold. At this point it destabilises totally and the cooling algorithm destroys it.

Multi-instanton configurations appear to remain permanently stable. Further work will be needed to determine if this stability is indeed permanent, but all indications at present suggest that such analysis will require precision cooling studies for durations (measured in sweep numbers) orders of magnitude longer than those hitherto performed. Such analyses will probably have to await the arrival of a new generation of supercomputers, and a new generation of PhD students.

# Appendix A

# *Mathematica* package for expanding Wilson loops

The following Mathematica code calculates the form of the expansion of the closed rectangular loop defined by the range $\{x_1, x_2\}$ in the $x$-direction and $\{y_1, y_2\}$ in the $y$-direction.

```
(* Expansion of the term A.dx as a double integral over
   the rectangular area defined by (x1,x2) and (y1,y2) *)

(* NC denotes non-commutative multiplication, which is
   necessary to make the chain rule easy to implement
   when we want to differentiate. These rules also show
   how to perform the chain rule, with a change of
   variable from dee to Dee to avoid recursion problems *)
```

```
NC[x___,NC[y___],z___]:= NC[x,y,z]
NC[x___, 1,y___]:= NC[x,y]
NC[x___, a_ + b_, y___]:= NC[x,a,y] + NC[x,b,y]
NC[y___, dee[mu],x[a[n_]],z___]:=(NC[y,x[a[n]],dee[mu],z]+
                        NC[y,Dee[mu],x[a[n]],z])
                                    (* Chain rule *)
NC[y___, dee[nu],x[a[n_]],z___]:=(NC[y,x[a[n]],dee[nu],z]+
                        NC[y,Dee[nu],x[a[n]],z])
                                    (* Chain rule *)


(* Starting from the assumed form of the expansion
     \partial_{\mu} A_{\nu}(x_0 + x)
          - \partial_{\nu} A_{\mu}(x_0 + x)
   we create a Taylor expansion. The displ and deriv
   functions recursively give us the displacement and
   derivative terms, and combi combines them to give us the
   required coefficients in the expansion. stretch[n_Integer]
   expands the Taylor series' out to n orders in the lattice
   spacing (for n even). *)

displ[0]:=1
displ[n_Integer]:= NC[displ[n-1],x[a[n]]]

deriv[0]:=1
deriv[n_Integer]:= NC[deriv[n-1],dee[a[n]]]

combi[n_Integer]:= NC[displ[n],deriv[n]]
```

```
stretch[n_Integer]:= ExpandAll[
         (Sum[NC[(1/i!),combi[i],dee[mu],A[nu]], {i,0,n}] -
          Sum[NC[(1/i!),combi[i],dee[nu],A[mu]], {i,0,n}])]

(* DAtoF converts dee A - dee A terms into F's *)

DAtoF[expr_]:=
   (expr //. NC[x___, dee[mu],A[nu]] -
             NC[x___, dee[nu],A[mu]] :> NC[x, F[mu,nu]])

(* XpandMuNu expands out the a[n] indices
   into mu's and nu's *)

XpandMuNu[expr_]:= (expr //.
 NC[XX___, x[a[n_Integer]],YY___,dee[a[n_Integer]],ZZ___]
  :> NC[XX,x[mu],YY,dee[mu],ZZ]+NC[XX,x[nu],YY,dee[nu],ZZ])

(* CleanUp takes the integer factors outside the
   NC brackets *)

CleanUp[expr_]:=
     ( expr /. NC[XX___, n_ , YY___] :> n NC[XX,YY] )

(* XsOut moves all the x's outside the NC brackets. Some
   will already have been moved outside by the previous
   function *)
```

```
XsOut[expr_]:= ( expr //. NC[XX___, x[n_], YY___]
                                    :> x[n] NC[XX,YY] )

(* ReorderDs moves all the dee terms together and orders
   them in the same way, so we can cancel and add to
   simplify terms properly *)

ReorderDs[expr_]:= ( expr //. NC[X_ ,dee[a_],Y___]
                                    :> NC[X dee[a], Y])

(* XpandTheLot brings it all together *)

XpandTheLot[n_Integer]:= ExpandAll[
                          ReorderDs[
                            XsOut[
                              CleanUp[
                                XpandMuNu[
                                  DAtoF[
                                    stretch[n]]]]]]]

(* Now we start to integrate around our chosen path *)

IntegRectangle[x1_, x2_, y1_, y2_, expr_]:=
                          ExpandAll[Integrate[
                            expr, {x[mu], a x1, a x2},
                              {x[nu], a y1, a y2}]]

(* CleanNC gets rid of that annoying factor of NC[], purely
```

```
   for aesthetic reasons *)

CleanNC[expr_]:= (expr /. NC[] :> 1 )

(* WilsonLoop gives us the whole lot in one package *)

WilsonLoop[x1_, x2_, y1_, y2_, n_Integer]:=
            CleanNC[
              IntegRectangle[x1,x2,y1,y2,XpandTheLot[n-2]]
                    ]
(* Plaquette gives us the expansion of the plaquette *)

Plaquette[n_Integer]:= WilsonLoop[-1/2,1/2,-1/2,1/2,n]

(* CloverTerm gives us the clover term expansion for the
   calculation of F_munu *)

CloverTerm[em_Integer,en_Integer,n_Integer]:=
      ExpandAll[(
                 WilsonLoop[0,em,0,en,n] +
                 WilsonLoop[-em,0,0,en,n] +
                 WilsonLoop[0,em,-en,0,n] +
                 WilsonLoop[-em,0,-en,0,n] +
                     WilsonLoop[0,en,0,em,n] +
                     WilsonLoop[-en,0,0,em,n] +
                     WilsonLoop[0,en,-em,0,n] +
                     WilsonLoop[-en,0,-em,0,n]
                     )/8]
```

# Appendix B

# Possible topics for future work

The scope of the research carried out in this PhD project by no means exhausts the range of applications possible with the mathematical tools developed. Possible future applications include the following;

- Analysis on lattices with various sizes and spacings, and for differing choices of improvement scheme (3-loop, 4-loop, 5-loop), to determine more accurately how the critical size at which single pseudo-instantons "drop through" the lattice is affected by the lattice parameters and the analytic reduction of discretization errors.

- The improved field-strength tensor $F_{\mu\nu}$ could be decomposed into its colour magnetic and colour electric components, which could in turn be used to create hybrid and glueball source operators, to investigate the spectra of glueball and hybrid states [40].

- The work detailed herein could be adapted to the study of glueball spectra by transferring the improved operators to an anisotropic lattice, similarly to the work with the Lüscher-Weisz action by Morningstar and Peardon [24].

- As mentioned in the Introduction, the Atiyah-Singer index theorem [9] relates the number of chiral fermion zero modes in the continuum to the topological charge. Comparative calculations of topological charge to test the index theorem on the lattice have been performed [41][42][43][44]. The 3-loop gluonic topological charge described in this thesis has been used in a paper (see Section C.1) to assess the Atiyah-Singer index theorem on uncooled and cooled field configurations.

- Further investigations could be performed to assess the performance of the improved action and topological charge operators against other types of improvement (e.g., the Iwasaki action [22]), and to investigate how coarse the lattice can be made before a substantial reduction in the quality of data results.

# Appendix C

# Related papers by the author

## C.1 Submitted papers by the author

- **Hadron masses from novel Fat-Link fermion actions.**

  James M .Zanotti, Sundance O. Bilson-Thompson, Frédéric D. R. Bonnet, Paul D. Coddington, Derek B. Leinweber, Anthony G. Williams, and Jian Bo Zhang.

  *Special Research Centre for the Subatomic Structure of Matter and The Department of Physics and Mathematical Physics, University of Adelaide, Adelaide SA 5005, Australia.*

  Wally Melnitchouk.

  *Jefferson Lab, 12000 Jefferson Avenue, Newport News, VA 23606, USA, and Special Research Centre for the Subatomic Structure of Matter and The Department of Physics and Mathematical Physics, University of Adelaide, Adelaide SA 5005, Australia.*

  Frank X. Lee.

  *Center for Nuclear Studies, Department of Physics, The George Washington University, Washington, D.C. 20052, USA, and Jefferson Lab, 12000*

*Jefferson Avenue, Newport News, VA 23606, USA.*
hep-lat/0110216. Report-no: ADP-01-39/T471, JLAB-THY-01-32.
*Physical Review* **D65** (2002) 074507.

- **Excited Baryons in Lattice QCD.**
  Wally Melnitchouk.
  *Jefferson Lab, 12000 Jefferson Avenue, Newport News, VA 23606, USA, and Special Research Centre for the Subatomic Structure of Matter and The Department of Physics and Mathematical Physics, University of Adelaide, Adelaide SA 5005, Australia.*
  Sundance O. Bilson-Thompson, Frédéric D. R. Bonnet,
  Derek B. Leinweber, Anthony G. Williams, James M. Zanotti,
  and Jian Bo Zhang.
  *Special Research Centre for the Subatomic Structure of Matter and The Department of Physics and Mathematical Physics, University of Adelaide, Adelaide SA 5005, Australia.*
  Frank X. Lee.
  *Center for Nuclear Studies, Department of Physics, The George Washington University, Washington, D.C. 20052, and Jefferson Lab, 12000 Jefferson Avenue, Newport News, VA 23606, USA.*
  hep-lat/0202022. Report-no: ADP-01-63-T503, JLAB-THY-01-36.
  Submitted to *Physical Review D.*

- **Numerical study of lattice index theorem using improved cooling and overlap fermions.**
  Jian Bo Zhang, Sundance O. Bilson-Thompson, Frédéric D. R. Bonnet,
  Derek B. Leinweber, and Anthony G. Williams.
  *Special Research Centre for the Subatomic Structure of Matter and The Department of Physics and Mathematical Physics, University of Adelaide,*

*Adelaide SA 5005, Australia.*

hep-lat/0111060. Report-no: ADP-01-45/T477.

*Physical Review* **D65** (2002) 074510.

- **Cooling for Instantons and The Wrath of Nahm.**

  Sundance O. Bilson-Thompson, Frédéric D. R. Bonnet,

  Derek B. Leinweber, and Anthony G. Williams

  *Special Research Centre for the Subatomic Structure of Matter and The Department of Physics and Mathematical Physics, University of Adelaide, Adelaide SA 5005, Australia.*

  hep-lat/0112034. Report-no: ADP-01-58/T490.

  Talk presented at the Workshop on Lattice Hadron Physics, Cairns Australia, July 2001.

  *Nucl. Phys. Proc. Suppl.* **109** 116 (2002).

- **Highly-improved lattice field-strength tensor.**

  Sundance O. Bilson-Thompson, Derek B. Leinweber,

  and Anthony G. Williams.

  *Special Research Centre for the Subatomic Structure of Matter and The Department of Physics and Mathematical Physics, University of Adelaide, Adelaide SA 5005, Australia.*

  hep-lat/0203008. Report-no: ADP-01-50/T482.

  Submitted to *Physical Review D.*

## C.2 Forthcoming related papers by the author

- **Behaviour of instantons under cooling with improved lattice operators.**

  Sundance O. Bilson-Thompson, Derek B. Leinweber,

  and Anthony G. Williams.

  *Special Research Centre for the Subatomic Structure of Matter and The Department of Physics and Mathematical Physics, University of Adelaide, Adelaide SA 5005, Australia.*

  Gerald Dunne.

  *Department of Physics, University of Connecticut, Storrs CT 06269, USA*

  Report-no: ADP-01-51/T483.

# Bibliography


[1] G. P. LePage, *Redesigning Lattice QCD*, in *Schladming 1996, Perturbative and nonperturbative aspects of quantum field theory*, 1 (1996), [hep-lat/9607076].

[2] G. P. LePage and P. B. MacKenzie, *Viability of Lattice Perturbation Theory*, *Phys. Rev.* **D48**, 2250 (1993).

[3] P. de Forcrand, M. G. Pérez, I-O. Stamatescu *Nucl. Phys* **B499**, 409 (1997).

[4] H. Schenk, *Comm. Math. Phys.* **116**, 177 (1988).

[5] M. E. Peskin and D. V. Schroeder, *Introduction to Quantum Field Theory*, Addison-Wesley Publishing Company (1995).

[6] K. G. Wilson, *Confinement of Quarks*, *Phys. Rev.* **D10**, 2445 (1974).

[7] G. P. LePage *Lattice QCD for small computers*, in *Boulder 1993, Proceedings, The building blocks of creation*, 207 (1994), [hep-lat/9403018].

[8] A. A. Belavin, A. M. Polyakov, A. S. Schwartz and Yu. S. Tyupkin, *Phys. Lett.* **B59**, 85 (1975).

[9] M. F. Atiyah, I. M. Singer, *Ann. Math.* **87**, 484 (1968); *ibid.* **93**, 119 (1971).

[10] T. V. Schaëfer and E. V. Shuryak, *Rev. Mod. Phys.* **70**, 323 (1998).

[11] H. Aoyama, T. Harano, H. Kikuchi, I. Okouchi, M. Sato, and S. Wada, *Prog. Theor. Phys. Suppl.* **127**, 1 (1997).

[12] I. I. Balitskii and V. M. Braun, *Phys. Lett.* **B314**, 237 (1993).

[13] A. Ringwald and F. Schrempp, *Proceedings of the International Seminar Quarks 94*, Vladimir, Russia (1994) [hep-ph/9411217].

[14] G. W. Buschhorn, talk given at Crimean Summer School-Seminar on New Trends in High-Energy Physics, *Jalta 2000, New trends in high-energy physics*, 167 (2000) [hep-ph/0009064].

[15] K. Symanzik *Nucl. Phys.* **B226**, 187 (1983).

[16] W. Nahm, *Phys. Rev.* **B90**, 413 (1980).

[17] H. J. Rothe, *Lattice Gauge Theories an introduction*, World Scientific (1992).

[18] R. Gupta, *Introduction to Lattice QCD*, Lectures given at *Les Houches Summer School in Theoretical Physics*, Les Houches, France, 28 Jul - 5 Sep 1997. [hep-lat/9807028].

[19] M. Lüscher and P. Weisz, *Phys. Lett.* **B158**, 250 (1982).

[20] I. Montvay and G. Munster, *Quantum Fields on a Lattice*, Cambridge University Press (1994).

[21] F. D. R. Bonnet, D. B. Leinweber, and A. G. Williams, *J. Comput. Phys.* **170**, 1 (2001).

[22] Y. Iwasaki, University of Tsukuba report UTHEP-118 (1983).

[23] P. Hasenfratz and F. Niedermayer, *Nucl. Phys.* **B414**, 785 (1994).

[24] C. Morningstar and M. Peardon, *Phys. Rev.* **D56**, 4043 (1997).

[25] G. t'Hooft,*Phys. Rev.* **D14**, 3432 (1976).

[26] S. Coleman, in *The whys of subnuclear physics.* Proc. 1977 Int. Sch. Subnucl. Phys. 'Ettore Majorana' (ed. A. Zichichi). Plenum Press, New York (1977).

[27] G. t'Hooft, lectures given at the *5th WE Heraeus Summer School*, Saalburg, Germany, 1999, (2000) [hep-th/0010225].

[28] T-P. Cheng and L-F. Li, *Gauge Theory of Elementary Particle Physics*, Oxford Science Publications (1988).

[29] C. Itzykson and J. B. Zuber, *Quantum Field Theory*, McGraw-Hill (1980).

[30] G. Dunne, *Towards torus instantons*, unpublished notes of a lecture presented at the Special research Centre for the Subatomic Structure of Matter (CSSM), Adelaide, South Australia, July 2001.

[31] D. A. Smith and M. J. Teper, *Phys. Rev.* **D58**, (1998) 014505, [hep-lat/9801008].

[32] B. Sheikholeslami and R. Wohlert, *Nucl. Phys.* **B259**, 572 (1985).

[33] C. Bernard, J. E. Hetrick, T. DeGrand, M. Wingate, C. DeTar, S. Gottleib, U. M. Heller, K. Rummukainen, D. Toussaint, and R. L. Sugar, *Phys. Rev.* **D56**, 5584 (1997).

[34] N. Cabibbo and E. Marinari, *Phys. Lett.* **B119**, 387 (1982).

[35] M. G. Pérez, O. Philipsen, I-O. Stamatescu, *Nucl. Phys.* **B551**, 293 (1999) [hep-lat/9812006].

[36] H. D. Trottier, R. M. Woloshyn, *Phys. Rev.* **D50**, 6939 (1994), [hep-lat/9409010].

[37] C. Taubes, *J. Diff. Geom.* **19**, 517 (1984).

[38] P. de Forcrand, M. G. Pérez, I-O. Stamatescu, *Nucl. Phys. Proc. Suppl.* **53**, 557 (1997) [hep-lat/9608032].

[39] P. de Forcrand, M. G. Pérez, J. E. Hetrick, I-O. Stamatescu, in *Buckow 1997, Theory of elementary particles*, 221 (1997) [hep-lat/9802017].

[40] D. Toussaint, *Nucl. Phys. Proc. Suppl.* **83**, 151 (2000).

[41] R. Narayanan and P. Vranas, *Nucl. Phys.* **B506**, 373 (1998).

[42] C. Gattringer and I. Hip, *Nucl. Phys.* **B536**, 363 (1998).

[43] P. Hernández, *Nucl. Phys.* **B536**, 345 (1998).

[44] T. Fujiwara, *Prog. Theor. Phys.* **107**, 163 (2002) [hep-lat/0012007].